GOSAT-2 Quality Assessment Summary

Author(s): ***Michael Buchwitz, University of Bremen, Germany; Hannakaisa Lindqvist, Ella Kivimäki and Tomi Karppinen, FMI; Tobias Borsdorff, Trismono Krisna, Lianghai Wu, Jochen Landgraf***
Task 4 Mission Expert

Approval: ***Alessandro Piro***
Task 4 Lead

Accepted: ***Clément Albinet***
EDAP Technical Officer

EDAP.REP.073 *Issue: 2.0* *08/09/2022*

TELESPAZIO
a LEONARDO and THALES company

AMENDMENT RECORD SHEET

The Amendment Record Sheet below records the history and issue status of this document.

ISSUE	DATE	REASON
1.0 DRAFT	25/11/2021	Second DRAFT
2.0	08/09/2022	Addressed ESA comments

TABLE OF CONTENTS

1. EXECUTIVE SUMMARY

GOSAT-2 is a Japanese mission which was launched on October 29, 2018. The experiences gained from the operation of the GOSAT-1 mission with regard to payload calibration and validation activities served as input for the requirements of the GOSAT-2 mission. GOSAT-2 is equipped with two sensors: the Thermal and Near-infrared Sensor for Carbon Observation (TANSO)-Fourier Transform Spectrometer 2 (FTS-2) and the TANSO-Cloud and Aerosol Imager 2 (CAI-2). The FTS-2 is a Fourier transform spectrometer with along and cross track pointing mechanism. It observes the sun light reflected by the Earth's surface or scattered by clouds or aerosols (NIR and SWIR bands) and the thermal emission from both the Earth's surface and the atmosphere. Addition- ally to the spectral coverage of GOSAT, its successor GOSAT-2 includes the 2.3 µm band with CO, H2O, and CH4 absorption bands.

This document describes results from an assessment of:

1) the first GOSAT-2 XCO_2 operational data product (v01.04) as released by the GOSAT-2 team in Japan to the public end of 2020. This product is available from the GOSAT-2 Product Archive (https://www.gosat-2.nies.go.jp/about/data_products/) along with detailed documentation. Several criteria related to this data product and its documentation have been assessed in this EDAP ESA project as required to fill out the Mission Quality Assessment Matrix (MQAM). Overall, we conclude excellent quality for data product information and mostly good quality for several other entries of the MQAM. Product validation is based on comparisons with ground-based Total Carbon Column Observing Network (TCCON) XCO_2 retrievals. TCCON has been developed and established for satellite XCO_2 validation and is the core network for this purpose. Primarily because of the limited spatial coverage of the TCCON reference data used for validation the two criteria "Uncertainty Characterisation Method" and "Reference Data Representativeness" are classified as intermediate. Some fields are classified as "Not Assessed" because the relevant information was not available for us (which does not imply that this information does not exist) or because we consider the corresponding assessment as outside of the scope of this project. We have removed the "Information Not Public" tag for all entries as we do not know with certainty if this is true. Note that characterization of this GOSAT-2 product as given in the MQMA only refers to quality of documentation and data format and availability etc. but does not address "fitness for purpose", which has not been assessed;
2) GOSAT-2 L2 retrievals over snow show higher retrieval error than over land, but due to the limited amount of data it is not possible to make very accurate conclusions
3) Bias in the GOSAT-2 XCO_2NIES v01.04 product varies between -4.2 – 6.9 ppm against different TCCON FTS; corresponds to < 1.7%. Precision (1-sigma) varies between 2.2 – 5.1 ppm.
4) Bias in the GOSAT-2 XCH_4NIES v01.04 product varies between -23.2 - 21 ppb against different TCCON FTS; corresponds to < 1.3%. Precision (1-sigma) varies between 10.4 – 23.1 ppb.
    a. Outlier Zugspitze: bias 47.3 ppb
5) GOSAT-2 L2 prior profiles of CH_4 and CO_2 agree well with high-latitude AirCore profile measurements
    a. Posterior profiles seem somewhat unstable but our comparison dataset is limited in number of observations and spatial coverage

The quality of the operational GOSAT-2 XCO_2 version 01.04 data product has been assessed by comparisons with ground-based TCCON XCO_2 retrievals and by comparisons with GOSAT XCO_2products and with GOSAT-2 XCO_2 data products, which have been retrieved using European retrieval algorithms as developed, for example, in the context of the ESA Climate Change Initiative (CCI) GHG-CCI+ project (https://climate.esa.int/en/projects/ghgs/). Our validation and comparison results can be summarized as follows: based on comparisons with TCCON we conclude that the operational GOSAT-2 v01.04 product has an overall high bias (global offset) of approximately 3.2 ppm. We also determined the "spatial bias" computed as standard deviation of the biases as obtained at the various TCCON sites. This spatial bias or site-to-site bias is ±2.43 ppm (1-sigma). For applications such as inverse modelling of regional CO_2 fluxes the overall offset or global bias is not critical as this is a single number and a data product can be easily corrected for this. The spatial bias can typically not be corrected and is therefore critical. The estimated value of the spatial bias of ±2.43 ppm is significantly larger compared to the other satellite XCO_2 data products including the two other GOSAT-2 data products. We also determined the "Precision", which quantifies the single observation random error. This quantity has been computed as standard deviation of satellite minus TCCON differences. We estimate that the precision is ±3.54 ppm (1-sigma). This is significantly larger compared to the other satellite XCO_2 data products including the two other GOSAT-2 data products and indicates that the scatter of the operational GOSAT-2 XCO_2data product is higher compared to the other products. We also identified a large difference between the reported uncertainty and the scatter of the data, which is not observed for the other satellite data products. From this we conclude that the reported XCO_2 uncertainty is too optimistic. The comparison results in terms of mean values and standard deviations in 30^o latitude bands indicate that the NIES GOSAT-2 XCO_2 product often shows a high bias, which is consistent with the findings based on the comparison with TCCON, i.e., with the overall high bias of 3.2 ppm.

Moreover, in this study, the scientific full-physics and proxy GOSAT-2 XCH4data product has been improved using the RemoTeC algorithm that is retrieved from L1B measurements of the GOSAT-2 mission. The coverage of the data products was enhanced by updating the posteriori filter criteria that were, in particular for the full-physics retrieval, too strict resulting in a poor spatial coverage. For the GOSAT-2 data product, a new bias correction scheme was developed that is not based anymore on GOSAT-1 data but derived from collocated measurements of the TCCON Total Carbon Column Observing Network of ground-based Fourier Transform Spectrometers. The bias correction deploys the retrieved surface albedo from one year (5th February 2019 to 29th Feb 2020) of GOSAT-2 data in window 1 (765 nm) and 2 (1593 nm). Furthermore, we corrected the definition of the instrument Mueller matrix, which defines the instrument polarization sensitivity. The retrieval scheme is now compatible with GOSAT-2 L1B v102102 (May 2020) and we reprocessed the full GOSAT-2 dataset from Feb. 2019 until July 2020 with the updated version of the RemoTeC processor. The retrieved GOSAT-2 XCH4data sets is validated with TCCON ground-based observation and compared with GOSAT-1, and TROPOMI data. The validation with TCCON measurements at 13 selected sites results in a good agreement. The global mean bias between TCCON and GOSAT-2 is -0.34 ppb and -0.06 ppb for the full-physics and proxy product, a corresponding mean scatter is 13.61 ppb and 16.15 ppb with a station-to-station bias of 1.94 ppb and 2.63 ppb, respectively. A similar good agreement can be achieved with GOSAT-2 glint measurements using TCCON stations near the coast. Here, the global mean bias between TCCON and GOSAT-2 is -2.57 ppb and 5.36 ppb for the full-physics and proxy product, a corresponding mean scatter is 10.93 ppb and 10.29 ppb with a station- to-station bias of 1.49 ppb and 5.16 ppb, respectively. Furthermore, we find a good agreement over land between the GOSAT-1 XCH4retrievals and GOSAT-2 full physics (correlation=0.78, bias=2.2 ppb, std=13.4 ppb) and proxy (correlation=0.84, bias=-3.1 ppb, std=14.4 ppb) retrievals. For observations over ocean, the agreement between XCH4GOSAT-1 and GOSAT-2 full physics retrieval is similar (correlation=0.87, bias=0.6 ppb, std=9.8 ppb). Similar holds for the corresponding XCH4proxy products (correlation=0.93, bias=3.1 ppb, std=11.3 ppb) retrievals. The uncorrected TROPOMI XCH4retrieval agrees well with both the GOSAT-2 full physics (correlation=0.82, bias= 0.78 ppb, std=23.48 ppb) and the GOSAT-2 proxy product (correlation=0.85, bias= 16.65 ppb, std=20.51ppb). For the bias corrected TROPOMI XCH4retrievals the correlation and the standard deviation with the GOSAT-2 full physics (correlation=0.85, bias=16.51 ppb, std=22.26 ppb) and proxy retrievals (correlation=0.85, bias=16.65 ppb, std= 22.26 ppb) are significantly improved. The increase of the mean bias when applying the correction to the TROPOMI data is of minor relevance because it can easily be corrected and is of little scientific relevance.

Overall, we conclude that there is need and also room to improve the quality of the operational GOSAT-2 XCO_2version 01.04 data product, which is the first GOSAT-2 XCO_2 product released to the public by the National Institute for Environmental Studies (NIES) in Japan. Probably product quality can (also) be improved by implementing a stricter quality filtering procedure and to also implement and appropriate bias correction procedure. Also, the reported uncertainty is too optimistic and we also recommend to also improve this aspect.

1.1 Mission Quality Assessment Matrix

Product Information	Product Generation	Ancillary Information	Uncertainty Characterisation	Validation
Product Details	Sensor Calibration & Characterisation Pre-Flight	Product Flags	Uncertainty Characterisation Method	Reference Data Representativeness
Availability & Accessibility	Sensor Calibration & Characterisation Post-Launch	Ancillary Data	Uncertainty Sources Included	Reference Data Quality
Product Format	Retrieval Algorithm Method		Uncertainty Values Provided	Validation Method
User Documentation	Retrieval Algorithm Tuning		Geolocation Uncertainty	Validation Results
Metrological Traceability Documentation	Additional Processing			

Key
Not Assessed
Not Assessable
Basic
Intermediate
Good
Excellent

Information Not Public

Figure 1: GOSAT-2 Product Quality Evaluation Matrix.

2. MISSION ASSESSMENT OVERVIEW

2.1 Product Information

Product Details	
Product Name	*L2 CO2 column amount (SWIR)* *GOSAT-1&2 Operational XCO2 and XCH4*
Sensor Name	*GOSAT-2* *GOSAT-1*
Sensor Type	*NIR/SWIR – Multichannel spectrometer*
Mission Type	*1 satellite (follow-on of GOSAT, which is still in orbit)*
Mission Orbit	*Sun Synchronous*
Product Version Number	*V01.04* *02.95bc*
Product ID	*GOSAT-2 FTS-2 SWIR L2 Column-averaged Dry-air CO2 Mole Fraction* *GOSATTFTS*
Processing level of product	*Level 2*
Measured Quantity Name	*XCO2 (column-averaged dry-air mole fraction of* CO_2*)* *XCO2 and XCH4*
Measured Quantity Units	*ppm (micromole / mole) and ppb (part per billion)*
Stated Measurement Quality	*Approx. 2-4 ppm (according to official GOSAT-2 validation report and assessment results presented in this document)* *XCO2 and XCH4 uncertainty provided for each retrieval in the product*
Spatial Resolution	*10 km*
Spatial Coverage	*Global (but non-consecutive sampling)*
Temporal Resolution	4s
Temporal Coverage	Earth dayside April 2009 – now (GOSAT) and March 2019 – now (GOSAT-2)
Point of Contact	gosat-2-info@nies.go.jp
Product locator (DOI/URL)	*https://www.gosat-2.nies.go.jp/about/data_products/*
Conditions for access and use	*http://www.nies.go.jp/soc/en/documents/datapolicy/*
Limitations on public access	None
Product Abstract	GOSAT-2 TANSO-FTS-2 SWIR L2Column-averagedDry-airMoleFractionProduct stores column-averaged dry-air mole fraction of atmospheric gases retrieved by a full-physics method from Band1-3 radiancespectrumdatainTANSO-FTS-2L1B products using MAP (maximum a posterior) method. TANSO-FTS-2 SWIR data, acquired under the condition where no cloud or only optically thin cirrus clouds are present within the TANSO-FTS-2 instantaneous field of view, are used to generate this product. Source: *https://prdct.gosat-2.nies.go.jp/documents/pdf/GOSAT-2_Data_Users_Handbook_1stEdition_en.pdf*

Availability & Accessibility	
Compliant with FAIR principles	*Yes*
Data Management Plan	*N.A.*
Availability Status	*Available and accessible from:* *Data: https://www.gosat-2.nies.go.jp/about/data_products/* *Documents: https://prdct.gosat-2.nies.go.jp/documents/documents.html.en*

Product Format	
Product File Format	*HDF5*
Metadata Conventions	*N.A.*
Analysis Ready Data?	*Yes*

User Documentation		
Document	*Reference*	*QA4ECV Compliant*
Product User Guide	*https://prdct.gosat-2.nies.go.jp/documents/pdf/GOSAT-2_Data_Users_Handbook_1stEdition_en.pdf*	*Yes*
ATBD	*https://prdct.gosat-2.nies.go.jp/documents/pdf/ATBD_FTS-2_L2_SWL2_en_00.pdf*	Yes

Metrological Traceability Documentation	
Document Reference	*https://prdct.gosat-2.nies.go.jp/documents/documents.html.en*
Traceability Chain / Uncertainty Tree Diagram Available	*N.A.* Complete traceability chain or uncertainty tree was not provided in the documentations. The traceability has been considered as basic level basing on Excel sheet of radiometric measurements.

2.2 Product Generation

Sensor Calibration & Characterisation – Pre-Flight	
Summary	The test program characterized the radiometric, spatial, and spectral performance of all five spectral bands, including SNR, FWHM, co-registration, FOV size/shape, polarization, and intelligent pointing functionality. The dark level and dark noise between the data obtained from the pre-flight test on the ground and the data obtained from the on-orbit dark calibration. There was no significant change in the dark level and dark noise from the ground test. It was confirmed that the performance at the ground test was maintained.
References	*Test Performance and Verification of the TANSO-FTS-2 Sensor, September 2018, SPIE Asia-Pacific Remote Sensing Conference* *Thermal and near-infrared sensor for carbon observation Fourier transform spectrometer-2 (TANSO-FTS-2) on the Greenhouse gases Observing SATellite-2 (GOSAT-2) during its first year in orbit, Atmos. Meas. Tech., 14, 2013–2039, 2021* https://doi.org/10.5194/amt-14-2013-2021

Sensor Calibration & Characterisation – Post-Launch	
Summary	To evaluate the geometric performance of the CAI-2, the observation of ground control point (GCP) and cross-correlation methods were used. At first, the absolute direction vector of each pixel in the reference bands (Band 4 and Band 9) derived using GCP was calculated. After that, the difference of the direction vector for the other bands with respect to the reference band was calculated using cross-correlation between images. The direction vector data ware calibrated using these observation data. In the radiometric calibration, the lunar calibration is performed using the Moon as the reference light source to evaluate the radiometric performance of the CAI-2. The CAI-2 acquires dark calibration data by imaging the ocean around midnight. To avoid the influence of sunshine, the data is acquired during the time when the satellite is in the shade of the Earth.
References	*"The development and on-orbit calibration status of GOSAT-2 TANSO-CAI-2 instrument" Proceedings Volume 11852, International Conference on Space Optics — ICSO 2020; 1185257 (2021)* https://doi.org/10.1117/12.2599936 *Thermal and near-infrared sensor for carbon observation Fourier transform spectrometer-2 (TANSO-FTS-2) on the Greenhouse gases Observing SATellite-2 (GOSAT-2) during its first year in orbit, Atmos. Meas. Tech., 14, 2013–2039, 2021* https://doi.org/10.5194/amt-14-2013-2021

Retrieval Algorithm Method	
Summary	Maximum APosteriori (MAP) method based on detailed radiative transfer modelling of radiance spectra
References	https://prdct.gosat-2.nies.go.jp/documents/pdf/ATBD_FTS-2_L2_SWL2_en_00.pdf

Retrieval Algorithm Tuning	
Summary	In the TIR, the agreement between TANSO-FTS-2 and AIRS–IASI is better than 1 K for scenes brighter than 220 K. The GOSAT-2's intelligent pointing mechanism based on active cloud avoidance indicates that the number of scenes useful for spectral analysis increased by a factor of 1.8 over a stiff pointing schedule.
References	*Algorithm development for the TIR bands of GOSAT-2/TANSO-FTS-2: lessons from GOSAT/TANSO-FTS TIR CO2 and CH4 measurement* *Thermal and near-infrared sensor for carbon observation Fourier transform spectrometer-2 (TANSO-FTS-2) on the Greenhouse gases Observing SATellite-2 (GOSAT-2) during its first year in orbit, Atmos. Meas. Tech., 14, 2013–2039, 2021https://doi.org/10.5194/amt-14-2013-2021*

Additional Processing	
Additional Processing	
Description	N.A.
Reference	N.A.

2.3 Ancillary Information

Product Flags	
Product Flag Documentation	*https://prdct.gosat-2.nies.go.jp/documents/pdf/ATBD_FTS-2_L2_SWL2_en_00.pdf*
Comprehensiveness of Flags	*Yes, contained in data product files*

Ancillary Data	
Ancillary Data Documentation	*https://prdct.gosat-2.nies.go.jp/en/documents/ATBD_FTS-2_L2_SWL2_en_00.pdf*
Comprehensiveness of Data	*Yes*
Uncertainty Quantified	*Yes, contained in data product files*

2.4 Uncertainty Characterisation

Uncertainty Characterisation Method	
Summary	*Via error propagation (MAP method) and via comparison with reference data (e.g., TCCON)*
Reference	https://prdct.gosat-2.nies.go.jp/en/documents/ValidationResult_FTS-2_L2_SWFP_ver0104_en_00.pdf https://prdct.gosat-2.nies.go.jp/en/documents/ATBD_FTS-2_L2_SWL2_en_00.pdf

Uncertainty Sources Included	
Summary	*Many sources considered (e.g., aerosols, clouds, surface reflectivity, meteorology)*
Reference	https://prdct.gosat-2.nies.go.jp/documents/pdf/ValidationResult_FTS-2_L2_SWFP_ver0104_en_01.pdf https://prdct.gosat-2.nies.go.jp/documents/pdf/ATBD_FTS-2_L2_SWL2_en_00.pdf

Uncertainty Values Provided	
Summary	*See variable xco2_uncert contained in each product file*
Reference	https://prdct.gosat-2.nies.go.jp/documents/pdf/ValidationResult_FTS-2_L2_SWFP_ver0104_en_01.pdf https://prdct.gosat-2.nies.go.jp/documents/pdf/ATBD_FTS-2_L2_SWL2_en_00.pdf
Analysis Ready Data?	*Yes*

Geolocation Uncertainty	
Summary	*N.A.*
Reference	

2.5 Validation

Validation Activity #1	
Independently Assessed?	Yes
Reference Data Representativeness	
Summary	*Good reference data representativeness as TCCON reference measures the same quantity, namely XCO2.*
Reference	*https://prdct.gosat-2.nies.go.jp/documents/pdf/ATBD_FTS-2_L2_SWL2_en_00.pdf* *This document*
Reference Data Quality & Suitability	
Summary	*Primarily TCCON XCO2.* *Perfectly suitable (as same quantity) but limitations due to sparse spatial coverage.* *In comparison with in-situ airborne measurements, the uncertainty (1σ) of XCO2 is0.4 ppm.*
Reference	*https://prdct.gosat-2.nies.go.jp/documents/pdf/ATBD_FTS-2_L2_SWL2_en_00.pdf* *This document*
Validation Method	
Summary	*Direct comparison of TCCON with satellite XCO2*
Reference	*https://prdct.gosat-2.nies.go.jp/documents/pdf/ATBD_FTS-2_L2_SWL2_en_00.pdf* *This document*
Validation Results	
Summary	*Findings GOSAT-2 team in Japan:* *Regarding XCO2in the GOSAT-2 product over land, the biases from the TCCON data ranged from 3.75 to 4.06 ppm (from 0.91 to 0.99%) and their standard deviations ranged from 3.11 to 3.91 ppm (from 0.76 to 0.95%). Regarding those over ocean, the biases from the TCCON data ranged from 1.64 to 5.36 ppm (from 0.40 to 1.30%) and their standard deviations ranged from 5.22 to 5.82 ppm (from 1.27 to 1.42%). However, the number of data and the degree of latitudinal coverage over ocean are yet sufficient. Source: Ref 1.* *Findings: This document:* *Our findings (Ref. 2) are consistent with the findings of the GOSAT-2 team*
Reference	*Ref 1: https://prdct.gosat-2.nies.go.jp/documents/pdf/ATBD_FTS-2_L2_SWL2_en_00.pdf* *Ref 2: This document*

3. DETAILED ASSESSMENT

In this section the validation and comparison results as conducted in the framework of this study are presented.

In Sect. 3.1 the comparisons of GOSAT-2 (Suto et al., 2020) operational XCO_2 (v01.04) with ground-based XCO_2 retrievals from the Total Carbon Column Observation Network (TCCON) are presented (Wunch et al., 2010, 2011).

In Sect. 3.2 we present comparisons with other satellite XCO_2 data products. For comparison also these products have been compared with TCCON and an overview about all satellite products used for comparisons is provided in Table 1.

Table 1: satellite XCO_2 data products as used for this document.

Product ID (Algorithm)	Version	Sensor	Comments
CO2_GO2_NIES (NIES)	01.04	GOSAT-2	Operational GOSAT-2 XCO_2 data product assessed in this document
CO2_GO2_SRFP (RemoTeC)	1.0	GOSAT-2	ESA GHG-CCI+ product from SRON (Krisna et al., 2020)
CO2_GO2_FOCA (FOCAL)	1.0	GOSAT-2	Univ. Bremen product (under development) (Noël et al., 2020)
CO2_GOS_NIES (NIES)	02.9bc	GOSAT	NIES GOSAT product (Yoshida et al., 2013)
CO2_GOS_SRFP (RemoTeC)	2.3.8	GOSAT	SRON product (Butz et al., 2011)
CO2_GOS_OCFP (UoL-FP)	7.3	GOSAT	Univ. Leicester product (Cogan et al., 2012)
CO2_GOS_BESD (BESD)	NRT	GOSAT	Univ. Bremen product (Heymann et al., 2015)
CO2_GOS_FOCA (FOCAL)	1.0	GOSAT	Univ. Bremen product (Noël et al., 2020)

In Sect. 3.3 the comparisons of GOSAT-2 (Suto et al., 2020) operational XCH_4 with ground-based XCH_4 retrievals from the Total Carbon Column Observation Network (TCCON) are presented.

In Sect. 3.4 the improvement of the scientific full-physics and proxy GOSAT-2 XCH4data product using the RemoTeC algorithm is presented.

In Sect. 3.5the evaluation of the GOSAT-2 CH4 and CO2 over the snow is shown (in Sect. 3.9 the same evaluation with GOSAT-1).

In Sect. 3.6 assessment of prior and posteriori profiles of GOSAT-2 CO2 and CH4 against AIRCORE soundings is presented (in Sect. 3.10 the same evaluation with GOSAT NIES).

In Sect. 3.7 the evaluation of SIF products on Northern Finland has been done and presented.

In Sect. 3.8 the comparisons of GOSAT operational XCO_2 and XCH_4 with ground-based retrievals from the Total Carbon Column Observation Network (TCCON) are presented

3.1 Comparisons with ground-based TCCON XCO_2

The GOSAT-2 XCO_2 data product from NIES ("CO2_GOS_NIES") and the other satellite XCO_2 data products as listed in Table 1 have been compared with TCCON XCO_2.

The comparison method is the "QA/QC method" as described in Reuter et al., 2020.

The time period covered is March – December 2019. The comparison method is identical for all satellite data products. The only difference is the time coverage of product CO2_GO2_SRFP, which is only available until end of October 2019, i.e., the used period is 2 months shorter as for the other products.

The following settings have been used for all comparisons to ensure that "enough data" are available in order to obtain robust conclusions:

- Colocation criteria:
  - Temporal colocation: ± 2 hours
  - Spatial colocation: ± 2 deg latitude and ± 4 deg longitude
- Other criteria:
  - Minimum number of satellite data per overpass of a given TCCON site: 1
  - Minimum number of overpasses of a given TCCON site to accept that site: 10

Comparison results for the three GOSAT-2 products are shown in Figure 2 and the numerical results are shown in Table 2.

The first quantity listed in Table 2 is the "Precision" which quantifies the single observation random error in ppm. This quantity has been computed as standard deviation of satellite minus TCCON differences. As can be seen, the estimated precision is ±3.54 ppm (1-sigma) for product CO2_GO2_NIES. This is significantly worse compared to the other satellite XCO_2 data products including the two other GOSAT-2 data products and indicates that the scatter or noise of the operational GOSAT-2 data product is higher compared to the other products.

The second quantity is the "Bias" and is reported as mean value of the satellite – TCCON differences at the various TCCON sites and as the standard deviation of these differences. As can be seen, product CO2_GO2_NIES has a high bias of 3.20 ppm relative to TCCON. As can also be seen, the standard deviation, which is interpreted as "spatial bias" or site-to-site bias, is ±2.43 ppm (1-sigma). For applications such as inverse modelling of regional CO_2 fluxes the overall offset or global bias is not critical as this is a single number and a data product can be easily corrected for this. The spatial bias can typically not be corrected and is therefore critical. The estimated value of the spatial bias is ±2.43 ppm which is significantly worse compared to the other satellite XCO_2 data products including the two other GOSAT-2 data products. This indicates that the accuracy of spatial XCO_2 pattern of the operational GOSAT-2 XCO_2 product is the lowest of all products.

Quantities “Ndays” and “Nobs” shows how many days (= TCCON overpasses) have been used for comparisons taking into account the colocation and other criteria listed above. These numbers are highest for product CO2_GO2_NIES indicating that the other products are more strongly filtered for “good quality”.

Quantity “R” is the linear correlation coefficient of the satellite and the TCCON data. For product CO2_GO2_NIES R is lowest, namely only 0.50. This also shows the poor quality of this product compared to the other products.

In the last columns the quantity “UncR” is shown. This Uncertainty Ratio is a measure of the reliability of the reported XCO_2 uncertainty (which is contained in all products). UncR is the mean value of the reported uncertainty (which is supposed to be the statistical (random) error (1-sigma) of XCO_2) divided by the actual random error estimated as “Precison” as reported in the first column. If the reported uncertainty is approximately correct, then UncR should be a value close 1o 1.0. As can be seen, UncR is only 0.14 for product CO2_GO2_NIES. This indicates that the reported uncertainty is much too optimistic. The “real uncertainty” is probably approximately 7 (= 1.0/0.14) times larger, i.e., about 3.5 ppm instead of the reported value of approximately (typically) 0.5 ppm.

(a)

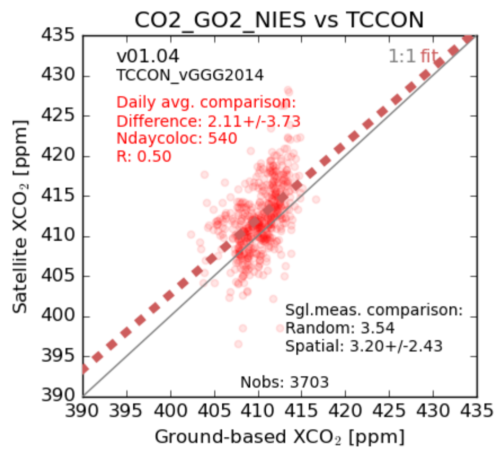

(b)

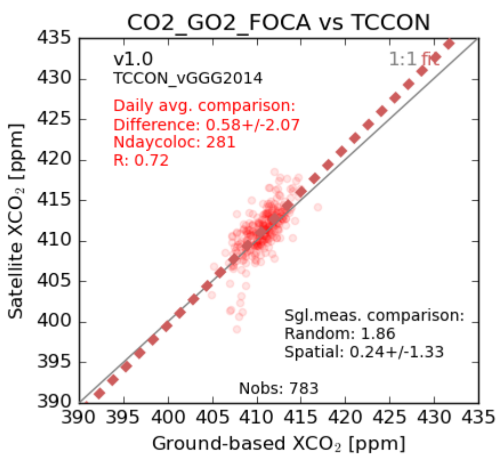

(c)

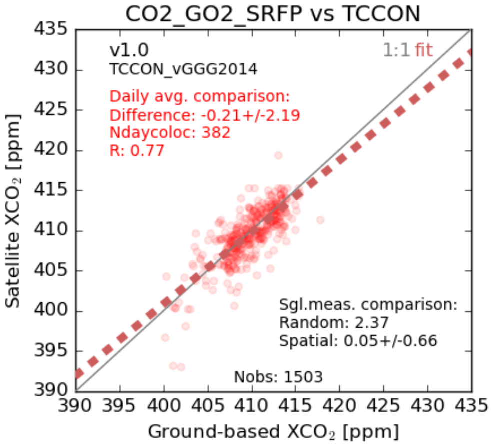

Figure 2: comparison of 3 GOSAT-2 XCO2 data product with TCCON. (a) CO2_GO2_NIES, (b) CO2_GO2_FOCA and (c) CO2_GO2_SRFP.

Table 2: overview satellite XCO_2 data product validation by comparison with TCCON. Precision is an estimate of single observation random error. Bias is the mean value of the satellite-TCCON difference± the standard deviation of the difference at the various TCCON sites. Ndays is the number of days (overpasses) used for comparison and Nobs the number of observations which have been compared. R is the linear correlation coefficient. UncR is the Uncertainty Ratio defined as the mean value of the reported uncertainty divided by the standard deviation of the satellite-TCCON XCO_2 difference.

Product ID	Precision [ppm]	Bias [ppm]	Ndays [-]	Nobs [-]	R [-]	UncR [-]
CO2_GO2_NIES	3.54	3.20 ± 2.43	540	3703	0.50	0.14
CO2_GO2_SRFP	2.37	0.05 ± 0.66	382	1503	0.77	1.08
CO2_GO2_FOCA	1.86	0.24± 1.33	281	783	0.72	0.58
CO2_GOS_NIES	1.98	0.79 ± 0.87	451	2640	0.80	0.58
CO2_GOS_SRFP	2.42	0.60± 1.12	368	1319	0.66	0.87
CO2_GOS_OCFP	2.13	0.70 ± 0.69	412	2126	0.75	0.98
CO2_GOS_BESD	2.26	0.00 ± 0.84	447	3270	0.77	0.97
CO2_GOS_FOCA	1.63	0.37± 0.77	427	2116	0.80	1.20

The operational GOSAT-2 XCO2 Level 2 product (GOSAT-2 NIES XCO2 v01.04) was evaluated also against 22 ground-based FTS instruments that participate in the Total Carbon Column Observing Network (TCCON; Wunch et al., 2011). The product was available for the period 1.3.2019–18.5.2020. The spatiotemporal co-location criteria for the evaluation were same-day soundings within 2.5 degrees in latitude and 5.0 degrees in longitude.

Product quality flags of QF = 0 (good) and QF = 1 (fair) were included in the evaluation. We present an evaluation of the daily mean values which mostly correspond to overpass-averaged statistics.

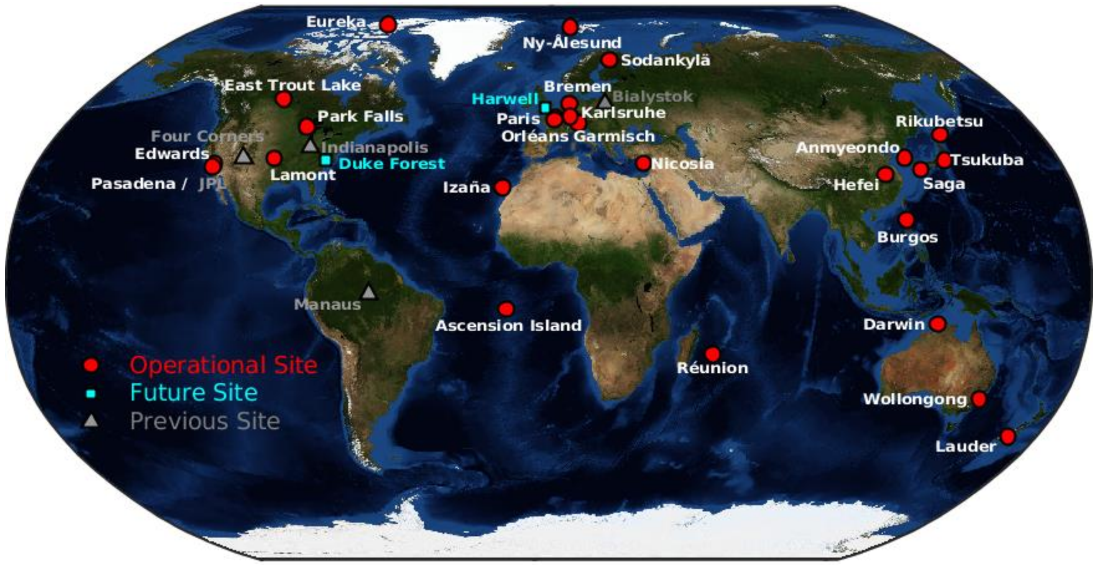

Figure 3: the Total Carbon Column Observing Network of ground-based Fourier Transform Spectrometers used in the evaluation of GOSAT and GOSAT-2 data. From: tccondata.org.

The biases for daily averaged GOSAT-2 XCO2 against 22 ground-based FTS as well as the standard deviations are listed in Table 3 and also presented in Figure 4. Bias in the GOSAT-2 XCO_2 NIES v01.04 product varies between -4.2 – 6.9 ppm against different TCCON instruments. This corresponds to smaller than 1.7% relative errors. The magnitude of the bias varies between the sites, and the largest bias of 6.9 ppm is obtained at Saga. Precision (1-sigma) varies between 2.2 – 5.1 ppm. Figure 4shows that the bias is systematically positive globally, with only three exceptions where the bias is negative. The resulting statistics show significant improvement over the earlier product evaluation (NIES v01.00) presented in the last report. Still, the product is statistically not yet as mature as the GOSAT-1 product.

In addition to the evaluation of the bias, i.e., the average difference in daily-averaged GOSAT-2 XCO2 – TCCON XCO2, an attempt was made to evaluate the seasonal cycle amplitude and the growth rate. However, the temporal data coverage was not yet sufficiently long for this purpose. Nevertheless, we present the individual site time series in Figure 5. These help to analyse the quality of data more systematically at the single-site level. It is apparent from Figure 5 that the single GOSAT-2 observations have significant scatter, shown by the high (typically 5 ppm or more) uncertainty estimates connected to the daily mean values. Due to the high scatter, it is difficult to reliably estimate the potential of seasonal biases, although some of the results suggest that seasonal biases may exist (e.g., Lamont).

Table 3: Evaluation of GOSAT-2 NIES v01.04 XCO_2 against XCO_2 of ground-based Fourier Transform Spectrometers in the Total Carbon Column Observing Network (TCCON) sites, using the GGG2014 retrieval. The table shows the mean bias (GOSAT-2 – TCCON; in ppm), the relative bias (in %) and the standard deviation (STD; in ppm) at a given site.

TCCON site	#days	Bias	Rel. b. %	STD	TCCON site	#days	Bias	Rel. b. %	STD
Bremen	8	4.0	1.00	2.2	Lauder	108	3.5	0.90	2.4
Burgos	38	0.2	0.00	5.1	Orleans	28	5.0	1.20	3.5
Caltech	152	0.4	0.10	2.4	Paris	23	5.5	1.30	2.8
Darwin	46	-4.2	-1.00	2.7	Park Falls	83	5.0	1.20	4.2
East Trout Lake	46	4.0	1.00	4.6	Reunion	53	-0.8	-0.20	2.8
Edwards	175	2.1	0.50	2.5	Rikubetsu	9	5.6	1.40	3.6
Eureka	7	3.0	0.70	3.8	Saga	53	6.9	1.70	4.0
Garmisch	23	6.2	1.50	3.9	Sodankylä	17	5.0	1.20	3.4
Izana	68	2.4	0.60	3.9	Tsukuba	40	3.7	0.90	4.2
Karlsruhe	48	6.2	1.50	3.1	Wollongong	118	0.6	0.20	3.3
Lamont	116	-0.2	0.00	2.6	Zugspitze	21	3.9	1.00	3.1

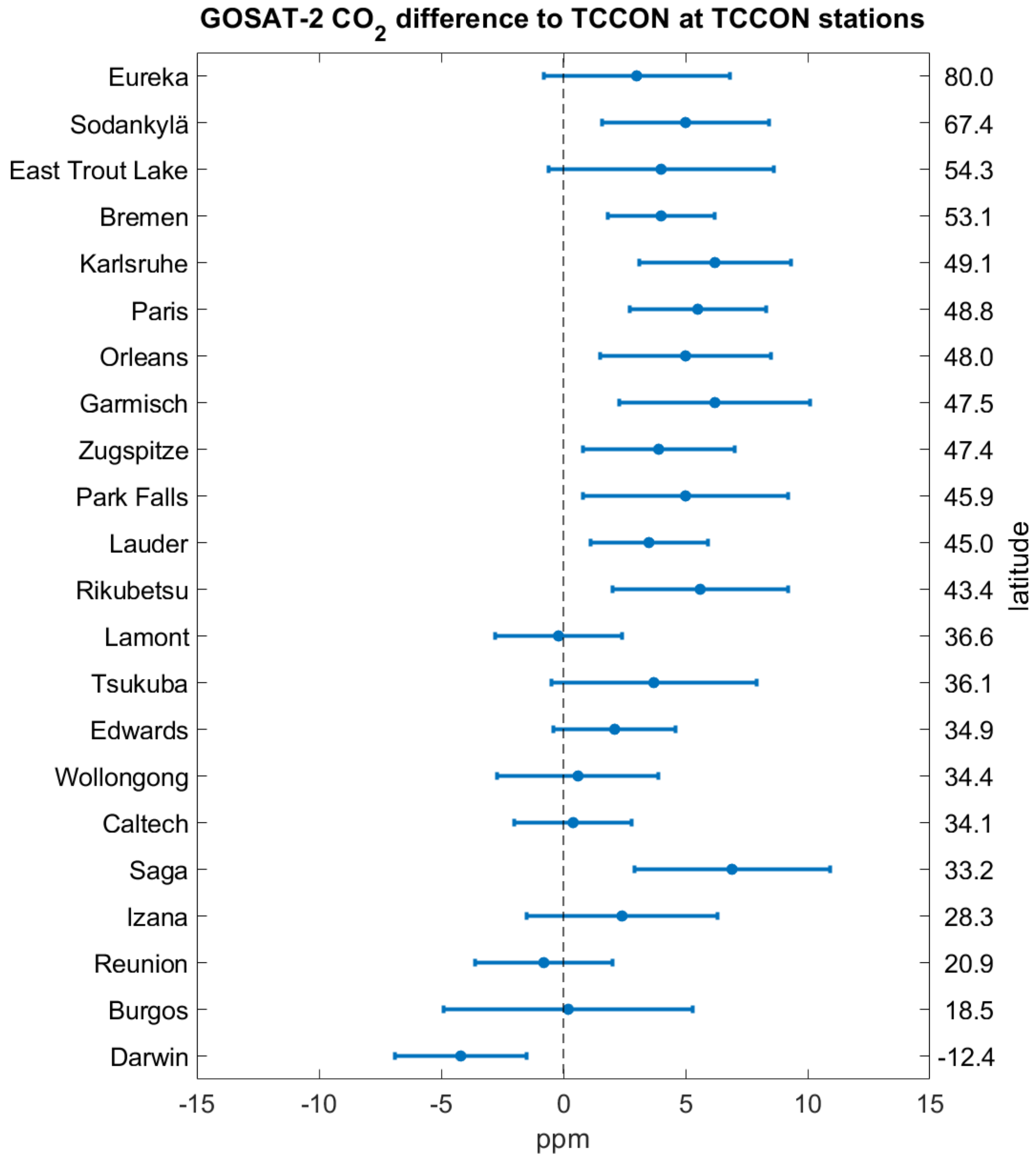

Figure 4: the accuracy and precision of GOSAT-2 NIES v01.04 XCO_2 at the TCCON sites, presented as the mean of GOSAT-2 – TCCON daily-averaged XCO_2. The error bars denote the standard deviation (in ppm). The evaluation sites are organised according to their latitude.

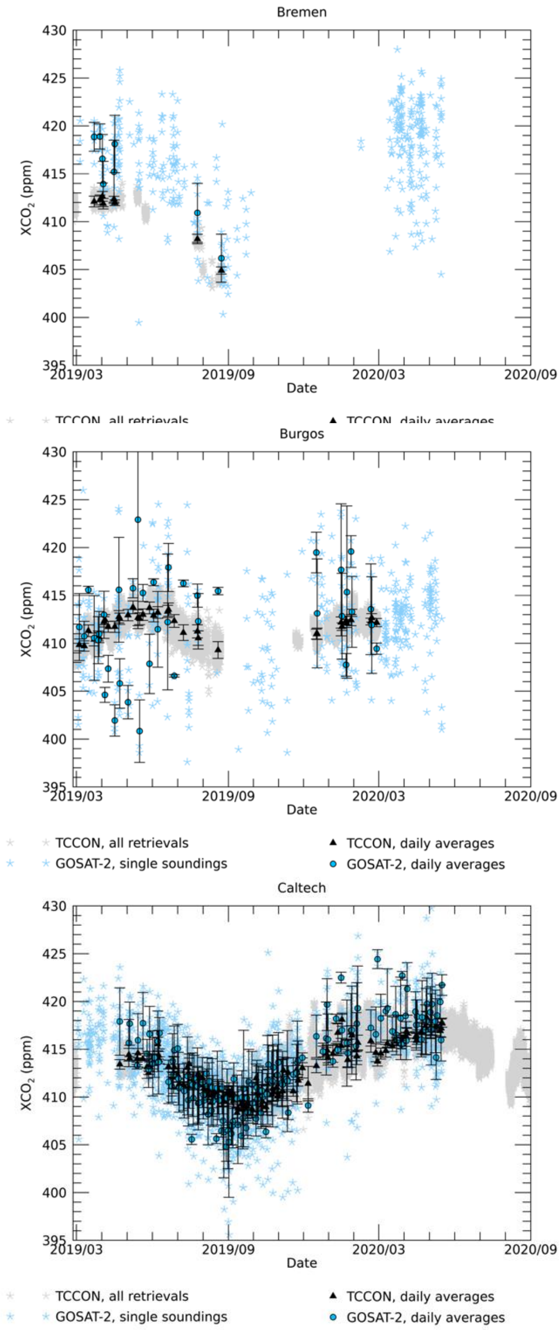
Bremen
XCO$_2$ (ppm)
Date
Burgos
XCO$_2$ (ppm)
Date
TCCON, all retrievals
GOSAT-2, single soundings
TCCON, daily averages
GOSAT-2, daily averages
Caltech
XCO$_2$ (ppm)
Date
TCCON, all retrievals
GOSAT-2, single soundings
TCCON, daily averages
GOSAT-2, daily averages

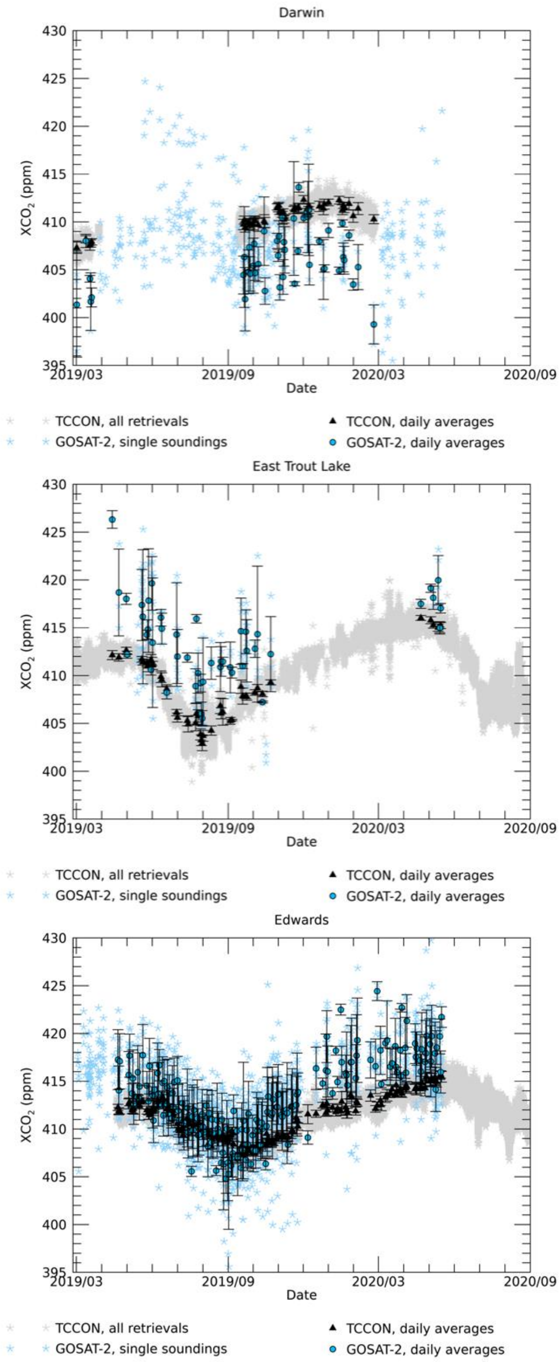
Darwin
XCO2 (ppm)
Date
2019/03
2019/09
2020/03
2020/09
TCCON, all retrievals
GOSAT-2, single soundings
TCCON, daily averages
GOSAT-2, daily averages
East Trout Lake
XCO2 (ppm)
Date
TCCON, all retrievals
GOSAT-2, single soundings
TCCON, daily averages
GOSAT-2, daily averages
Edwards
XCO2 (ppm)
Date
TCCON, all retrievals
GOSAT-2, single soundings
TCCON, daily averages
GOSAT-2, daily averages

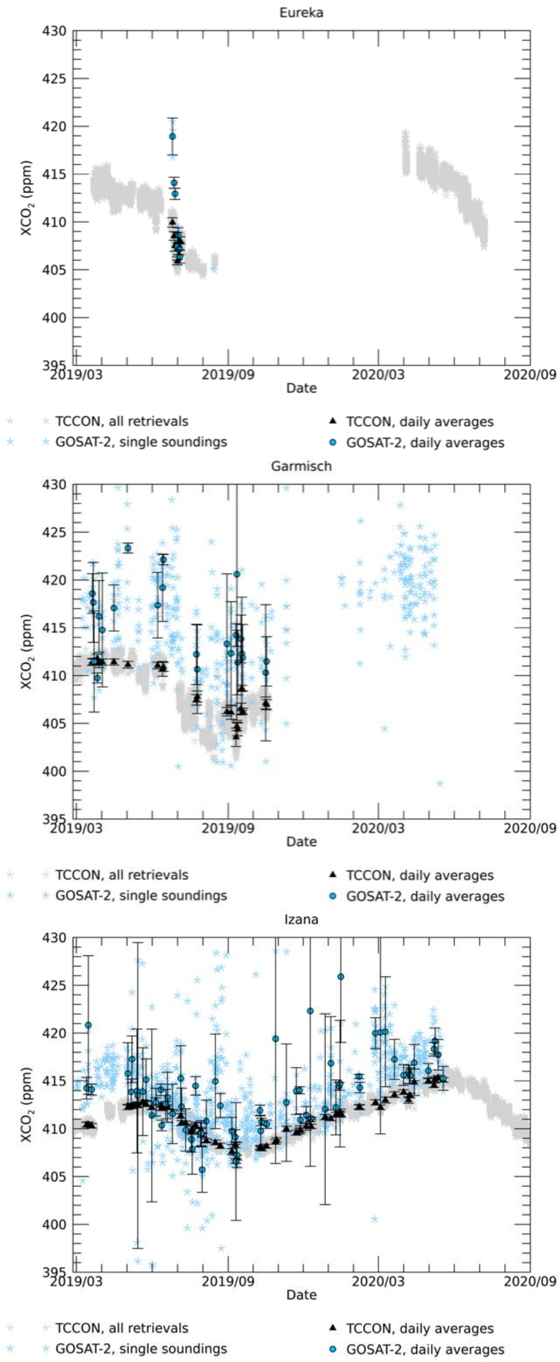
Eureka
430
425
420
415
410
405
400
395
XCO2 (ppm)
2019/03
2019/09
2020/03
2020/09
Date
TCCON, all retrievals
GOSAT-2, single soundings
TCCON, daily averages
GOSAT-2, daily averages
Garmisch
Izana

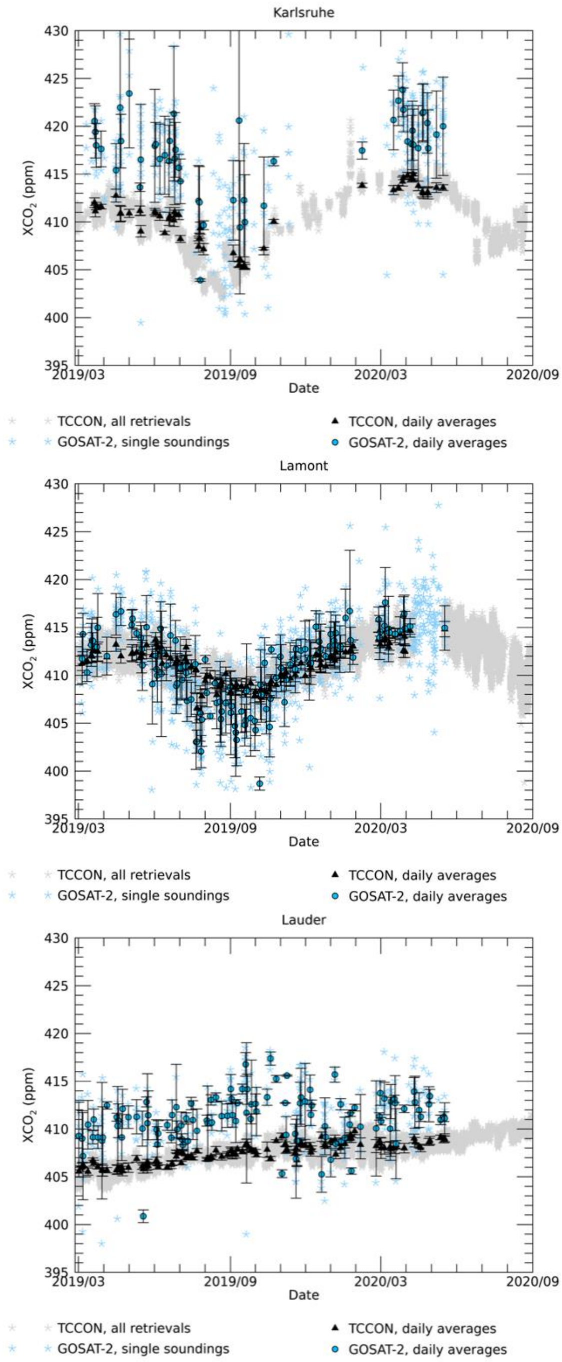
Karlsruhe
XCO2 (ppm)
Date
2019/03
2019/09
2020/03
2020/09
TCCON, all retrievals
GOSAT-2, single soundings
TCCON, daily averages
GOSAT-2, daily averages
Lamont
XCO2 (ppm)
Date
TCCON, all retrievals
GOSAT-2, single soundings
TCCON, daily averages
GOSAT-2, daily averages
Lauder
XCO2 (ppm)
Date
TCCON, all retrievals
GOSAT-2, single soundings
TCCON, daily averages
GOSAT-2, daily averages

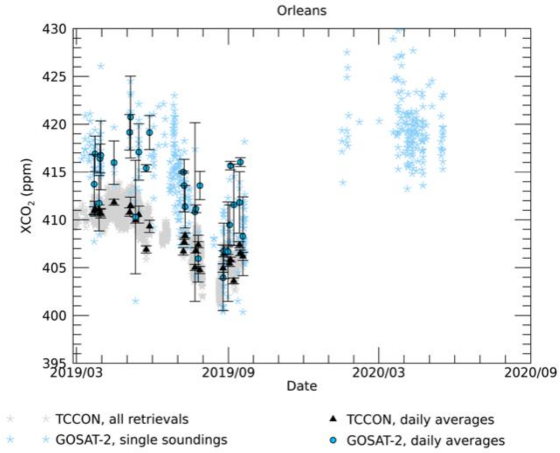
Orleans
430
425
420
415
410
405
400
395
XCO$_2$ (ppm)
2019/03
2019/09
2020/03
2020/09
Date
TCCON, all retrievals
GOSAT-2, single soundings
TCCON, daily averages
GOSAT-2, daily averages

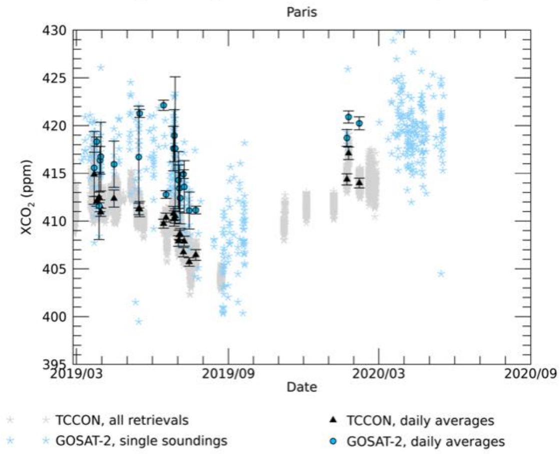
Paris
430
425
420
415
410
405
400
395
XCO$_2$ (ppm)
2019/03
2019/09
2020/03
2020/09
Date
TCCON, all retrievals
GOSAT-2, single soundings
TCCON, daily averages
GOSAT-2, daily averages

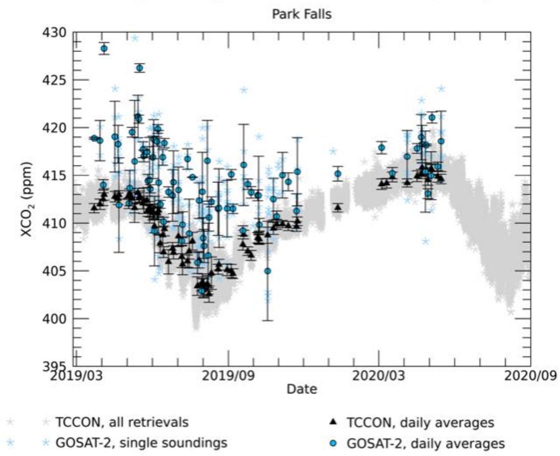
Park Falls
430
425
420
415
410
405
400
395
XCO$_2$ (ppm)
2019/03
2019/09
2020/03
2020/09
Date
TCCON, all retrievals
GOSAT-2, single soundings
TCCON, daily averages
GOSAT-2, daily averages

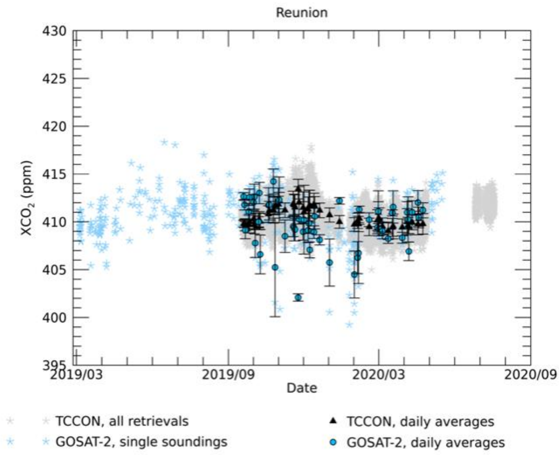
Reunion
XCO$_2$ (ppm)
Date
TCCON, all retrievals
GOSAT-2, single soundings
TCCON, daily averages
GOSAT-2, daily averages

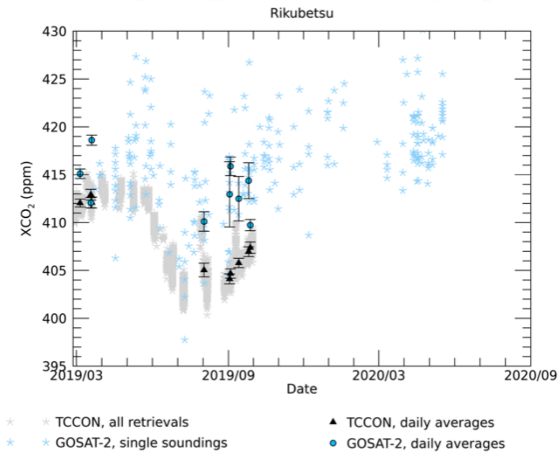
Rikubetsu
XCO$_2$ (ppm)
Date
TCCON, all retrievals
GOSAT-2, single soundings
TCCON, daily averages
GOSAT-2, daily averages

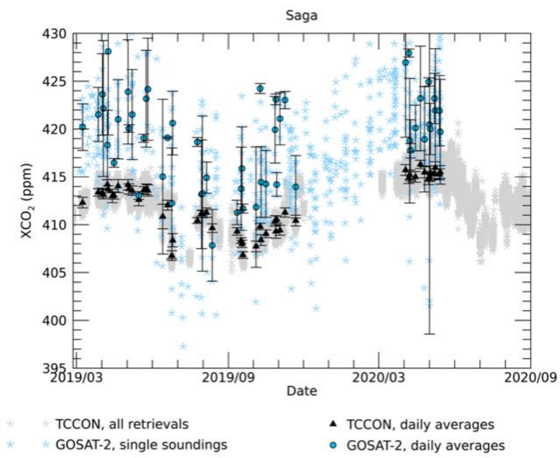
Saga
XCO$_2$ (ppm)
Date
TCCON, all retrievals
GOSAT-2, single soundings
TCCON, daily averages
GOSAT-2, daily averages

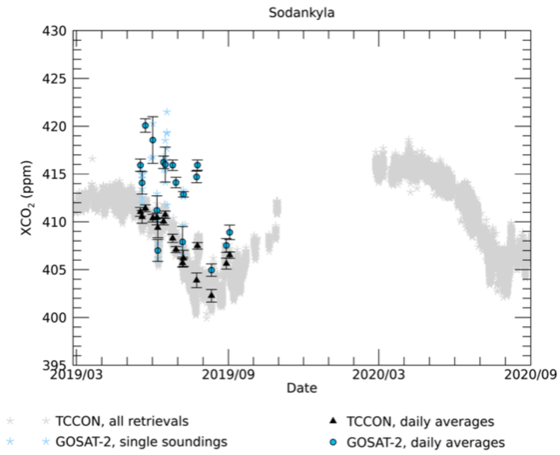
Sodankyla
430
425
420
415
410
405
400
395
XCO2 (ppm)
2019/03
2019/09
2020/03
2020/09
Date
TCCON, all retrievals
GOSAT-2, single soundings
TCCON, daily averages
GOSAT-2, daily averages

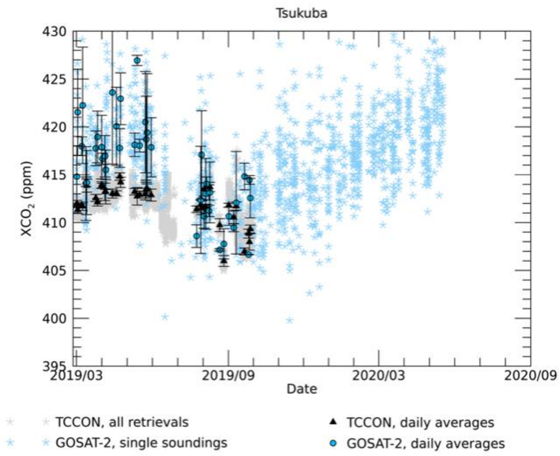
Tsukuba
430
425
420
415
410
405
400
395
XCO2 (ppm)
2019/03
2019/09
2020/03
2020/09
Date
TCCON, all retrievals
GOSAT-2, single soundings
TCCON, daily averages
GOSAT-2, daily averages

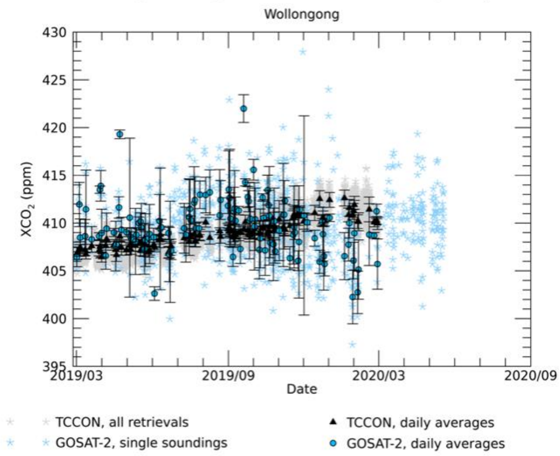
Wollongong
430
425
420
415
410
405
400
395
XCO2 (ppm)
2019/03
2019/09
2020/03
2020/09
Date
TCCON, all retrievals
GOSAT-2, single soundings
TCCON, daily averages
GOSAT-2, daily averages

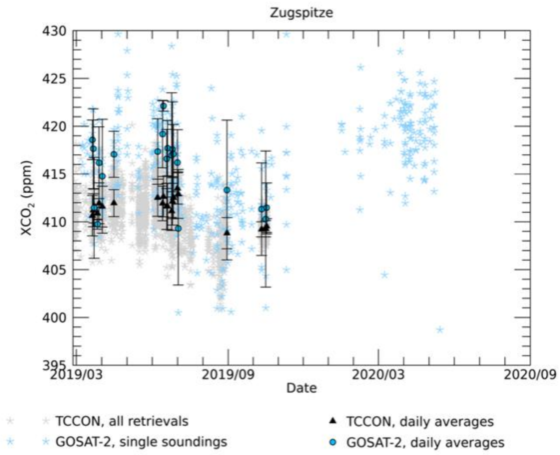

Figure 5: the evaluation of the daily-averaged XCO_2 from GOSAT-2 NIES v01.04 against TCCON GGG2014 at individual TCCON sites. Single soundings are presented in addition to daily mean values.

3.2 Comparisons with other satellite XCO_2 data products

The operational GOSAT-2 XCO_2 data product, i.e., product CO2_GO2_NIES, version 01.04, has been compared with the other satellite XCO_2 data products listed in Table 1.

For comparison all products have been averaged (gridded) to compute monthly maps at a spatial resolution of 5ºx5º.

For product CO2_GO2_NIES and August 2019 the corresponding maps are shown in Figure 6. This figure shows the spatial pattern of XCO_2 (top left), its reported uncertainty (top right), the number of observations per grid cell (bottom left) and the XCO_2 standard deviation (bottom right). One can see, for example, that the reported uncertainty, which is about 0.5 ppm, is much smaller compared to the standard deviation, which is about 2.3 ppm. This indicates that the reported uncertainty is too optimistic (see also Table 2 and the related discussion).

This large difference between the reported uncertainty and the scatter of the data is not observed for any of the other products shown in Figure 7 - Figure 9. These products are however spatially much sparser, especially product CO2_GO2_FOCA (Figure 8). Product CO2_GO2_FOCA is the very first GOSAT-2 product obtained with the FOCAL algorithm and needs to be significantly improved to obtain better coverage over land; note that so far FOCAL algorithm development focussed on GOSAT product CO2_GOS_FOCA (Figure 9).

The comparison results in terms of mean values and standard deviations in 30º latitude bands are shown in Figure 10 - Figure 12. As can be seen, product CO2_GO2_NIES (thick red dots and solid lines) often differs from the other products in terms of a high bias and large scatter, a finding that is consistent with the TCCON validation results shown in Table 2.

Overall, we conclude that there is need and also room to improve the quality of product CO2_GO2_NIES, version 01.04, which is the first NIES GOSAT-2 XCO_2 product released to the public. Probably product quality can be improved by implementing a stricter quality filtering procedure and to also implement and appropriate bias correction procedure.

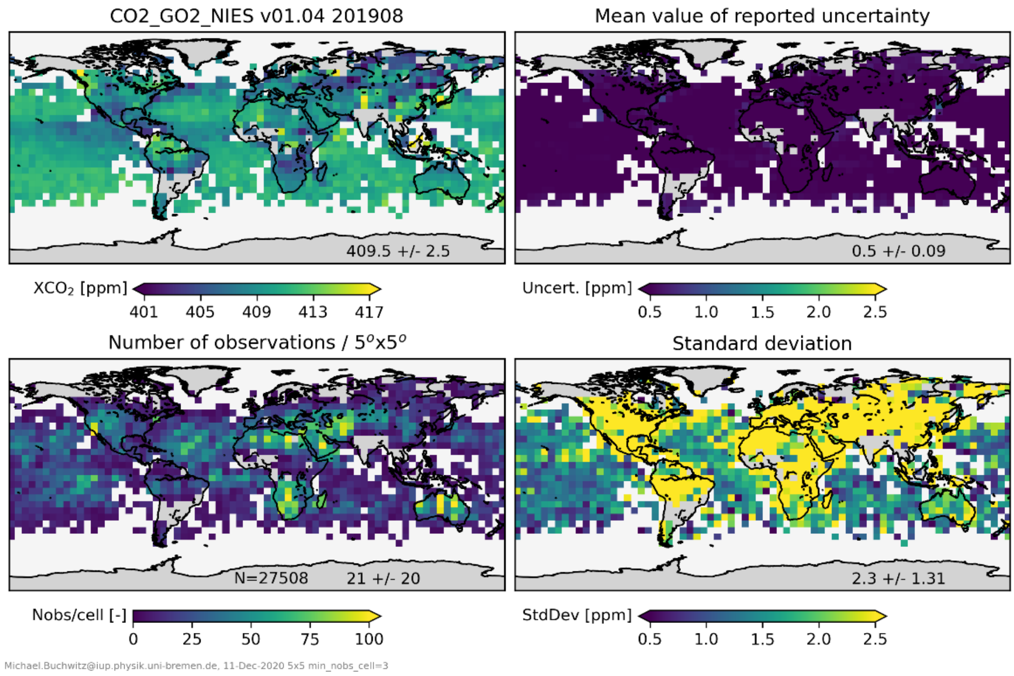

Figure 6: gridded maps at 5°x5° spatial resolution as computed from the Level 2 CO2_GO2_NIES product files for August 2019. Top left: XCO_2. Top right: mean values of reported XCO_2 uncertainty. Bottom left: Number of observations per 5°x5° grid cell. Bottom right: XCO_2 standard devation.

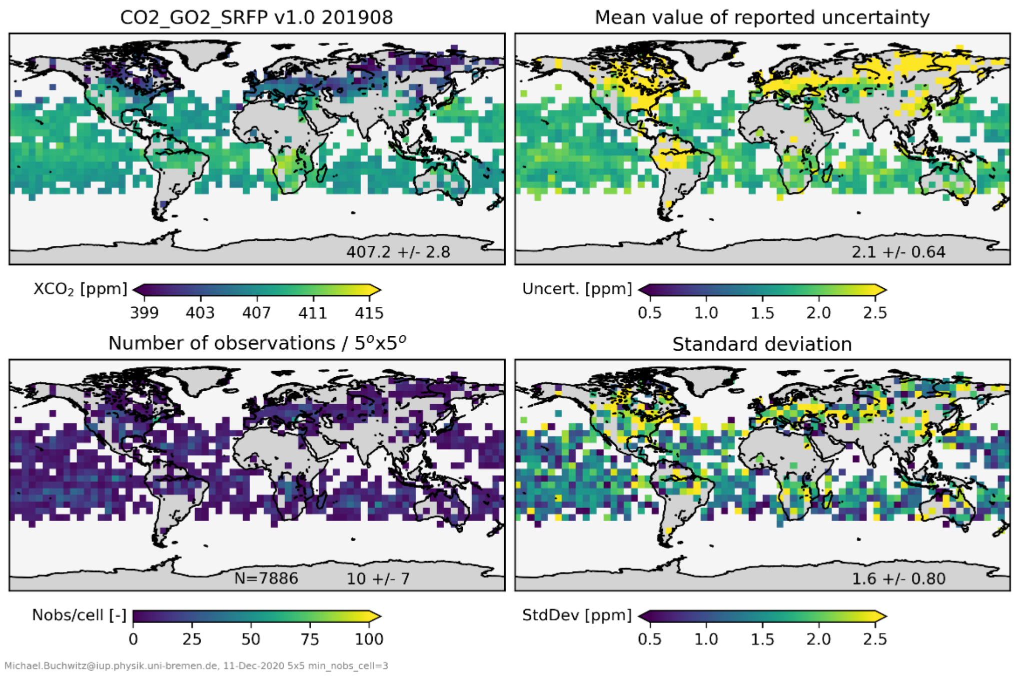

Figure 7: as Figure 6 but for product CO2_GO2_SRFP.

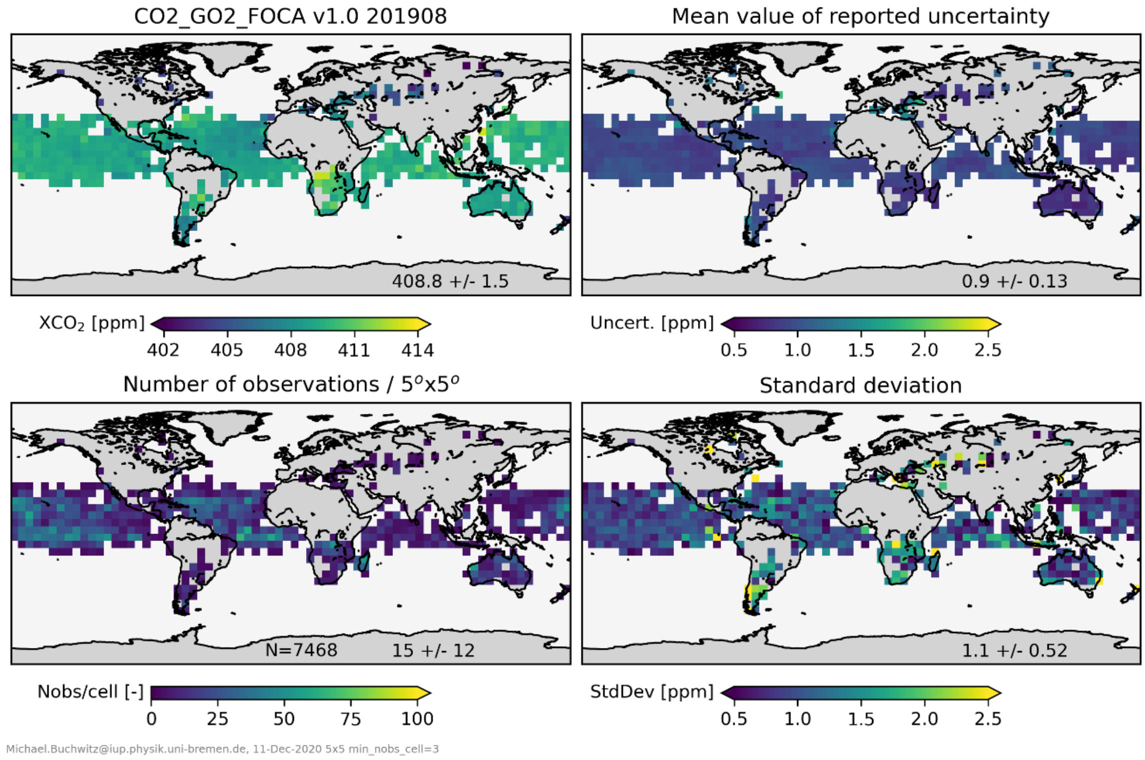

Figure 8: as Figure 6 but for product CO2_GO2_FOCA.

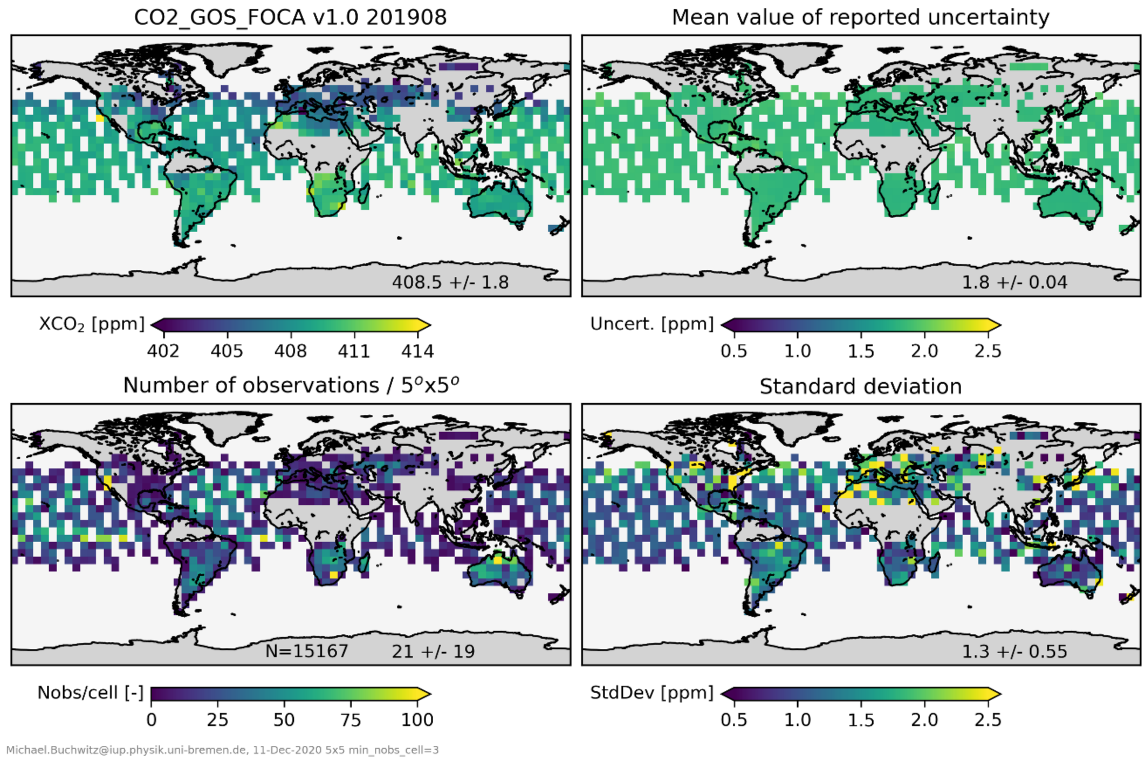

Figure 9: as Figure 6 but for product CO2_GOS_FOCA.

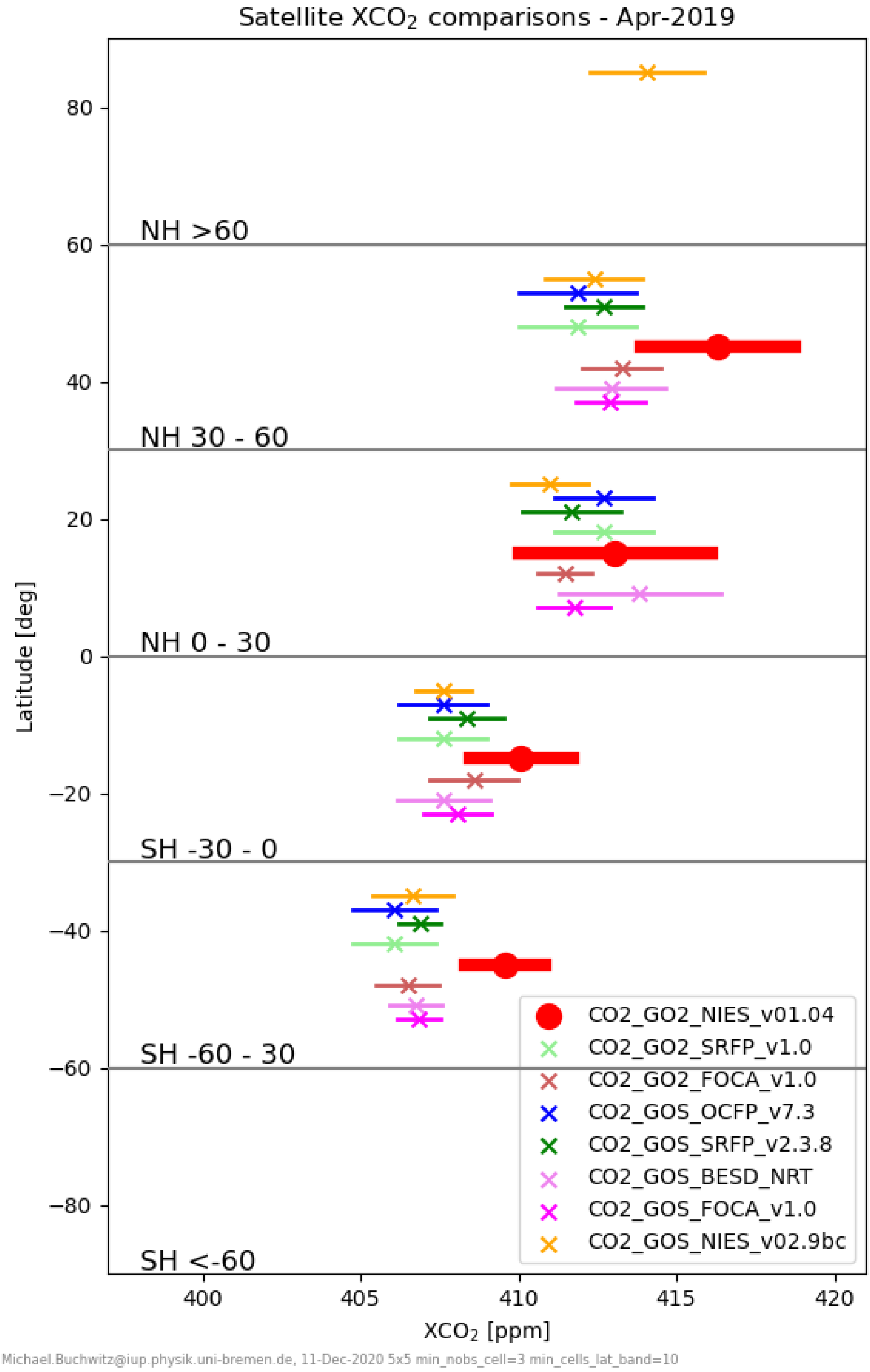

Figure 10: comparison of product CO2_GO2_NIES (thick red dots and solid lines) with the other satellite data products in 30º latitude bands.

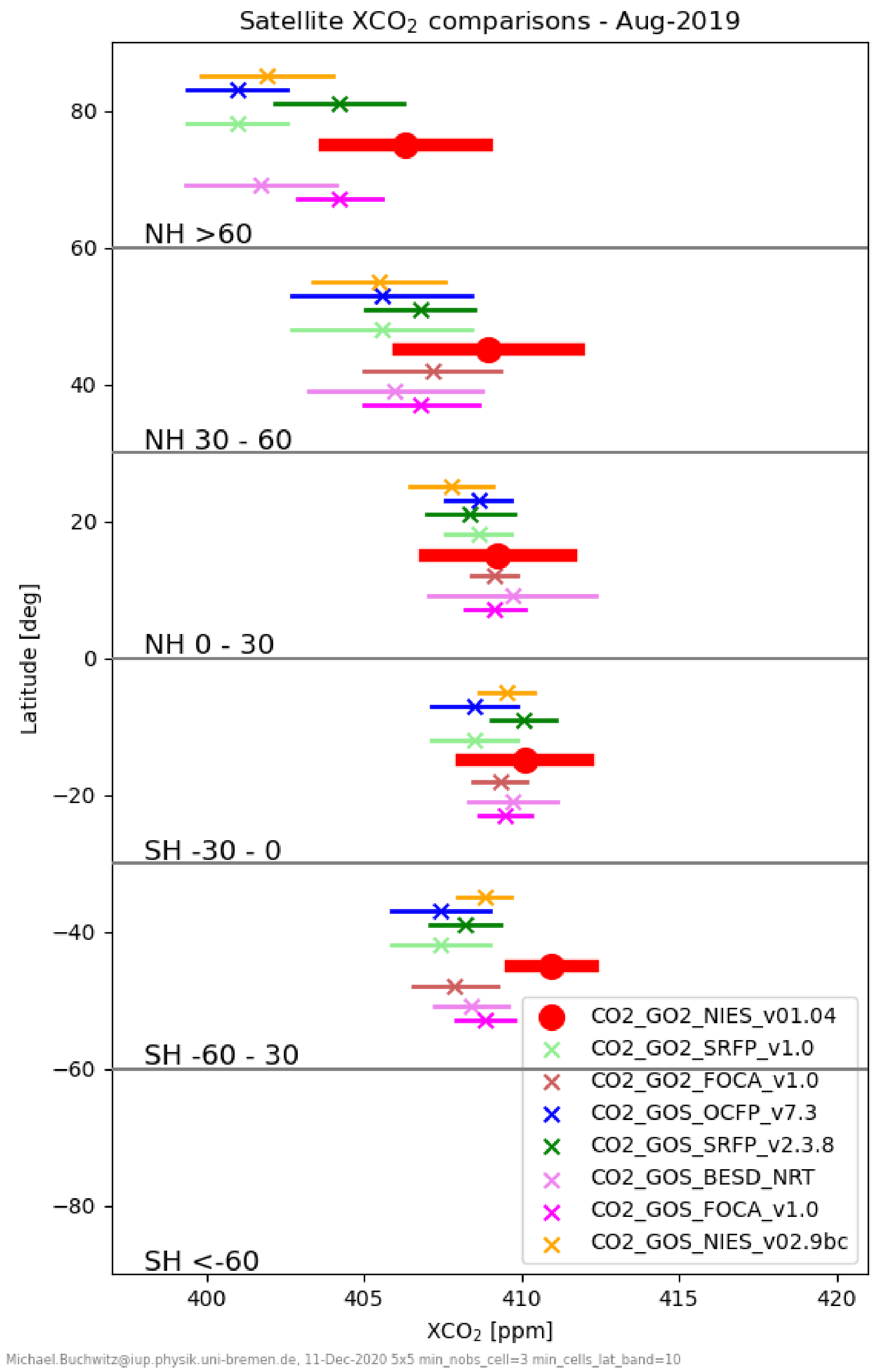

Figure 11: as Figure 10 but for August 2019.

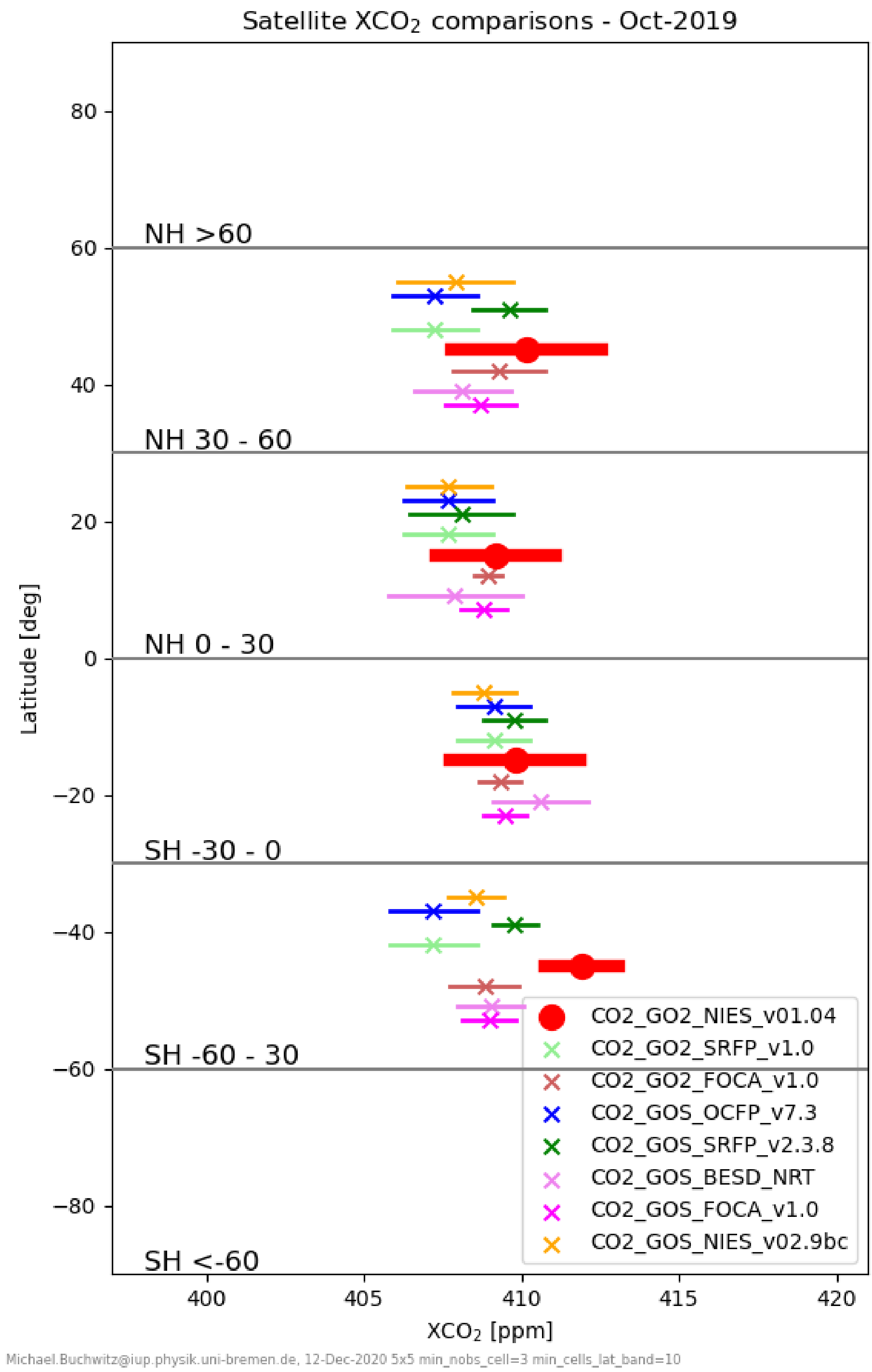

Figure 12: as Figure 10 but for October 2019.

3.3 Comparisons with ground-based TCCON GOSAT-2 XCH4

The operational GOSAT-2 XCH_4 Level 2 product (GOSAT-2 NIES XCH_4 v01.04) was evaluated against 22 ground-based FTS instruments in the TCCON. The product was available for the period 1.3.2019–18.5.2020, similarly to XCO_2. The spatiotemporal co-location criteria for the evaluation were same-day soundings within 2.5 degrees in latitude and 5.0 degrees in longitude. Product quality flags of QF = 0 (good) and QF = 1 (fair) were included in the evaluation. We present an evaluation of the daily mean values which mostly correspond to overpass-averaged statistics.

The biases for daily averaged GOSAT-2 XCH_4 against 22 ground-based FTS as well as the standard deviations are listed in Table 4 and also presented in Figure 13. Bias in the GOSAT-2 XCH_4 NIES v01.04 product varies generally between -23.2 – 21 ppb against different TCCON instruments. This corresponds to smaller than 1.3% relative errors. An outlier is Zugspitze with a bias of 47.3 ppb, comparable to the high XCH_4 bias found for GOSAT at the same site. Precision (1-sigma) varies between 10.4 – 23.1 ppb. Figure 13shows that the bias is systematically positive globally, with six exceptions where the bias is negative at the Southern and lower Northern latitudes. The resulting statistics show significant improvement over the earlier product evaluation (NIES v01.00) presented in the last report. Still, similarly to our evaluation on GOSAT-2 XCO_2, the product is statistically not yet as mature as the GOSAT-1 product.

In addition to the evaluation of the bias, an attempt was made to evaluate the seasonal cycle amplitude and the growth rate. However, the temporal data coverage was not yet sufficiently long for this purpose. Nevertheless, we present the individual site time series in **Figure 14**. These help to analyse the quality of data more systematically at the single-site level. It is seen from **Figure 14**that the single GOSAT-2 XCH_4 observations are scattered comparably to the TCCON observations. Obvious seasonal biases are not identified due to the significant gaps in the data, although the existence of seasonal biases cannot yet be reliably excluded, either.

Table 4: evaluation of GOSAT-2 NIES v01.04 XCH_4 against XCH_4 of ground-based Fourier Transform Spectrometers in the Total Carbon Column Observing Network (TCCON) sites, using the GGG2014 retrieval. The table shows the mean bias (GOSAT-2 – TCCON; in ppb), the relative bias (in %) and the standard deviation (STD; in ppb) at a given site.

TCCON site	#days	Bias	Rel. b. %	STD	TCCON site	#days	Bias	Rel. b. %	STD
Bremen	8	8.1	0.4	10.4	Lauder	108	6.7	0.4	12.2
Burgos	38	-9.6	-0.5	22.4	Orleans	28	12.1	0.7	15
Caltech	152	-6	-0.3	13.1	Paris	23	10.2	0.6	14.1
Darwin	54	-23.2	-1.3	11.9	Park Falls	83	12.7	0.7	16.6
East Trout Lake	46	10	0.5	19	Reunion	54	-14.9	-0.8	11.7
Edwards	175	3.6	0.2	14.8	Rikubetsu	9	14.8	0.8	20.8
Eureka	7	1.2	0.1	19.4	Saga	53	17.2	0.9	18.2
Garmisch	23	21	1.1	23.1	Sodankylä	17	11.2	0.6	16
Izana	69	15.5	0.8	18.7	Tsukuba	40	2.8	0.2	18.8
Karlsruhe	48	12.7	0.7	13.1	Wollongong	118	-7.9	-0.4	14.8
Lamont	116	-14.2	-0.8	13.5	Zugspitze	21	47.3	2.6	20.2

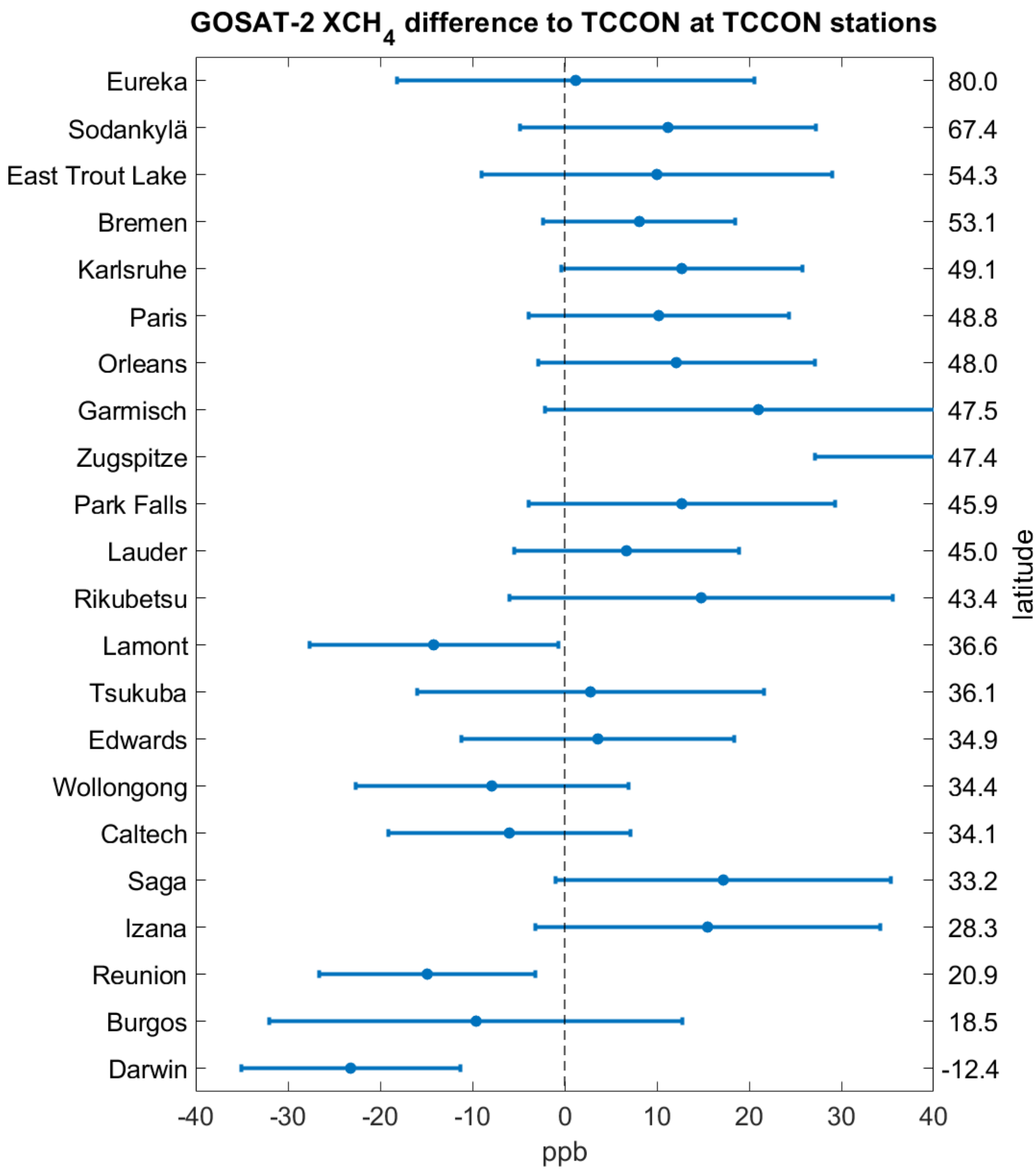

Figure 13: the accuracy and precision of GOSAT-2 NIES v01.04 XCH_4 at the TCCON sites, presented as the mean of GOSAT-2 – TCCON daily-averaged XCH_4. The error bars denote the standard deviation (in ppb). The evaluation sites are organised according to their latitude.

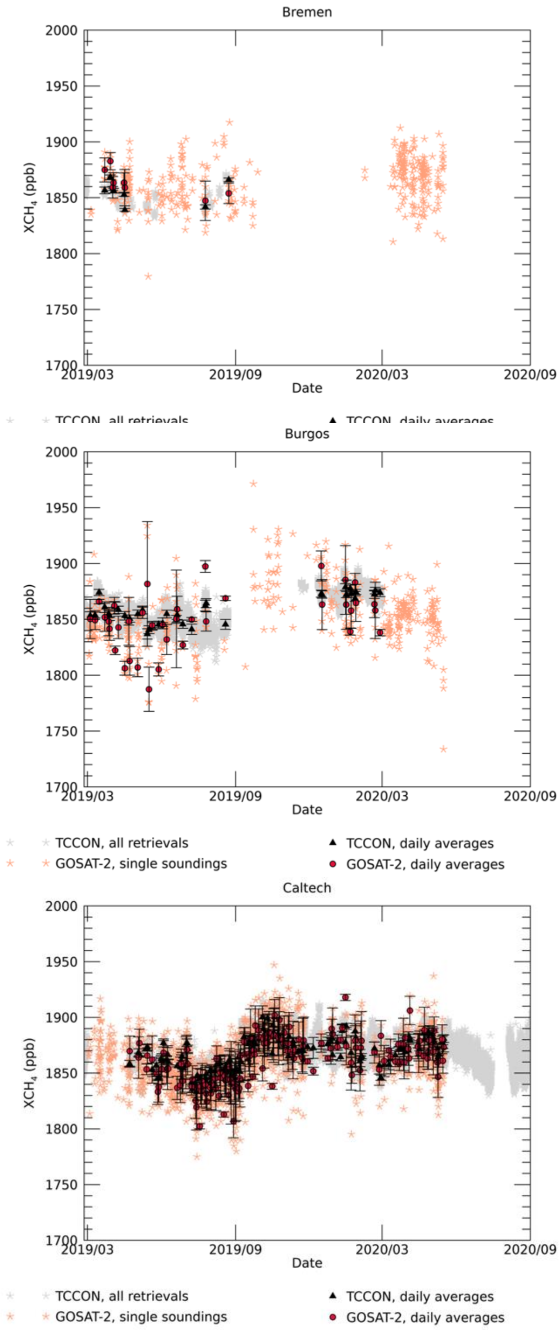
Bremen
2000
1950
1900
1850
1800
1750
1700
XCH4 (ppb)
2019/03
2019/09
2020/03
2020/09
Date
TCCON, all retrievals
TCCON, daily averages
Burgos
XCH4 (ppb)
Date
TCCON, all retrievals
GOSAT-2, single soundings
TCCON, daily averages
GOSAT-2, daily averages
Caltech
XCH4 (ppb)
Date
TCCON, all retrievals
GOSAT-2, single soundings
TCCON, daily averages
GOSAT-2, daily averages

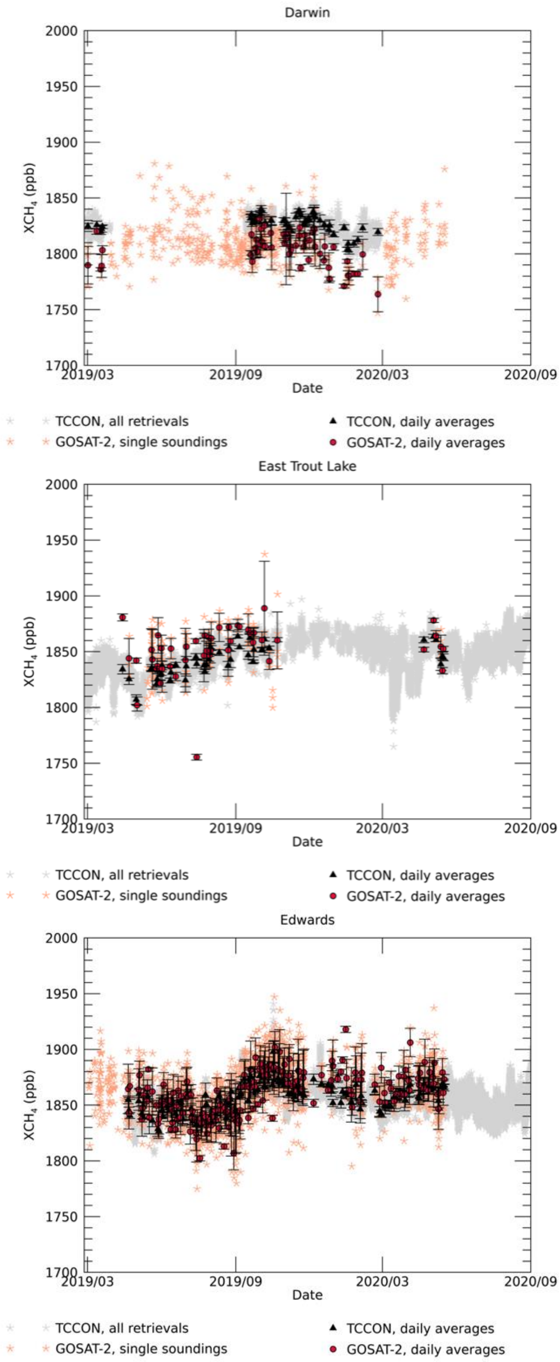
Darwin
XCH4 (ppb)
Date
TCCON, all retrievals
GOSAT-2, single soundings
TCCON, daily averages
GOSAT-2, daily averages
East Trout Lake
Edwards
2019/03
2019/09
2020/03
2020/09

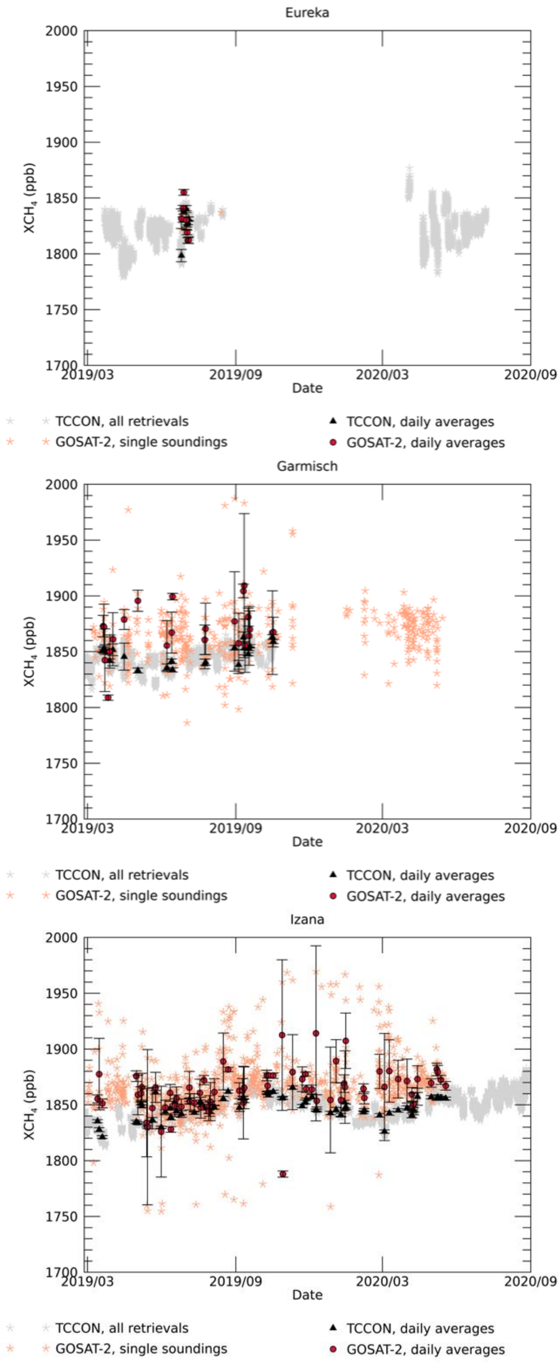
Eureka
XCH4 (ppb)
Date
TCCON, all retrievals
GOSAT-2, single soundings
TCCON, daily averages
GOSAT-2, daily averages
Garmisch
XCH4 (ppb)
Date
TCCON, all retrievals
GOSAT-2, single soundings
TCCON, daily averages
GOSAT-2, daily averages
Izana
XCH4 (ppb)
Date
TCCON, all retrievals
GOSAT-2, single soundings
TCCON, daily averages
GOSAT-2, daily averages

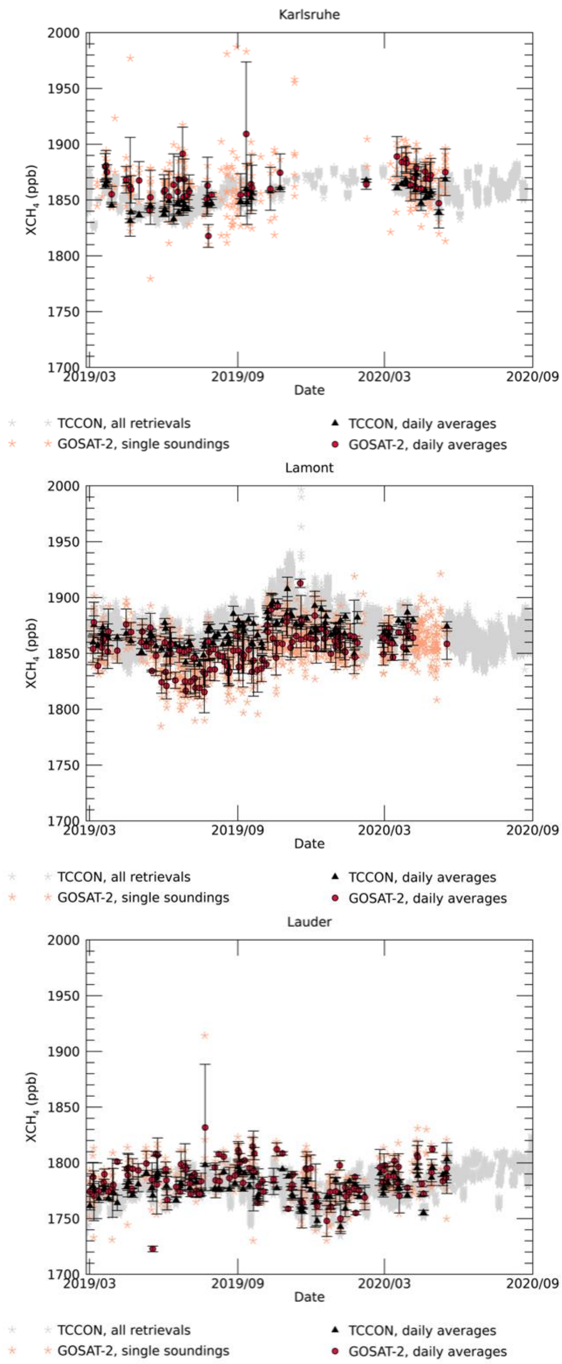
Karlsruhe
XCH$_4$ (ppb)
Date
TCCON, all retrievals
GOSAT-2, single soundings
TCCON, daily averages
GOSAT-2, daily averages
Lamont
XCH$_4$ (ppb)
Date
TCCON, all retrievals
GOSAT-2, single soundings
TCCON, daily averages
GOSAT-2, daily averages
Lauder
XCH$_4$ (ppb)
Date
TCCON, all retrievals
GOSAT-2, single soundings
TCCON, daily averages
GOSAT-2, daily averages

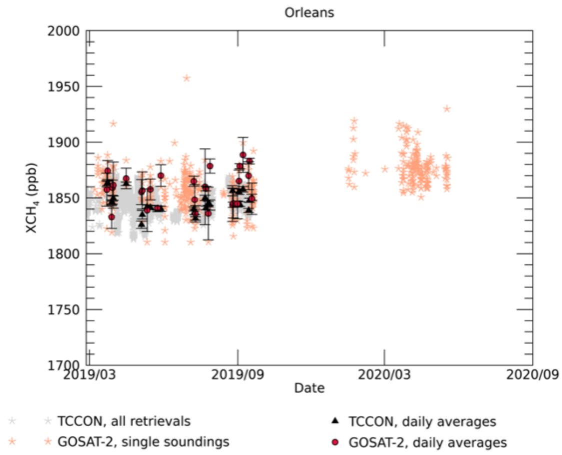
Orleans
2000
1950
1900
1850
1800
1750
1700
XCH4 (ppb)
2019/03
2019/09
2020/03
2020/09
Date
TCCON, all retrievals
GOSAT-2, single soundings
TCCON, daily averages
GOSAT-2, daily averages

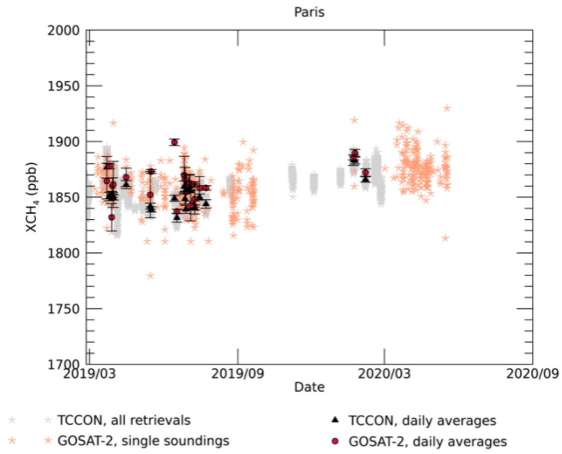
Paris
2000
1950
1900
1850
1800
1750
1700
XCH4 (ppb)
2019/03
2019/09
2020/03
2020/09
Date
TCCON, all retrievals
GOSAT-2, single soundings
TCCON, daily averages
GOSAT-2, daily averages

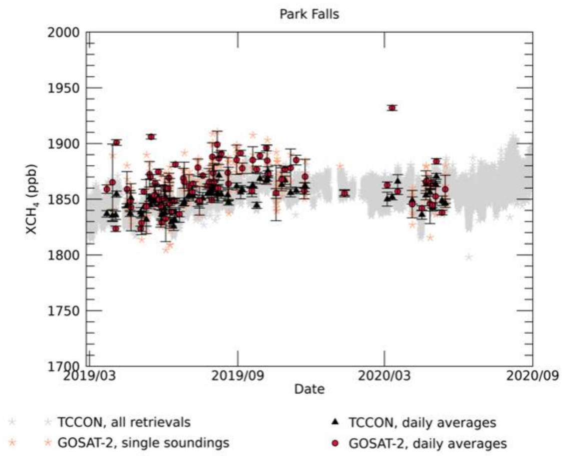
Park Falls
2000
1950
1900
1850
1800
1750
1700
XCH4 (ppb)
2019/03
2019/09
2020/03
2020/09
Date
TCCON, all retrievals
GOSAT-2, single soundings
TCCON, daily averages
GOSAT-2, daily averages

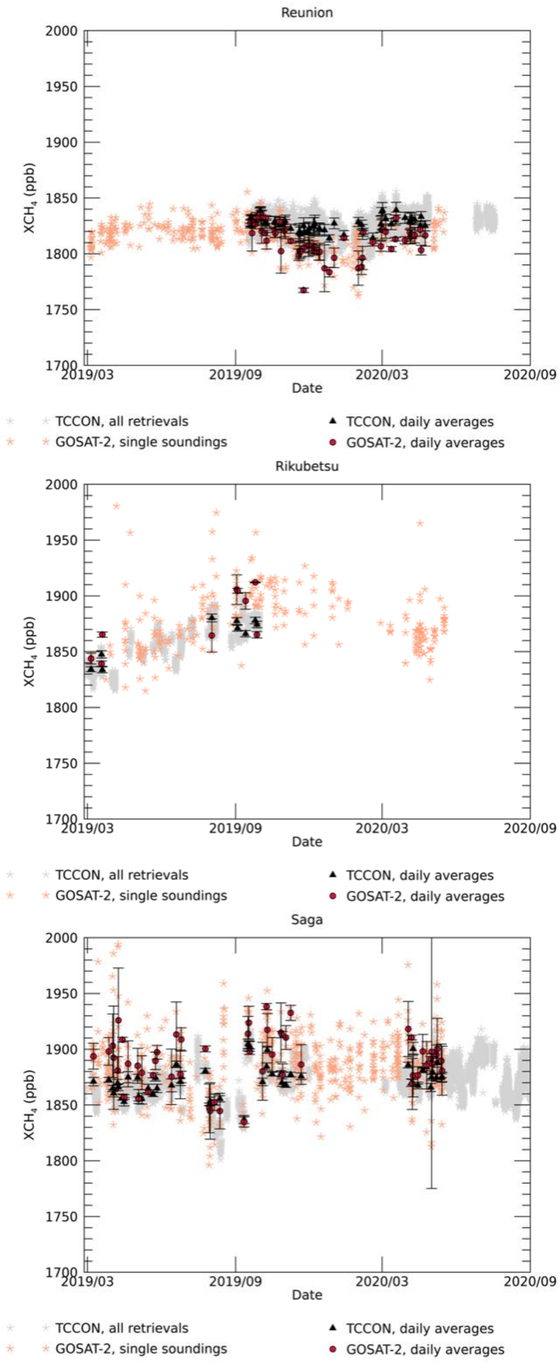
Reunion
XCH4 (ppb)
Date
2019/03
2019/09
2020/03
2020/09
TCCON, all retrievals
GOSAT-2, single soundings
TCCON, daily averages
GOSAT-2, daily averages
Rikubetsu
XCH4 (ppb)
Date
TCCON, all retrievals
GOSAT-2, single soundings
TCCON, daily averages
GOSAT-2, daily averages
Saga
XCH4 (ppb)
Date
TCCON, all retrievals
GOSAT-2, single soundings
TCCON, daily averages
GOSAT-2, daily averages

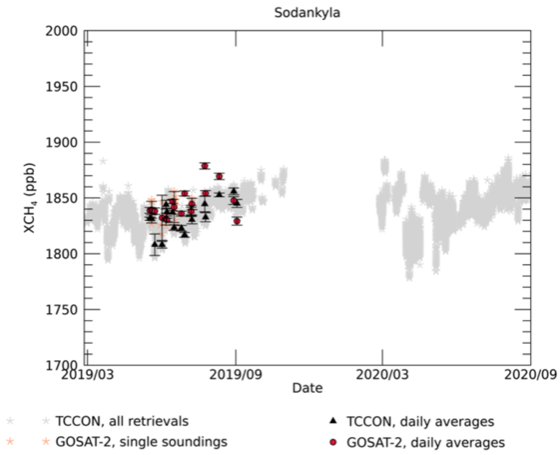
Sodankyla
XCH4 (ppb)
Date
TCCON, all retrievals
GOSAT-2, single soundings
TCCON, daily averages
GOSAT-2, daily averages

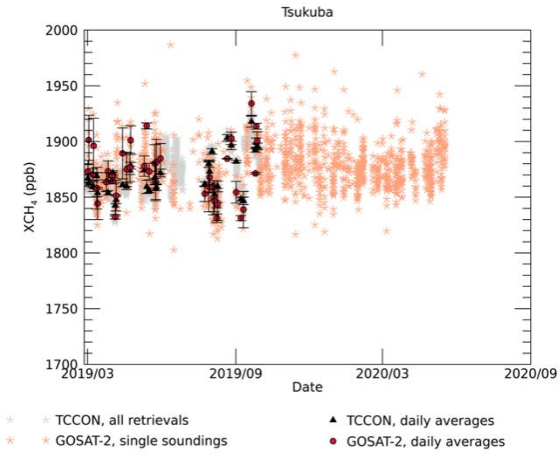
Tsukuba
XCH4 (ppb)
Date
TCCON, all retrievals
GOSAT-2, single soundings
TCCON, daily averages
GOSAT-2, daily averages

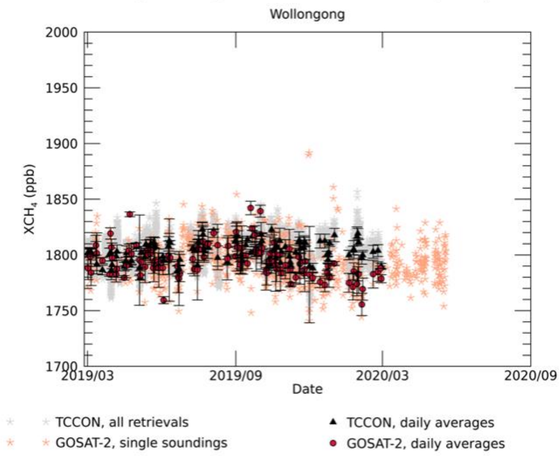
Wollongong
XCH4 (ppb)
Date
TCCON, all retrievals
GOSAT-2, single soundings
TCCON, daily averages
GOSAT-2, daily averages

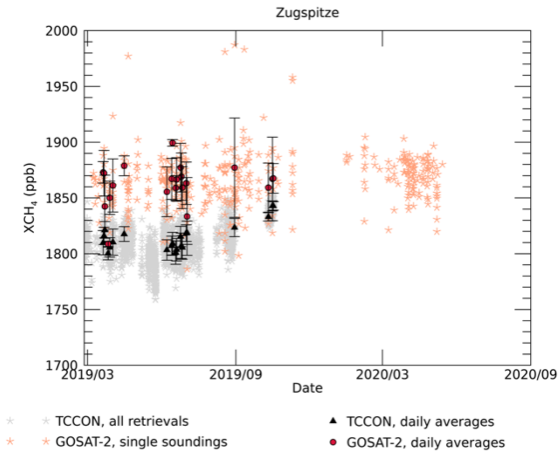

Figure 14: The evaluation of the daily-averaged XCH_4 from GOSAT-2 NIES v01.04 against TCCON GGG2014 at individual TCCON sites. Single soundings are presented in addition to daily mean values.

3.4 GOSAT-2 RemoTeC Quality Assessment

The RemoTeC full-physics GOSAT-2 retrieval approach simultaneously infers gas concentrations and scattering properties of the atmosphere in order to model the light path through the Earth's atmosphere. There- fore, RemoTeC aims at retrieving the CH4 vertical profile (with slightly more than 1 degree of freedom) and 3 scattering parameters characterising the particle amount, size and height using multiple spectral bands. Particle amount is represented through the total column number density of particles. The algorithm is fully flexible concerning the selected spectral measurement bands.

An alternative approach to the full-physics type retrieval method is the light path proxy method introduced by [1]. The proxy method is conceptually simple since it relies on non-scattering retrievals of the CH4 and CO2 total column from spectrally close absorption bands such as covered by the SWIR-1 channel around 1.6 µm. Under the assumption that scattering and calibration induced errors are the same for the spectrally close absorption bands, scattering induced errors cancel in the [CH4]/[CO2] ratio and XCH4 can be calculated via

$$XCH_4 = \frac{[CH_4]}{[CO_2]} \times XCO_2^{mod}, \qquad (1)$$

where XCOmod is the column-averaged dry air mole fraction of CO2, which we take from the Carbon Tracker model [2]. A comparison between the full-physics and proxy approach using GOSAT measurements was presented by [3] and [4]. Note that the proxy method cannot be applied to TROPOMI measurements, because there is no suitable light-path proxy for CH4 in the 2.3 µm band. The Tropospheric Monitoring Instrument (TROPOMI) is the single payload of the Copernicus Sentinel- 5 Precursor (S5P) satellite that was launched by the European Space Agency (ESA) on 13 October 2017.

The instrument provides spectral measurements of the solar radiance reflected by Earth and its atmosphere in the ultraviolet-visible (UV-VIS, 270-495 nm), near-infrared (NIR, 675-775 nm), and the shortwave-infrared (SWIR, 2305-2385 nm) ([5]). The novelty of the mission is the daily global coverage, the high spatial resolution of 3.5 x 7 km^2 or 7x 7 km^2 depending on spectral range, and the higher signal-to-noise ratio (SNR). One of the primary goals of the mission is to measure the dry air column mixing ratio XCH4 of methane in the 2.2 µm band. The observation strategy relies on measuring spectra of sunlight, backscattered by the Earth's surface and the atmosphere.

The spectroscopic absorption by CH4 in the 2.3 µm band allows for the retrieval of its atmospheric abundance provided that the lightpath is accurately known. Scattering by aerosol and cirrus particles can modify the lightpath resulting in retrieval errors if not accounted for. For TROPOMI measurements, we employ the so-called full-physics method. Implemented in the RemoTeC software package [6, 4, 7, 8, 9], the approach uses TROPOMI radiance observations in the NIR and SWIR for CH4 retrievals to minimise these errors by simultaneously retrieving CH4 column concentrations and scattering properties of the atmosphere. The fitted parameters are the partial CH4 columns in twelve atmospheric layers, the total columns of water and carbon monoxide, two scattering parameters (total column of aerosol particles and aerosol layer centre height), the surface albedo (up to second-order spectral dependence), and wavelength shifts in Earth radiance and solar irradiance spectra. A detailed description of the operational algorithm is given by ([8]).

The accuracy requirement for the S5P XCH4 column mixing ratio product has originally been formulated as 2% uncertainty [10]. Veefkind et al., 2012 [5] modified this requirement to 2% accuracy and 0.6% precision (defined as the contribution of purely instrument noise). Applicable for this study are the requirement provided in [11] with a bias of 1% and a precision of 1%.

From the 1% bias 0.6% is reserved for instrument related errors and 0.8% for forward model errors. It is also important to keep in mind the performance of the Japanese GOSAT-1 satellite, launched 2009, which sets the current benchmark for methane retrievals from space. Performing GOSAT-1 methane retrievals using the same algorithm as the S5P prototype algorithm [3, 4], for methane we achieve a precision of 0.8% per individual measurement and a relative accuracy (between regions) of 0.25%.

In this study an updated version of the scientific GOSAT-2 XCH4full physics and proxy data product from SRON has been presented. The full GOSAT-2 L1 dataset with the new version of the retrieval code has been processed and validated it with the XCH44 measurements of TCCON network. Furthermore, the retrieval is inter-compared with the XCH4measurements of GOSAT-1 and TROPOMI. In the following sections an overview about the updates to the GOSAT-2 retrieval has provided. The validation with TCCON is given and the inter-comparison with GOSAT-1 and TROPOMI is discussed.

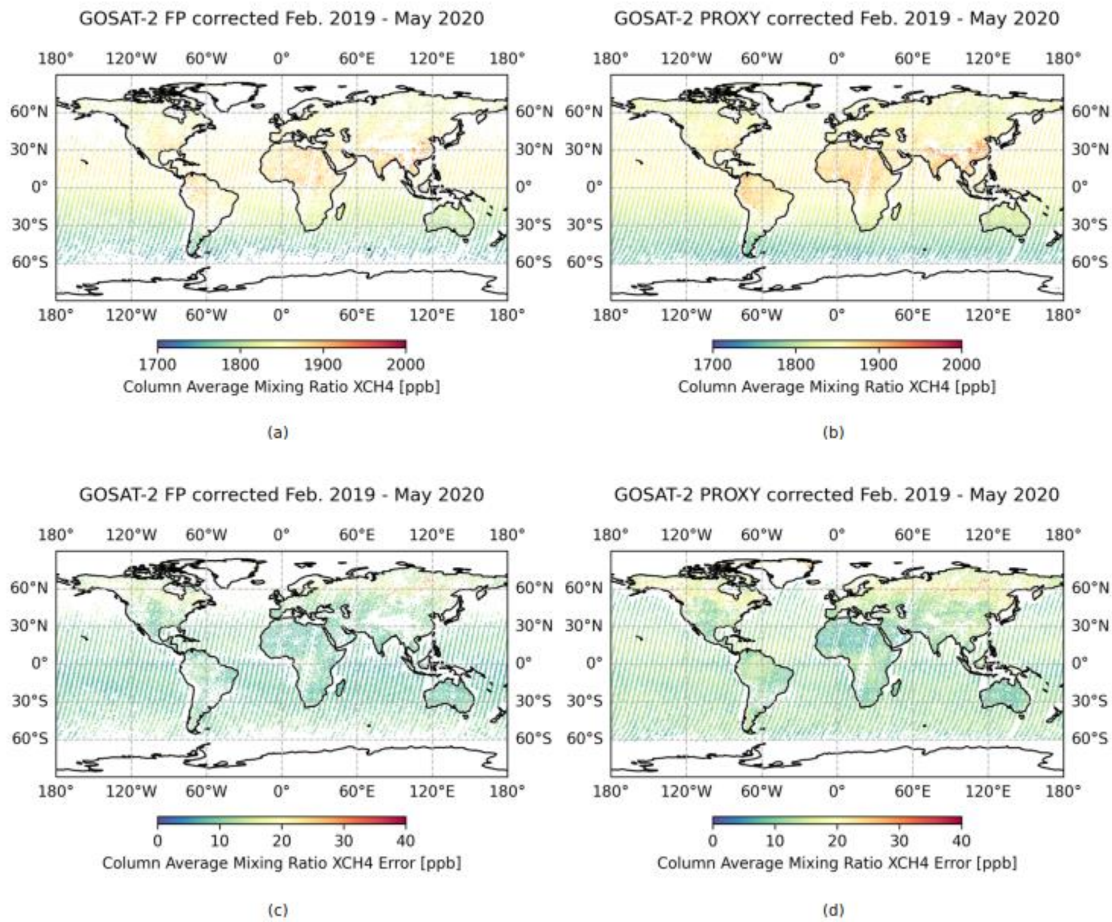

Figure 15: global GOSAT-2 XCH4distribution averaged between February 2019 and May 2020 on a 0.5 º x 0.5º resolution. (a) XCH4 proxy, (c) XCH4 proxy estimate, (b) XCH4 full physics, (e) XCH4 full physics error estimate.

3.4.1 GOSAT-2 Dataset

Figure 15 (b) shows the XCH4 full physics product that is retrieved from GOSAT-2 TANSO-FTS SWIR spectra using the RemoTeC algorithm [6, 4, 7, 8, 9]. The algorithm retrieves simultaneously XCH4 and XCO2. For the retrieval, we analyse four spectral regions: the 0.77 µm oxygen band, two CO2 bands at 1.61 and 2.06 µm, and a CH4 band at 1.64 µm. Within the retrieval procedure the sub-columns of CO2 and CH4 in different altitude layers are being retrieved. To obtain the column averaged dry air mixing ratios XCO2 and XCH4, the sub-columns are summed up to get the total column which is divided by the dry-air columns obtained from the surface pressure of the ECMWF model data in combination with a surface elevation data base. A small difference between the GOSAT-1 and -2 retrievals is that the GOSAT-2 retrieval uses a slightly shortened retrieval window for the O2-A Band as described in the ATBD document [12].

The methane full physics retrieval relies on strict cloud filtering of the observation. Currently, RemoTeC uses a cloud filter based on SWIR measurements for cloud clearing of GOSAT-1 observations. Here, we retrieve CH4 and H2O columns from weak and strong absorption bands in the SWIR channel assuming a non- scattering atmosphere. The difference in columns of the same trace gas retrieved from different bands in- creases with increasing cloud optical thickness and/or cloud fraction. Hence, it can be used for cloud filtering in a pre-processing step. Finally, the RemoTeC full physics data product consists of the dry air total column mol fraction XCH4, its noise estimate, the column-averaging kernel and the CH4 a priori information.

Figure 15 (a) shows the XCH4 proxy product that is retrieved from GOSAT-2 TANSO-FTS SWIR spectra also using the RemoTeC algorithm, which is also used for the GOSAT-1 retrievals. The algorithm infers simultaneously XCH4and XCO2. As the proxy retrievals perform a non-scattering retrieval, the retrieved XCH4column cannot be used directly, as effects of aerosol scattering modify the light path. To correct for this, the retrieved XCH4column is divided by the retrieved XCO2 column at the 1.61 µm band and then multiplied by a XCO2 total column obtained from the Copernicus Atmosphere Monitoring Service (CAMS) v18r2 product.

3.4.1.1 Improved bias correction

All GOSAT-1 and GOSAT-2 data are corrected for biases based on a comparison with TCCON data. Here, our philosophy is to keep the bias correction as simple as possible using a physical retrieved parameter that can explain and correct for most of the observed bias. TCCON measurements are used as the reference for the bias correction. When there are multiple TCCON measurements, data will be averaged. Eq. (2)-(6) show the formula used for the bias correction. Here Eq. (2)-(4) are used for the proxy retrieval while the full set is used for the full physics retrieval. The equations are found by data inspection.

$$XCH_{4,corr} = XCH_{4,raw}(a + b \times sza) \quad (2)$$

$$XCH_{4,corr} = XCH_{4,raw}(a + b \times alb\_win2) \quad (3)$$

$$XCH_{4,corr} = XCH_{4,raw}(a + b \times ratio\_O2) \quad (4)$$

$$XCH_{4,corr} = XCH_{4,raw} \times (a + b \times aer\_filter) \quad (5)$$

$$XCH_{4,corr} = XCH_{4,raw}(a + b \times aer\_filter + c \times sza) \quad (6)$$

where the aerosol filter aer_filter is defined as,

$$\frac{aot\_win1 \times aer\_height}{aer\_size} \quad (7)$$

aot_win1, aer_height (m), and aer_size are the aerosol optical thickness at window 1 (765 nm), aerosol height (m) and aerosol size parameter. sza, alb_win2, and ratio_o2 are the solar zenith angle, surface albedo at window 2 (1593 nm), and ratio of O2, respectively. Coefficients a, b, and c are the subject to be found by the fitting algorithm. Table 2 shows the coefficients and statistics from the bias correction based on the equations above. Further details about the bias correction can be found in [13, 14, 15, 16, 12, 16].

3.4.1.2 Improved post-filtering

The previous filter criteria for the GOSAT-2 retrieval cannot be applied anymore. It would mean that most of the retrieved data were discarded. Therefore, the data filtering required adjustments and this section summarizes the changes of the thresholds for each parameter of the post-filtering. Figure 17 shows the changes of the filter criteria over land and Figure 18over oceans for the full physics and proxy XCH4 retrieval from GOSAT-2, respectively. Further details about the derivation of the filtering approach can be found in [13, 14, 15, 16, 12, 16].

Nr	Parameter	Coefficients			Statistics			
		a	b	C	N_data	Mean_Bias [ppb]	Std_Bias [ppb]	R
#	no-correction	-	-	-	862	-12.96	17.80	0.68
1	aer_filter_sza	1.003625	5.4E-05	-5.7E-05	862	-0.12	16.29	0.72
2	aer_filter	1.001305	5.25E-05	-	862	-0.12	16.36	0.73
3	sza	1.007669	-1.7E-05	-	862	-0.14	17.90	0.68
4	albedo_b2	0.998898	0.016459	-	862	-0.15	17.51	0.71
5	ratio_o2	0.977977	0.029048	-	862	-0.14	17.89	0.68

(a)

Nr	Parameter	Coefficients		Statistics			
		a	b	N_data	Mean_Bias [ppb]	Std_Bias [ppb]	R
#	no-correction	-	-	2534	12.52	16.96	0.78
1	sza	0.991323	4.44E-05	2534	-0.14	16.81	0.78
2	albedo_b2	0.987652	0.012794	2534	-0.14	16.53	0.79
3	ratio_o2	0.967934	0.025596	2534	-0.14	16.80	0.78

(b)

Figure 16: coefficients and statistics of the bias correction (a) full physics approach (b) proxy approach.

Nr.	Criteria	Threshold		Description
		Old	New	
1	n_iter	< 31	< 31	Number of iteration
2	dfs_tar*	> 1	> 1	Degree of freedom
3	xco2_err	< 2.0	< 1.3	XCO2 error [ppm]
4	chi2	< 4.5	< 9	Chi2
5	chi2_win1_tar*	< 8	< 16	Chi2 window 1
6	var_elev	< 80	< 80	Surface elevation [m]
7	snr*	> 50	> 50	Signal to noise ratio
8	sza	< 70	< 75	Solar zenith angle [°]
9	aerosol_filter	0 < x < 300	0 < x < 550	Aerosol filter
10	aot_win1	< 0.6	< 0.3	Aerosol optical thickness at window 1
11	aero_size	3 < x < 5	2 < x < 6	Aerosol size parameter
12	int_offset_o2a	2E-9 < x < 5E-9	Not-applicable	Offset o2a
13	blended_alb	< 0.9	0 < x < 1.5	Blended albedo
14	ratio_co2	0.99 < x < 1.015	0.99 < x < 1.015	Ratio CO2
15	ratio_o2	0.95 < x < 1.02	0.95 < x < 1.02	Ratio O2
16	ratio_h2o	0.95 < x < 1.08	0.95 < x < 1.08	Ratio H2O

Note: * = all window/target.

(a)

Nr.	Criteria	Threshold		Description
		Old	New	
1	n_iter	< 10	< 14	Number of iteration
2	chi2	< 7	< 14	Chi2
3	var_elev	< 150	< 150	Elevation
4	snr	> 50	> 50	Signal to noise ratio
6	sza	< 75	< 75	Solar zenith angle
7	ratio_co2	0.98 < x < 1.15	0.98 < x < 1.15	Ratio CO2
8	ratio_o2	0.88 < x < 1.035	0.88 < x < 1.035	Ratio O2
9	ratio_h2o	0.90 < x < 1.50	0.90 < x < 1.50	Ratio H2O
10	xch4_err	> 1.0	> 1.0	XCH4 non-scattering [ppm]

Note: * = all window/target.

(b)

Figure 17: Filter criteria and corresponding thresholds for measurements overland (a) full physics approach (b) proxy approach.

Nr.	Criteria	Threshold		Description
		Old	New	
1	n_iter	< 31	< 31	Number of iteration
2	dfs_tar*	> 1	> 1	Degree of freedom
3	cirrus_signal	< 8E-10	< 8E-10	Cirrus signal
4	chi2	< 4	< 9	Chi2
5	chi2_win1_tar*	< 4	< 16	Chi2 window 1
6	chi2_win4_tar*	< 10	< 20	Chi2 window 4
7	s_alb_win4	-13E-5 < x < -4.5E-5	Not-applicable	Slope of albedo at window 4
8	int_offset_o2a	1.5E-9 < x < 3.75E-9	Not-applicable	Offset o2a
9	ratio_co2	0.99 < x < 1.01	0.99 < x < 1.015	Ratio CO2
10	ratio_o2	0.965 < x < 1.0	0.95 < x < 1.02	Ratio O2
11	ratio_h2o	0.95 < x < 1.05	0.95 < x < 1.08	Ratio H2O

(a)

Nr.	Criteria	Threshold		Description
		Old	New	
1	n_iter	< 10	< 14	Number of iteration
2	chi2	< 7	< 14	Chi2
3	var_elev	< 150	< 150	Elevation
4	snr	> 50	> 50	Signal to noise ratio
6	sza	< 75	< 75	Solar zenith angle
7	ratio_co2	0.98 < x < 1.15	0.98 < x < 1.15	Ratio CO2
8	ratio_o2	0.88 < x < 1.035	0.88 < x < 1.035	Ratio O2
9	ratio_h2o	0.90 < x < 1.50	0.90 < x < 1.50	Ratio H2O
10	xch4_err	> 1.0	> 1.0	XCH4 non-scattering [ppm]

(b)

Figure 18: filter criteria and corresponding thresholds for measurements over oceans (a) full physics approach (b) proxy approach.

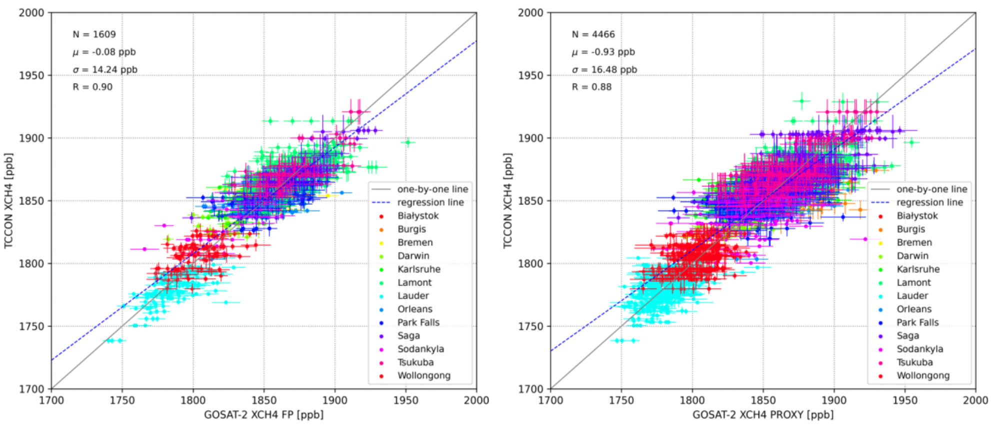

(a) (b)

Figure 19: validation of single soundings of the GOSAT-1 full physics and proxy XCH_4 product with collocated TCCON measurements at all TCCON sites for the period Feb.2019 - May 2020. Numbers in the figures: μ=bias, i.e., average of the difference; σ = single measurement precision, i.e., standard deviation of the difference; N = number of co-locations; R = Pearson correlation coefficient: (left panel a) full physics approach, (right panel b) proxy approach.

3.4.2 Validation

The ground-based FTIR measurements of the TCCON network represent the standard validation source for satellite trace gas retrievals. In 2004 the TCCON network was founded in preparation for the validation of the OCO mission, the first dedicated CO2 satellite mission to be launched. Since then, the network has become the standard for validating satellite-based column measurements of CO2 and CH4 [17, 18]. TCCON is a network of inter-calibrated ground-based Fourier transform spectrometers that measure the absorption in the NIR and SWIR of direct sunlight by trace gas species such as CO2, CH4, CO, HDO, etc. These measurements are much less influenced by atmospheric scattering by cirrus and aerosols than satellite observations of backscattered/reflected sunlight. TCCON XCH4 measurements have been calibrated and validated against the WMO-standard of in-situ measurements using dedicated aircraft campaigns of XCH4 profiles and their resulting accuracy have been estimated to 0.4% (2σ value) [17].

To demonstrate the absolute accuracy of the GOSAT-2 data set, TCCON measurements are compared to collocated GOSAT-1 data at 13 selected sites. Here data are considered as collocated if they are within a latitude/longitude box of ± 2.5° and if the TCCON observation time falls within ± 2 hr of each GOSAT-2 sounding time. Figure 19 shows the validation of single soundings of the GOSAT-1 full physics and proxy XCH4product with collocated TCCON measurements at all TCCON sites. The high data yield of the proxy product compared to the full-physics product is striking.

Furthermore, the agreement between both TCCON and GOSAT-2 observations is specified by the mean bias per station, the standard deviation of the difference, the standard deviation of the station biases (station-to-station bias) and an overall bias averaged over all stations. Figure 20 summaries our findings for GOSAT-2 observations over land and Figure 25 for GOSAT-2 glint retrievals over the oceans. Overall, we can conclude that the RemoTeC GOSAT-2 XCH4data product agrees well with the measurements of the TCCON network. The global mean bias between TCCON and GOSAT-2 is -0.34 ppb and -0.06 ppb for the full-physics and proxy product, a corresponding mean scatter is 13.61 ppb and 16.15 ppb with a station-to-station bias of 1.94 ppb and 2.63 ppb, respectively.

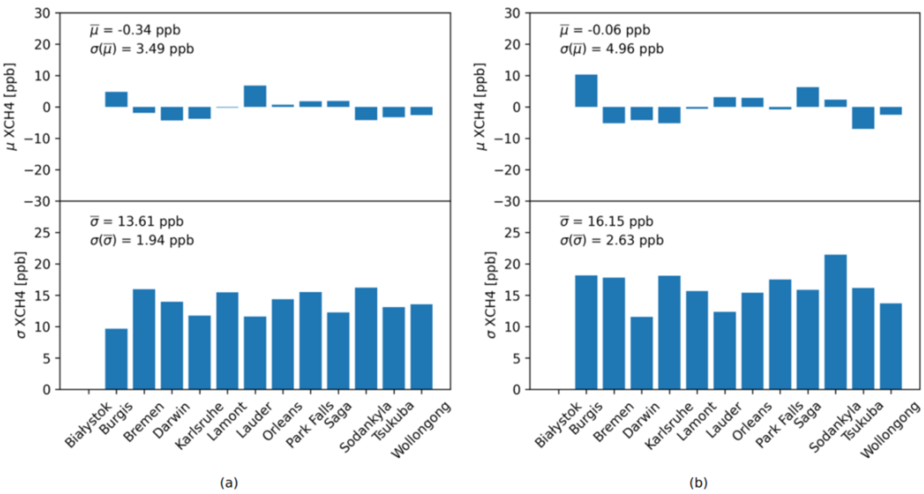

Figure 20: validation statistics bias (top panel) and scatter (lower panel) per TCCON site for land observation (bias corrected). The summarizing values represent the standard deviation of the site biases and the average scatter relative to TCCON. Figure (a) full physic approach, Figure (b) proxy approach.

A similar good agreement can be achieved with GOSAT-2 glint measurements using TCCON stations near the coast. Here, the global mean bias between TCCON and GOSAT-2 is -2.57 ppb and 5.36 ppb for the full-physics and proxy product, a corresponding mean scatter is 10.93 ppb and 10.29 ppb with a station-to-station bias of 1.49 ppb and 5.16 ppb, respectively.

Furthermore, we find a good agreement over land between the GOSAT-1 XCH4 retrievals and GOSAT-2 full physics (correlation=0.78, bias=2.2 ppb, std=13.4 ppb) and proxy (correlation=0.84, bias=-3.1 ppb, std=14.4 ppb) retrievals. Over the oceans the agreement is similar between GOSAT-1 XCH4 retrievals and GOSAT-2 full physics (correlation=0.87, bias=0.6 ppb, std=9.8 ppb) and proxy (correlation=0.93, bias=3.1 ppb, std=11.3 ppb) retrievals. These numbers demonstrate the potential of the GOSAT-2 data product, although the presented analysis is preliminary due to the limited temporal coverage of the investigated data set. Hence, we consider the GOSAT-2 RemoTeC product appropriate for cross-verification with the TROPOMI XCH4 operational product.

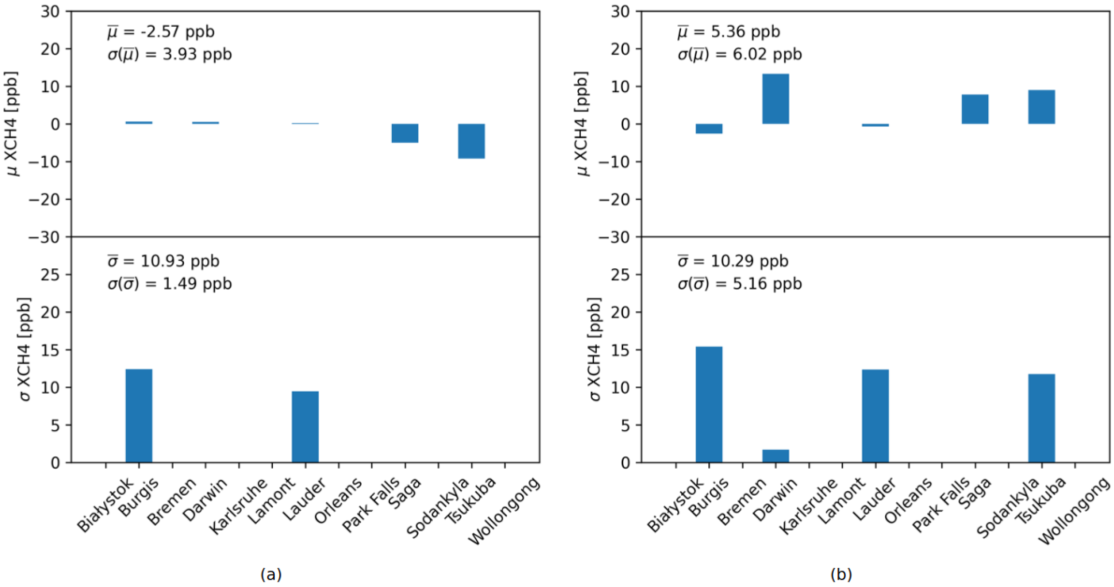

Figure 21: same as Figure 20 but for GOSAT-2 retrieval glint geometry.

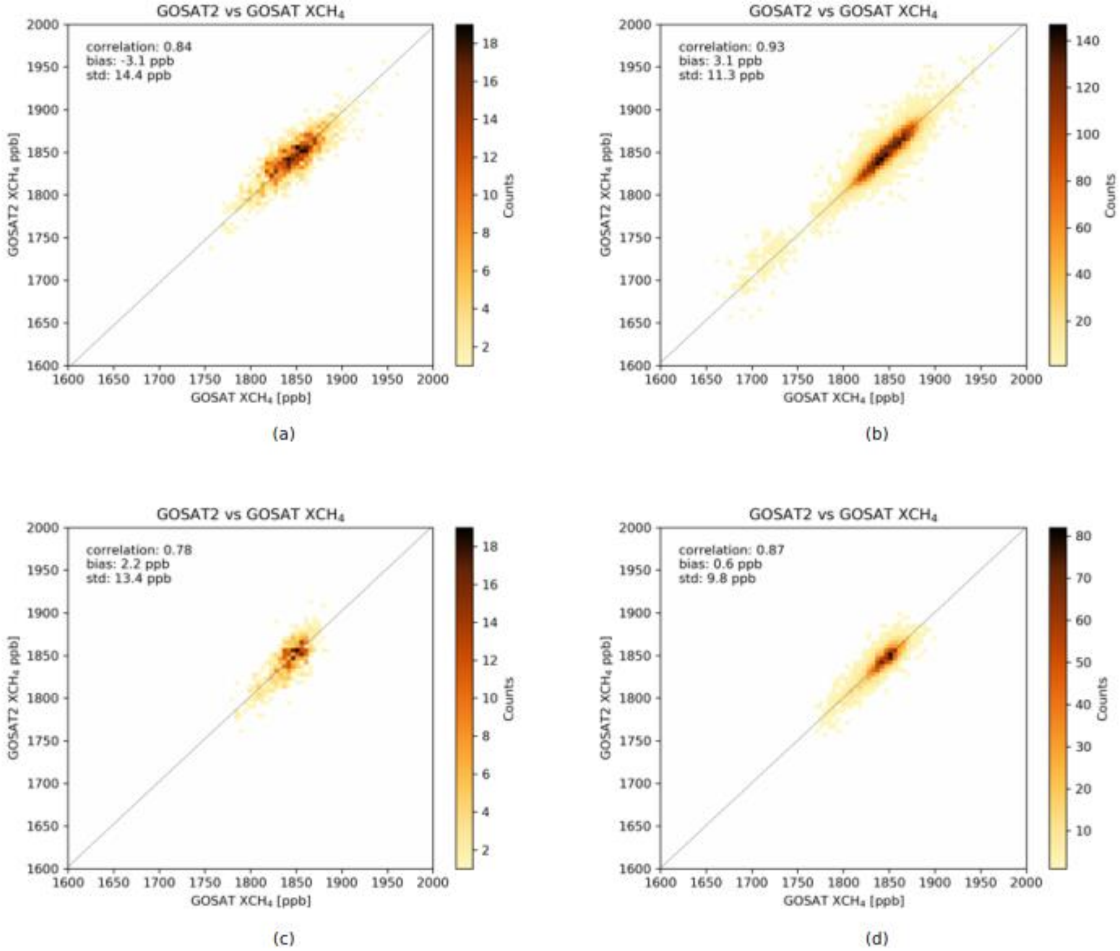

Figure 22: correlation between GOSAT-1 and GOSAT-2 XCH_4 retrievals for the period Feb-Aug 2019 for the full physics XCH_4 product (a, c) and XCH_4 proxy product (b, d) over land (a, b) and for glint geometries (c, d).

3.4.3 Inter-comparison of XCH4satellite data

The GOSAT-1 full physics and proxy retrieval has been extensively validated and offers an excellent opportunity for comparison. As the GOSAT-1 product reports both bias corrected and non-bias corrected value, we will compare it with the bias corrected and non-bias corrected GOSAT-2 values. We consider days for the period February 2019 – May 2020, split the GOSAT-2 observations into glint and non-glint ("land") sets and com- pare them separately. As both satellites observe at similar overpass times, we will co-locate the GOSAT-1 and GOSAT-2 footprints spatially by classing them into 2°x2° boxes and temporally by matching the overpasses by day. All groups are then averaged to create daily averaged 2°x2° values. Any GOSAT-2 group that does not have a corresponding match for GOSAT-1 is discarded. The results are shown in Figure 22.

We find a good agreement between GOSAT-1 and GOSAT-2 data over land both for the full physics (correlation=0.78, bias=2.2 ppb, std=13.4 ppb) and proxy data (correlation=0.84, bias=-3.1 ppb, std=14.4 ppb). Over the oceans the agreement is similar (full physics: correlation=0.87, bias=0.6 ppb, std=9.8 ppb and proxy: correlation=0.93, bias=3.1 ppb, std=11.3 ppb).

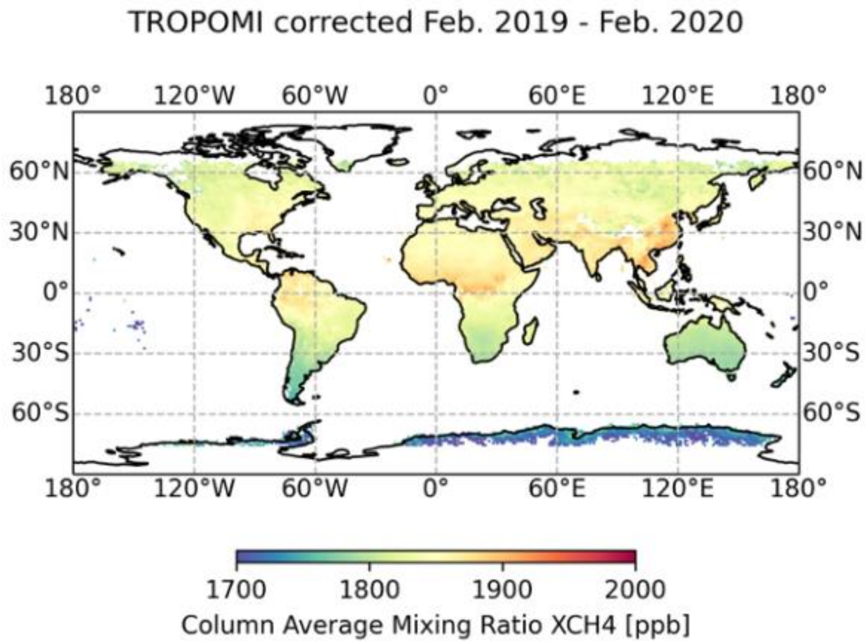

Figure 23 : TROPOMI XCH4 proxy retrieval. The data is bias corrected and averaged from Feb. 2019 to Feb. 2020

Finally, we inter-compare the GOSAT-2 data with collocated measurements of the TROPOMI instrument shown in Figure 23. Already during the commissioning phase of the TROPOMI instrument the XCH4 data product was compared with GOSAT-1 data from 31 May 2018 to 13 September 2018 [19]. Overall, the agreement was good. However, Hu et al. identified a dependency of the difference δ XCH4 between TROPOMI and GOSAT XCH4 on the retrieved surface albedo inferred from the TROPOMI SWIR measurement. The origin of this problem is not known yet and still under investigation but Hu et al., 2018 [19] suggested an empirical correction of the TROPOMI XCH4 further improved by [20]. This correction is already included in the operational TROPOMI XCH4 data product. A similar approach was followed for GOSAT-1 CO2 and CH4 and OCO-2 CO2 retrievals (e.g. [21], [22], [23]) and the data were corrected for their dependence on different parameters such as goodness of fit, surface albedo or aerosol parameters.

Figure 24shows the correlation for the corrected and uncorrected TROPOMI XCH4 data with the GOSAT- 2 full physics and proxy retrieval. The uncorrected TROPOMI XCH4 retrieval agree well with both the GOSAT- 2 full physics (correlation=0.82, bias= 0.78 ppb, std=23.48 ppb) and the GOSAT-2 proxy product (correlation=0.85, bias= 16.65 ppb, std= 20.51ppb). For the corrected TROPOMI XCH4 retrievals the correlation and the standard deviation with the GOSAT2 full physics (correlation=0.85, bias=16.51 ppb, std=22.26 ppb) and proxy retrievals (correlation=0.85, bias=16.65 ppb, std= 22.26 ppb) are significantly improved. We find an increase of the mean bias, which can be easily induced by erroneous spectroscopy in one of the retrievals and it is straight forward to correct for it when applying the correction to the TROPOMI or GOSAT data.

Another possible reason for the increased mean bias can be the sparse coverage of the TCCON network that is used for the correction applied to the GOSAT-1 and GOSAT-2 that does not cover all albedo scenes. This is still under investigation and could be possibly solved by following the approach presented by [20] that does not deploy TCCON measurements for the correction anymore. However, in general the mean bias is not relevant for the data interpretation as it mainly relies on spatial gradients in the data fields.

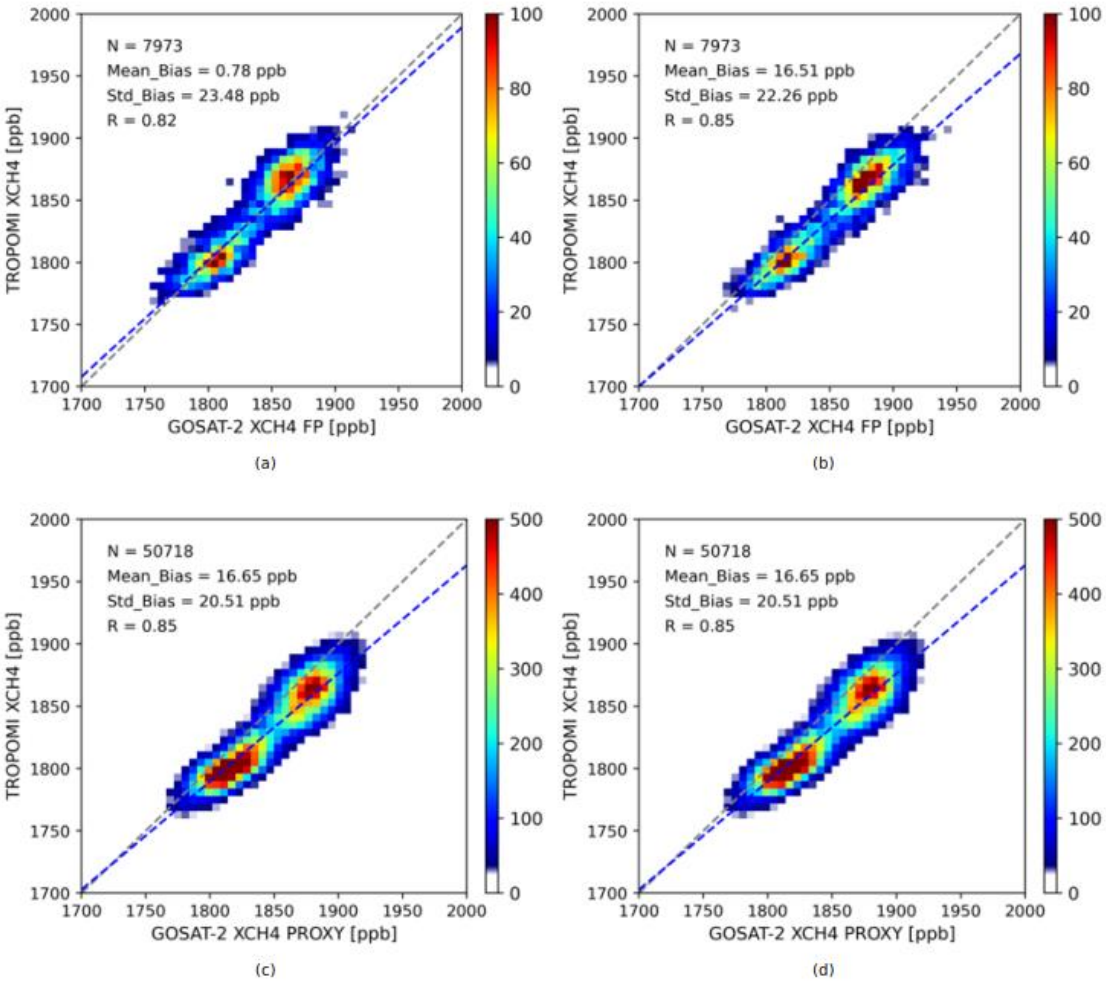

Figure 24: TROPOMI XCH_4 proxy retrieval compared to the GOSAT-2 full physics (a, b) and proxy retrieval approach (c, d). The panels (a, c) show the TROPOMI data without bias correction and (b, d) with bias correction applied. The data is collocated from Feb. 2019 to Feb. 2020.

3.4.4 Conclusions

A new scientific GOSAT-2 XCH4 data product (full physics and proxy approach) has been developed, that is bias corrected using ground-based TCCON measurements and does not deploy GOSAT-1 data anymore. The coverage of the data products was improved by updating the posteriori filter criteria that were, in particular for the full- physics retrieval, too strict, resulting in a poor spatial coverage. An error in the definition of the instrument Mueller matrix was corrected and the processing framework improved. The retrieval scheme was updated to use GOSAT-2 L1B v102102 (May 2020) and we reprocessed the full GOSAT-2 dataset from Feb. 2019 until July 2020 with the updated version of the retrieval processor.

The reprocessed data was validated with the measurements of the TCCON network. The global mean bias between TCCON and GOSAT-2 is -0.34 ppb and -0.06 ppb for the full-physics and proxy product, a corresponding mean scatter is 13.61 ppb and 16.15 ppb with a station-to-station bias of 1.94 ppb and 2.63 ppb, respectively. A similar good agreement can be achieved with GOSAT-2 glint measurements using TCCON stations near the coast. Here, the global mean bias between TCCON and GOSAT-2 is -2.57 ppb and 5.36 ppb for the full-physics and proxy product, a corresponding mean scatter is 10.93 ppb and 10.29 ppb with a station- to-station bias of 1.49 ppb and 5.16 ppb, respectively. Overall, we conclude that the two XCH4 data sets show good agreement. These numbers demonstrate the potential of the GOSAT-2 data product, although the presented analysis is preliminary due to the limited temporal coverage of the investigated data set.

To cope with the sparse coverage of the TCCON network we inter-compared our XCH4 GOSAT-2 data with the XCH4 retrievals of GOSAT-1 and TROPOMI. We found a good agreement over land between the GOSAT-1 XCH4 retrievals and GOSAT-2 full physics (correlation=0.78, bias=2.2 ppb, std=13.4 ppb) and proxy (correlation=0.84, bias=-3.1 ppb, std=14.4 ppb) retrievals. Over the oceans, the agreement is similar (full physics: correlation=0.87, bias=0.6 ppb, std=9.8 ppb, and proxy: correlation=0.93, bias=3.1 ppb, std=11.3 ppb).

The uncorrected TROPOMI XCH4 retrieval agree well with both the GOSAT-2 full physics (correlation=0.82, bias= 0.78 ppb, std=23.48 ppb) and the GOSAT-2 proxy product (correlation=0.85, bias= 16.65 ppb, std= 20.51ppb). For the corrected TROPOMI XCH4 retrievals the correlation and the standard deviation with the GOSAT2 full physics (correlation=0.85, bias=16.51 ppb, std=22.26 ppb) and proxy retrievals (correlation=0.85, bias=16.65 ppb, std= 22.26 ppb) are improved. The increase of the mean bias can be easily corrected for when applying the correction to the TROPOMI or GOSAT data.

With this study we could demonstrate the great potential of our scientific GOSAT-2 XCH4 data product. It comes basically with the same data quality as the official GOSAT-1 data product but provides better global coverage and spatial resolution and agrees well with the measurements of the TCCON network. Especially, for the satellite inter-comparisons with the TROPOMI data it is important to extend the GOSAT-2 data product to cover a longer time period. An interesting opportunity for future work represents the SWIR-3 channel measurements of the GOSAT-2 instrument. These measurements are spectrally overlapping with the SWIR measurement by the TROPOMI instrument. It will allow comparing the CO and CH4 retrievals of the two satellites excluding a bias caused by a different spectral range or a different retrieval algorithm. The TROPOMI XCH4 data used in this study does not include retrievals for sun glint geometries yet.

3.5 Evaluation of GOSAT-2 XCO2 AND XCH4 Over Snow

Similarly to GOSAT, the GOSAT-2 data coverage at high latitudes over snow and ice-covered ground has been evaluated. Figure 25shows the amount of data for GOSAT-2 XCH_4 product north from 40°N during the entire data record. The different colours describe the IMS classification at the ground point where the GOSAT-2 observation has been made. Based on Figure 25, GOSAT-2 has slightly less observations over snow than GOSAT, but this may be related to the observation breaks in GOSAT-2 and/or stricter filtering. Seasonal variability is also different compared to GOSAT, but this is related to the short temporal coverage of the GOSAT-2 record. In addition, there were maintenance breaks during the first operative months of the mission. The total number of high-latitude observations is significantly higher for GOSAT-2 already in this early stage, which is related to the shorter integration time of the instrument and potentially also to the intelligent pointing system for a reduced number of cloud-contaminated observations.

Figure 26 and Figure 27show the retrieval errors, given in the GOSAT-2 data files, for XCH_4 and XCO_2 observations north from 40°N. The y-axis in the left shows the number of observations for over land, and the y-axis in the right shows it for observations over snow. The retrieval errors are generally higher for observations over snow than those over snow-free landscape, systematically to GOSAT. In addition, especially for XCO_2, the retrieval error for observations over snow is not close to being normally distributed, unlike the error for observations over snow-free landscape. However, this might be related to the limited amount of data.

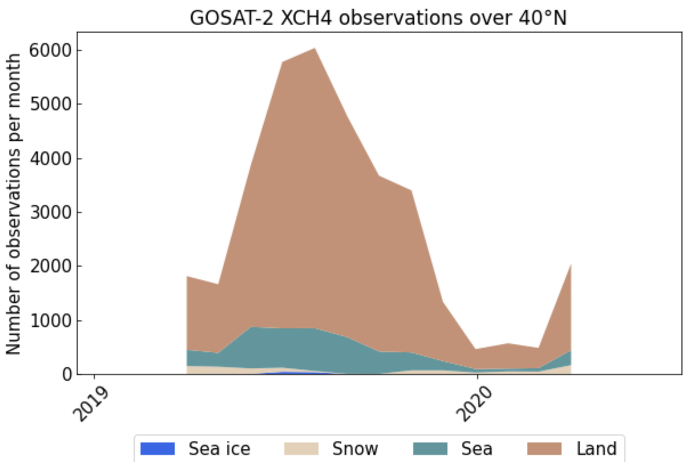

Figure 25: time series of the number of GOSAT-2 NIES v01.04 XCH_4 observations north from 40°N. Colours show the surface state at the ground observation footprint.

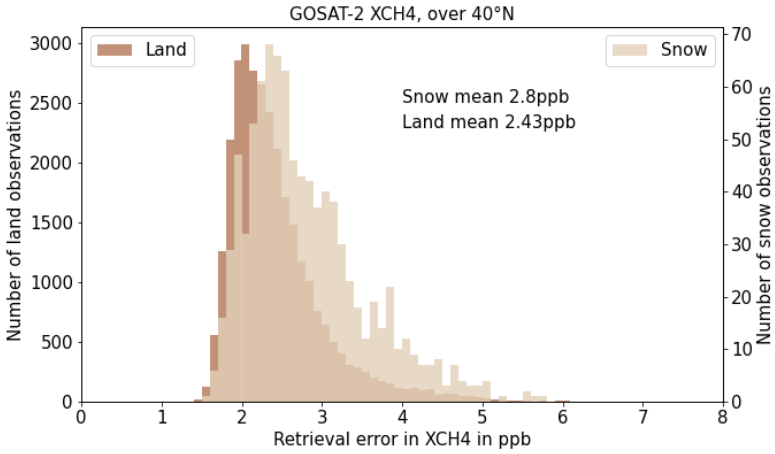

Figure 26: GOSAT-2 XCH_4 retrieval error for observations north from 40°N. Light brown shows the error for observations over snow and dark brown for observations over land. Note the different y-axis for observations over land and over snow.

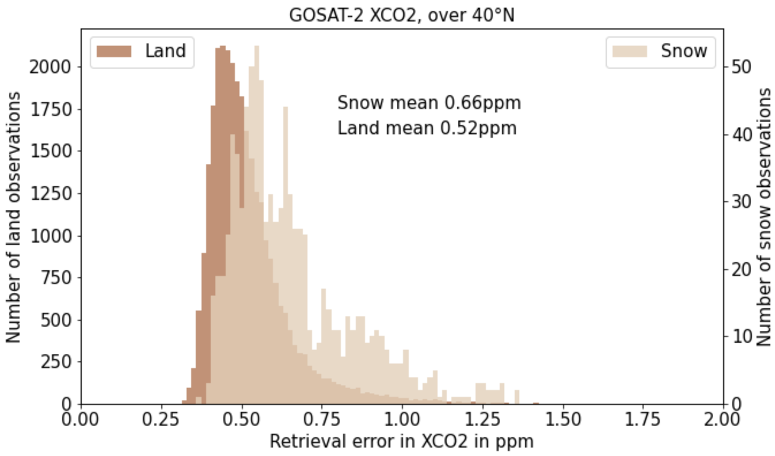

Figure 27: GOSAT-2 XCO_2 retrieval error for observations north from 40°N. Light brown shows the error for observations over snow and dark brown for observations over land. Note the different y-axis for observations over land and over snow.

3.6 Assessment Of Prior and Posterior Profiles Against AIRCORE Soundings

3.6.1 GOSAT-2 CO2 Profiles

Similarly to GOSAT, we evaluated the GOSAT-2 retrieval profiles against AirCore in Northern Finland where we carry out regular AirCore measurements of atmospheric profiles of greenhouse gases. Contrary to GOSAT, the GOSAT-2 NIES data files contain both prior profiles and posterior profiles. Posterior profiles are retrieved with the full-physics retrieval. Figure 28 shows GOSAT-2 prior and posterior profiles, TCCON GGG2014 prior profiles and AirCore profiles for CO_2 at Sodankylä TCCON site for three days from summer 2019. The GOSAT-2 profiles are collected within ±2 days from the AirCore soundings because without this expansion of the temporal co-location there would have been only one co-located day. For CO_2, the GOSAT-2 prior profiles agree much better with AirCore profiles than the GOSAT-2 posterior profiles. The posterior profiles show peaking CO_2 concentrations near 400 hPa which is not observed with AirCore or seen in the prior profiles. In addition, there is some instability near the surface, where the posterior profiles are in many cases either much larger or much smaller than the AirCore concentrations. The reasons behind these differences in the posterior profiles should be investigated in more detail.

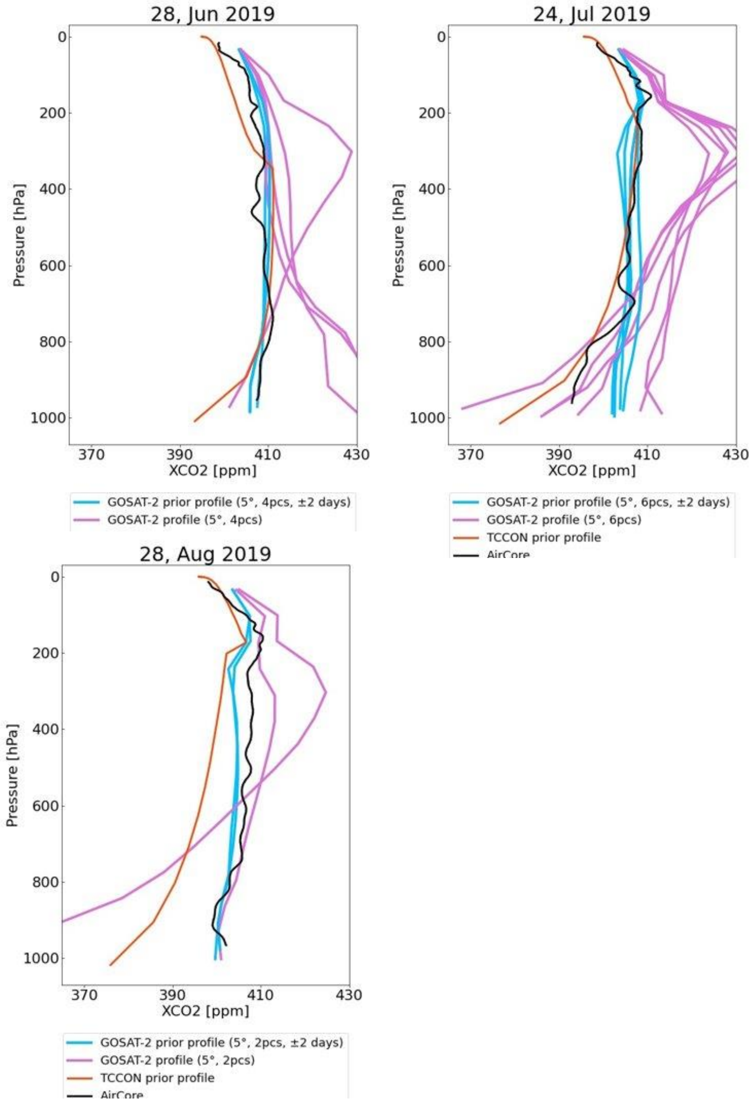

Figure 28.GOSAT-2 prior (blue) and posterior (purple) profiles, TCCON prior (red) profiles and AirCore (black) profiles for CO_2 at Sodankylä TCCON site on 28.6.2019 (left), 24.7.2019 (middle) and 28.8.2019 (right). The GOSAT-2 profiles are within ±2 days from the AirCore soundings.

3.6.2 GOSAT-2 CH_4 profiles

Figure 29 shows GOSAT-2 prior and posterior profiles, TCCON prior profiles and AirCore profiles for CH_4 at Sodankylä TCCON site for three days from summer 2019. The GOSAT-2 profiles are within ±2 days from the AirCore soundings. For CH_4 the GOSAT-2 prior and posterior profiles agree well with AirCores, there are small disagreements near the surface and in the upper atmosphere. The GOSAT-2 posterior profiles of CH_4 are much more realistic than the GOSAT-2 posterior profiles of CO_2, there are small peaks in the CH_4 posterior profiles near 100-200 hPa but these are small compared to the CO_2 peaks.

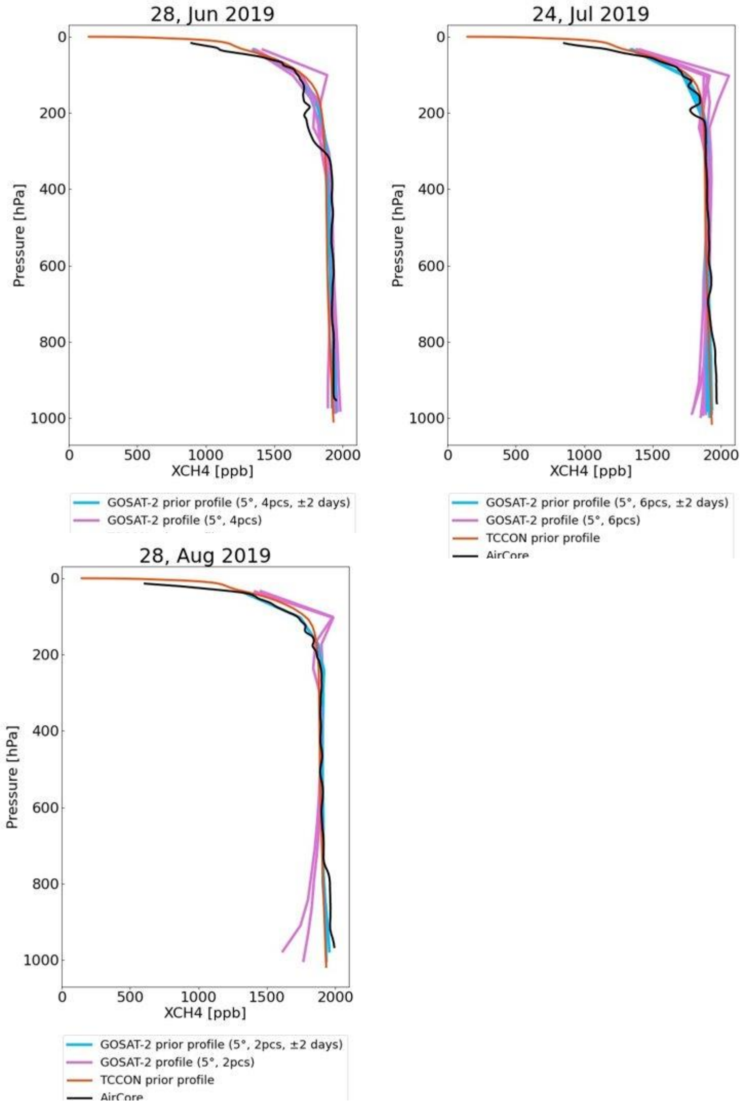

Figure 29: GOSAT-2 prior (blue) and posterior (purple) profiles, TCCON prior (red) profiles and AirCore (black) profiles for CH_4 at Sodankylä TCCON site on 28.6.2019 (left), 24.7.2019 (middle) and 28.8.2019 (right). The GOSAT-2 profiles are within ±2 days from the AirCore soundings.

3.7 GOSAT-2 SIF Evaluation in Northern Finland

GOSAT-2 Level 2 retrieval includes the retrieval of solar-induced fluorescence (SIF), which is an indicator of photosynthetic activity of vegetation and has been found to systematically correlate with the ecosystem's gross primary productivity (GPP), making it an important variable to detect from space. GOSAT-2 provides SIF as one of their official Level 2 products. Being a new product, it is important to evaluate this product. Here, we perform an evaluation of this product v01.03 over Northern Finland (mostly evergreen needleleaf forest vegetation) as an example of the quality of the product at high latitudes. Figure 30shows a time series of GOSAT-2 SIF at 755 nm. The SIF retrievals classified as "good" and "fair" quality (sif_quality_flag = 0 and sif_quality_flag = 1) are considered and averaged over ±1 degrees in latitude and longitude around Sodankylä (26.617ºE, 67.367ºN). Temporally, daily averaging is carried out, meaning essentially that the daily averages correspond also to satellite overpass averages. The evaluation is done against TROPOMI L2B TROPOSIF v2.0 product (Guanter et al. 2021). The TROPOSIF product uses a different retrieval window for SIF and corresponds to SIF at 743 nm wavelength. SIF radiation has a known spectral dependence and reduces towards larger near-infrared wavelengths beyond about 740 nm; therefore, it is not expected that the two products would yield equal SIF values. However, the seasonal variability (timings of spring recovery, maximum SIF, and the ending of active photosynthesis) should be comparable in both wavelengths. Based on Figure 30, the GOSAT-2 SIF product has significant scatter at all seasons, and a seasonal cycle cannot be reliably extracted. Therefore, we conclude that the GOSAT-2 SIF at high latitudes could benefit from a stricter data filtering and should be investigated in more detail before applying these data in carbon cycle related applications.

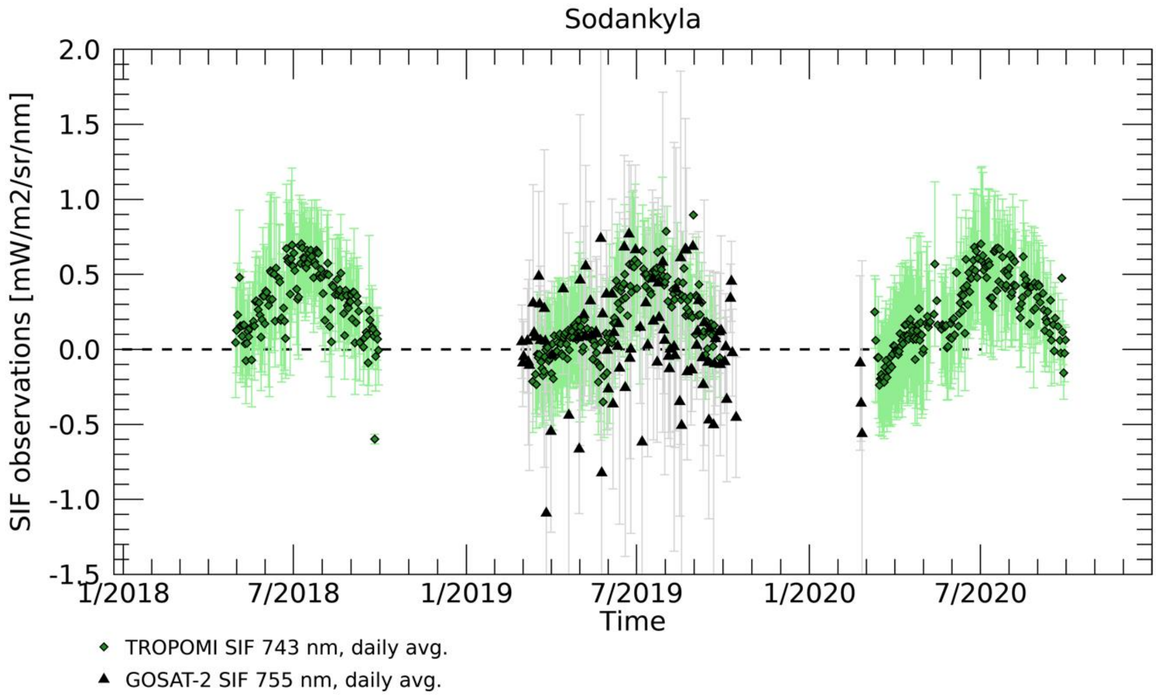

Figure 30: the evaluation of GOSAT-2 Level 2 SIF product v01.03 (black symbols) in mostly evergreen needleleaf forests in Northern Finland. The evaluation is carried out against TROPOSIF v2.0 product (green symbols). The figure shows daily (overpass) averages of SIF and their standard deviations as error bars.

3.8 Precision And Accuracy Of Gosat-1 Against TCCON

3.8.1 GOSAT XCO2 precision and accuracy

The operational, updated GOSAT XCO2 Level 2 product (GOSAT NIES XCO2 v02.95bc and v02.96bc) was evaluated against 29 ground-based FTS instruments that participate in the Total Carbon Column Observing Network (TCCON; Wunch et al., 2011; Figure 31). The spatiotemporal co-location criteria for the evaluation were same-day soundings within 2.5 degrees in latitude and 5.0 degrees in longitude, which have been applied also in other similar assessments (e.g., Boesch et al., 2021; Taylor et al., 2021). We present an evaluation of the daily mean values which mostly correspond to overpass-averaged statistics.

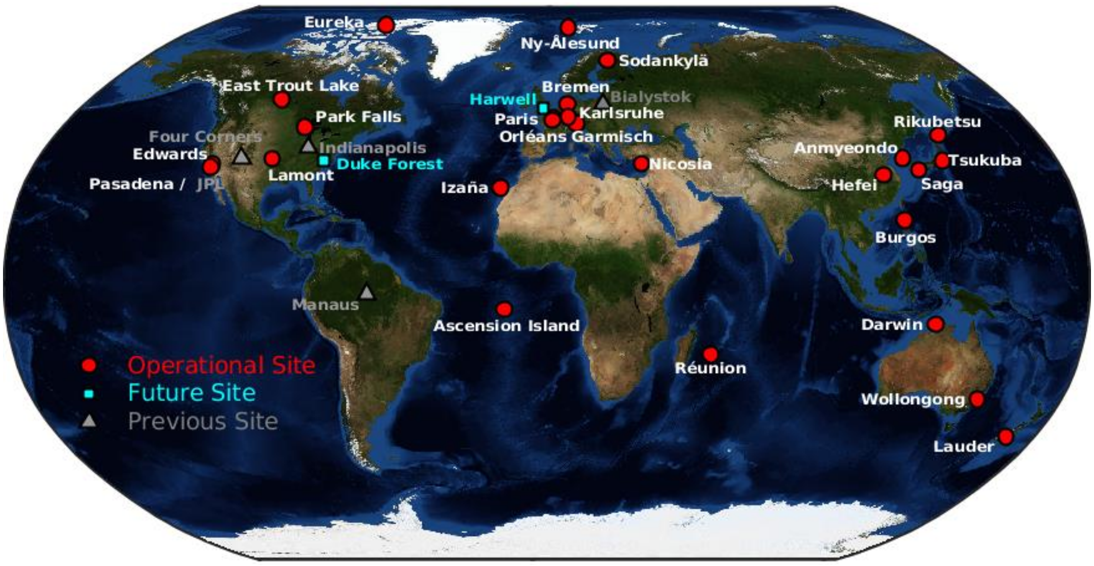

Figure 31: the Total Carbon Column Observing Network of ground-based Fourier Transform Spectrometers used in the evaluation of GOSAT and GOSAT-2 data. From: tccondata.org.

The biases for daily-averaged GOSAT XCO2 against 29 ground-based FTS as well as the standard deviations are listed in Table 1 and also presented in Figure 32. Relative biases at all sites are smaller than or equal to 0.35%. The magnitude of the bias varies between the sites, and the largest bias of 1.45 ppm is obtained at Tsukuba, corresponding to about 0.35%. Standard deviations of the bias vary between 1.1–2.5 ppm. Figure 32 shows that the bias is not systematic globally or latitudinally dependent but varies among the evaluation sites and FTS instruments. The resulting statistics show little to minor improvement over the previous product evaluation (NIES v02.75bc) presented in the last report.

In addition to the evaluation of the bias, i.e., the average difference in daily-averaged GOSAT XCO2 – TCCON XCO2, the seasonal cycle amplitude and the growth rate were evaluated at 25 sites using nonlinear time series fitting (see Lindqvist et al., 2015, for methodological details). The time series comparisons as well as the fitted functions for the estimation of the growth rate and the seasonal cycle amplitude are presented in the panels of Figure 33, separately for every site. The seasonal cycle amplitude (in ppm) and the growth rate (slope in ppm/year) are estimated for each FTS comparison, along with statistical error estimates. These are also collectively presented in Figure 34 and Figure 35with statistical uncertainty estimates derived from the parameter fitting procedure.

Table 5: evaluation of GOSAT NIES v02.95 XCO_2 against XCO_2 of ground-based Fourier Transform Spectrometers in the Total Carbon Column Observing Network (TCCON) sites, using the GGG2014 retrieval. The table shows the mean bias (GOSAT – TCCON; in ppm), the relative bias (in %) and the standard deviation (STD; in ppm) at a given site.

TCCON site	Bias	Rel. b. %	STD	TCCON site	Bias	Rel. b. %	STD
Anmyeondo	1.2	0.30	1.5	JPL	-0.4	-0.10	1.7
Ascension	0.0	0.00	1.1	Karlsruhe	0.7	0.17	1.8
Bialystok	0.5	0.12	1.9	Lamont	-0.5	-0.12	1.5
Bremen	0.5	0.12	1.9	Lauder	-0.1	-0.03	2.1
Burgos	1.3	0.31	2.1	Orleans	0.2	0.05	1.7
Caltech	-0.9	-0.22	1.6	Paris	-0.7	-0.17	2.3
Darwin	-0.1	-0.03	1.4	Park Falls	0.2	0.05	1.9
East Trout Lake	0.6	0.15	2.5	Reunion	0.2	0.04	1.4
Edwards	0.7	0.16	1.4	Rikubetsu	0.9	0.22	2.0
Eureka	-1.0	-0.25	2.4	Saga	0.3	0.07	1.9
Four Corners	0.2	0.05	1.8	Sodankylä	0.4	0.10	1.9
Garmisch	0.8	0.20	1.8	Tsukuba	1.5	0.35	1.8
Hefei	0.1	0.03	2.1	Wollongong	0.0	0.00	1.7
Influx	0.6	0.15	1.2	Zugspitze	0.0	0.01	2.0
Izana	-0.7	-0.16	1.5				

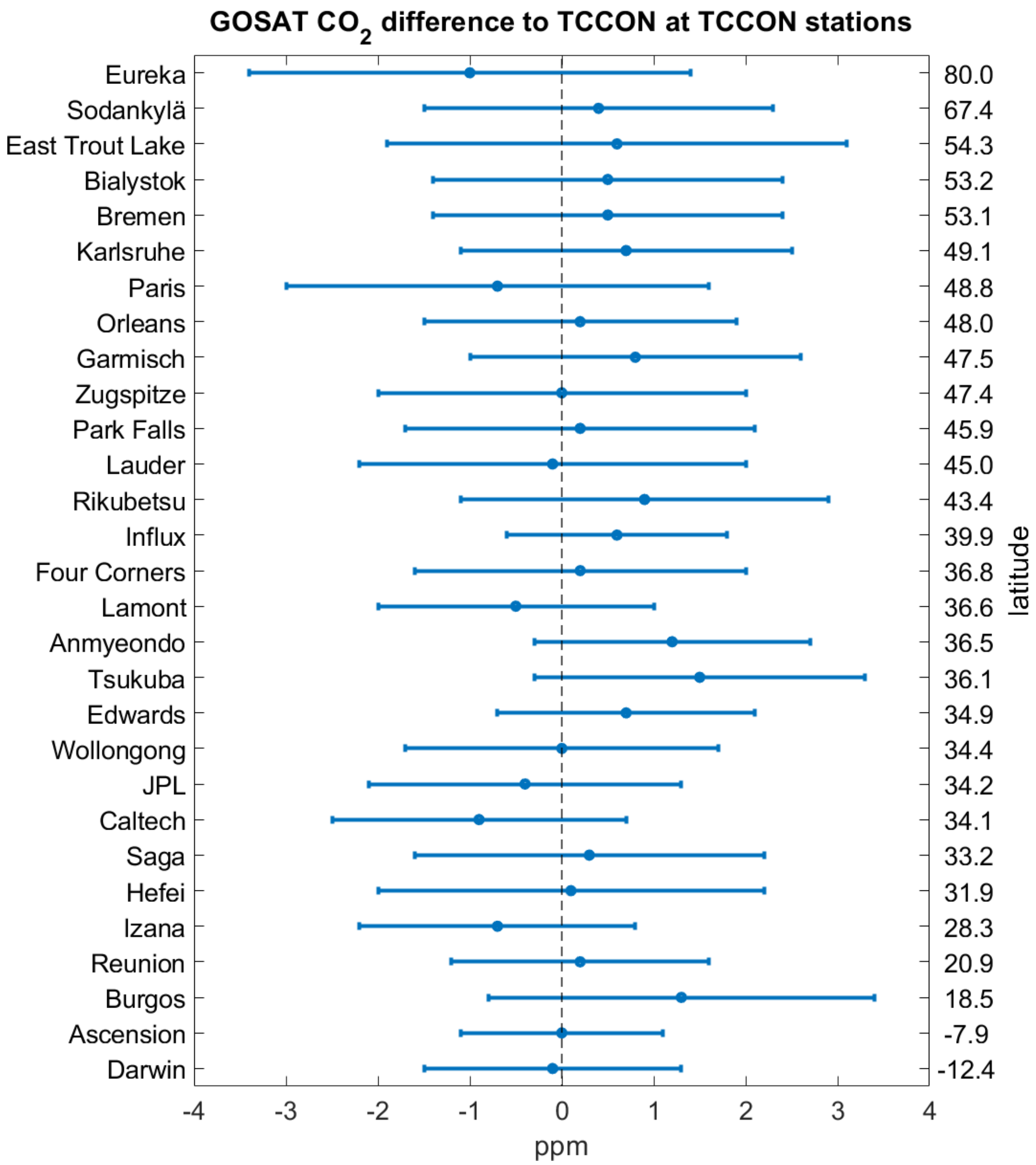

Figure 32: the accuracy and precision of GOSAT NIES v02.95 XCO2 at the TCCON sites, presented as the mean of GOSAT–TCCON daily-averaged XCO2. The error bars denote the standard deviation (in ppm). The evaluation sites are organised according to their latitude.

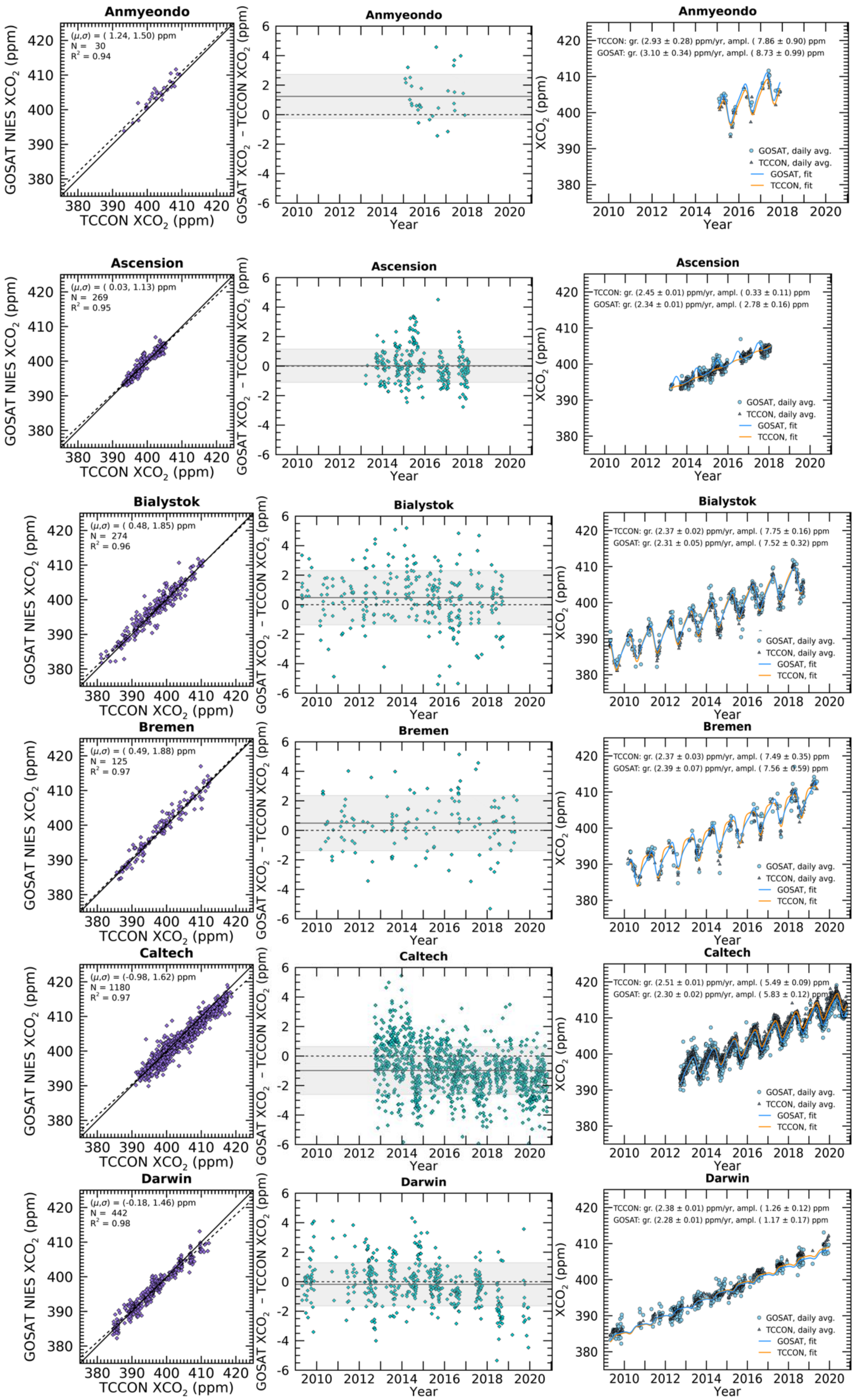
Anmyeondo
(μ,σ) = (1.24, 1.50) ppm
N = 30
R² = 0.94
GOSAT NIES XCO2 (ppm)
TCCON XCO2 (ppm)
GOSAT XCO2 – TCCON XCO2 (ppm)
Year
TCCON: gr. (2.93 ± 0.28) ppm/yr, ampl. (7.86 ± 0.90) ppm
GOSAT: gr. (3.10 ± 0.34) ppm/yr, ampl. (8.73 ± 0.99) ppm
XCO2 (ppm)
GOSAT, daily avg.
TCCON, daily avg.
GOSAT, fit
TCCON, fit
Ascension
(μ,σ) = (0.03, 1.13) ppm
N = 269
R² = 0.95
TCCON: gr. (2.45 ± 0.01) ppm/yr, ampl. (0.33 ± 0.11) ppm
GOSAT: gr. (2.34 ± 0.01) ppm/yr, ampl. (2.78 ± 0.16) ppm
Bialystok
(μ,σ) = (0.48, 1.85) ppm
N = 274
R² = 0.96
TCCON: gr. (2.37 ± 0.02) ppm/yr, ampl. (7.75 ± 0.16) ppm
GOSAT: gr. (2.31 ± 0.05) ppm/yr, ampl. (7.52 ± 0.32) ppm
Bremen
(μ,σ) = (0.49, 1.88) ppm
N = 125
R² = 0.97
TCCON: gr. (2.37 ± 0.03) ppm/yr, ampl. (7.49 ± 0.35) ppm
GOSAT: gr. (2.39 ± 0.07) ppm/yr, ampl. (7.56 ± 0.59) ppm
Caltech
(μ,σ) = (-0.98, 1.62) ppm
N = 1180
R² = 0.97
TCCON: gr. (2.51 ± 0.01) ppm/yr, ampl. (5.49 ± 0.09) ppm
GOSAT: gr. (2.30 ± 0.02) ppm/yr, ampl. (5.83 ± 0.12) ppm
Darwin
(μ,σ) = (-0.18, 1.46) ppm
N = 442
R² = 0.98
TCCON: gr. (2.38 ± 0.01) ppm/yr, ampl. (1.26 ± 0.12) ppm
GOSAT: gr. (2.28 ± 0.01) ppm/yr, ampl. (1.17 ± 0.17) ppm

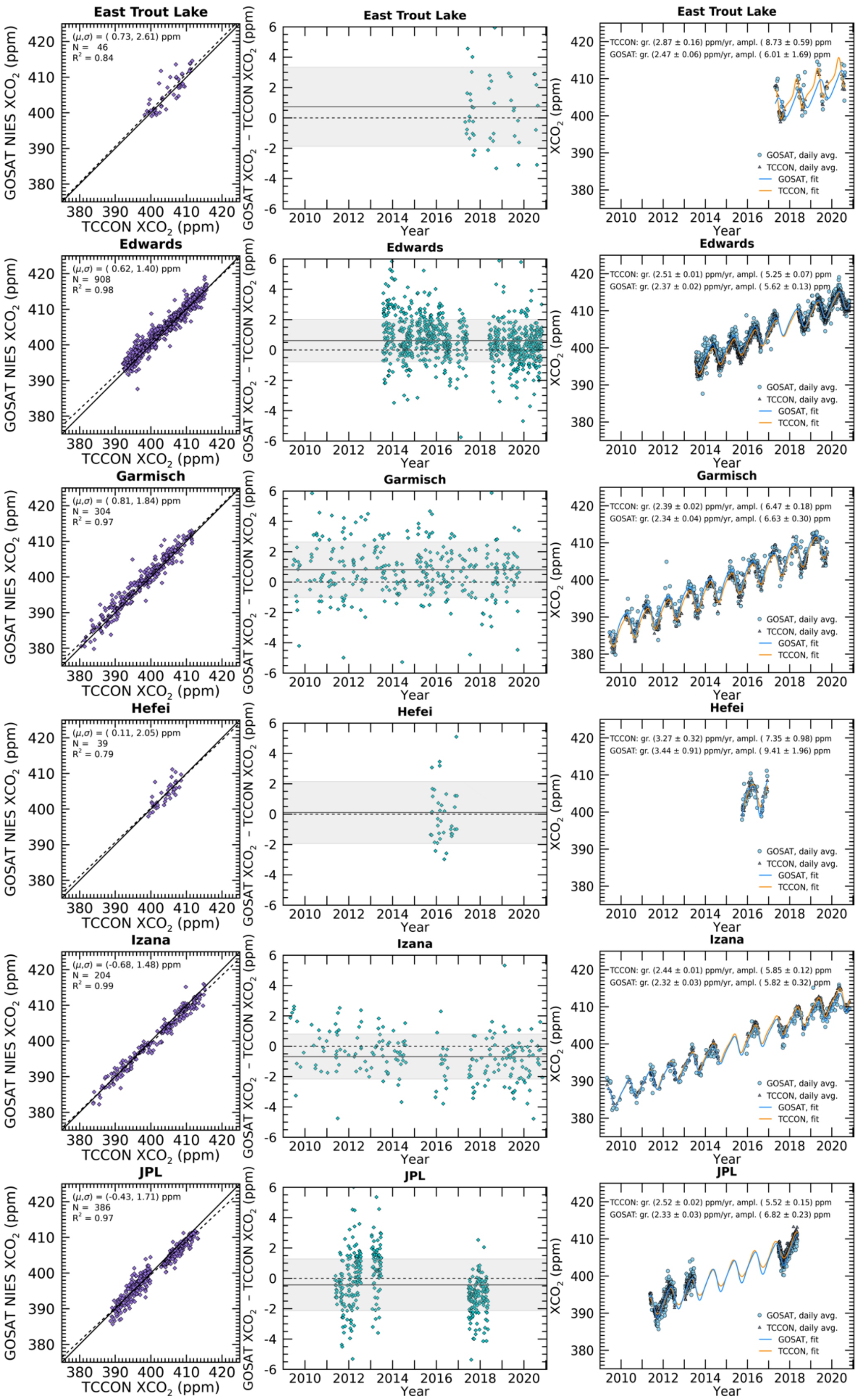
East Trout Lake
(μ,σ) = (0.73, 2.61) ppm
N = 46
R² = 0.84
TCCON: gr. (2.87 ± 0.16) ppm/yr, ampl. (8.73 ± 0.59) ppm
GOSAT: gr. (2.47 ± 0.06) ppm/yr, ampl. (6.01 ± 1.69) ppm
Edwards
(μ,σ) = (0.62, 1.40) ppm
N = 908
R² = 0.98
TCCON: gr. (2.51 ± 0.01) ppm/yr, ampl. (5.25 ± 0.07) ppm
GOSAT: gr. (2.37 ± 0.02) ppm/yr, ampl. (5.62 ± 0.13) ppm
Garmisch
(μ,σ) = (0.81, 1.84) ppm
N = 304
R² = 0.97
TCCON: gr. (2.39 ± 0.02) ppm/yr, ampl. (6.47 ± 0.18) ppm
GOSAT: gr. (2.34 ± 0.04) ppm/yr, ampl. (6.63 ± 0.30) ppm
Hefei
(μ,σ) = (0.11, 2.05) ppm
N = 39
R² = 0.79
TCCON: gr. (3.27 ± 0.32) ppm/yr, ampl. (7.35 ± 0.98) ppm
GOSAT: gr. (3.44 ± 0.91) ppm/yr, ampl. (9.41 ± 1.96) ppm
Izana
(μ,σ) = (-0.68, 1.48) ppm
N = 204
R² = 0.99
TCCON: gr. (2.44 ± 0.01) ppm/yr, ampl. (5.85 ± 0.12) ppm
GOSAT: gr. (2.32 ± 0.03) ppm/yr, ampl. (5.82 ± 0.32) ppm
JPL
(μ,σ) = (-0.43, 1.71) ppm
N = 386
R² = 0.97
TCCON: gr. (2.52 ± 0.02) ppm/yr, ampl. (5.52 ± 0.15) ppm
GOSAT: gr. (2.33 ± 0.03) ppm/yr, ampl. (6.82 ± 0.23) ppm
GOSAT NIES XCO₂ (ppm)
TCCON XCO₂ (ppm)
GOSAT XCO₂ – TCCON XCO₂ (ppm)
XCO₂ (ppm)
Year
GOSAT, daily avg.
TCCON, daily avg.
GOSAT, fit
TCCON, fit

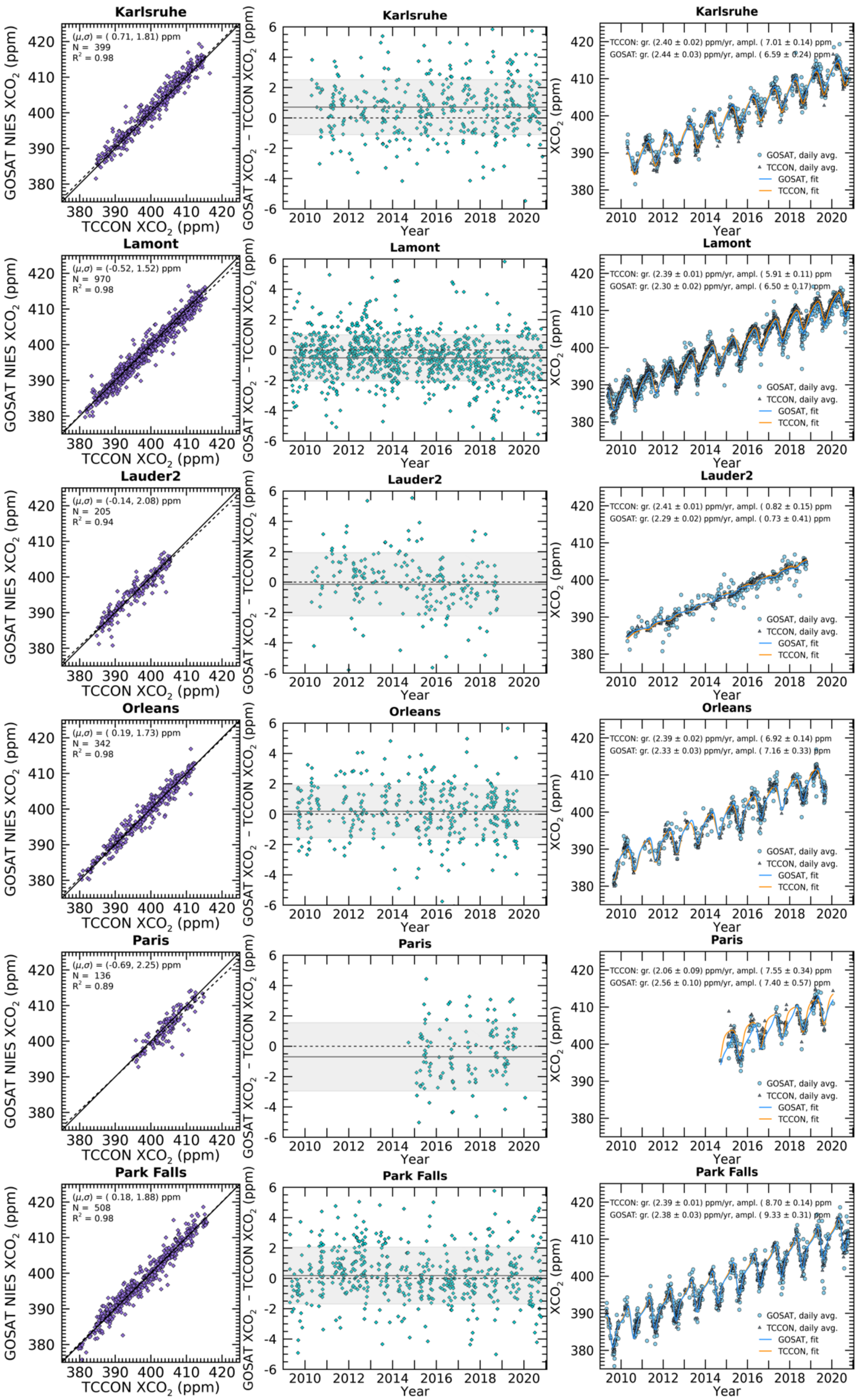
Karlsruhe
(μ,σ) = (0.71, 1.81) ppm
N = 399
R² = 0.98
TCCON: gr. (2.40 ± 0.02) ppm/yr, ampl. (7.01 ± 0.14) ppm
GOSAT: gr. (2.44 ± 0.03) ppm/yr, ampl. (6.59 ± 0.24) ppm
Lamont
(μ,σ) = (-0.52, 1.52) ppm
N = 970
R² = 0.98
TCCON: gr. (2.39 ± 0.01) ppm/yr, ampl. (5.91 ± 0.11) ppm
GOSAT: gr. (2.30 ± 0.02) ppm/yr, ampl. (6.50 ± 0.17) ppm
Lauder2
(μ,σ) = (-0.14, 2.08) ppm
N = 205
R² = 0.94
TCCON: gr. (2.41 ± 0.01) ppm/yr, ampl. (0.82 ± 0.15) ppm
GOSAT: gr. (2.29 ± 0.02) ppm/yr, ampl. (0.73 ± 0.41) ppm
Orleans
(μ,σ) = (0.19, 1.73) ppm
N = 342
R² = 0.98
TCCON: gr. (2.39 ± 0.02) ppm/yr, ampl. (6.92 ± 0.14) ppm
GOSAT: gr. (2.33 ± 0.03) ppm/yr, ampl. (7.16 ± 0.33) ppm
Paris
(μ,σ) = (-0.69, 2.25) ppm
N = 136
R² = 0.89
TCCON: gr. (2.06 ± 0.09) ppm/yr, ampl. (7.55 ± 0.34) ppm
GOSAT: gr. (2.56 ± 0.10) ppm/yr, ampl. (7.40 ± 0.57) ppm
Park Falls
(μ,σ) = (0.18, 1.88) ppm
N = 508
R² = 0.98
TCCON: gr. (2.39 ± 0.01) ppm/yr, ampl. (8.70 ± 0.14) ppm
GOSAT: gr. (2.38 ± 0.03) ppm/yr, ampl. (9.33 ± 0.31) ppm
GOSAT NIES XCO2 (ppm)
TCCON XCO2 (ppm)
GOSAT XCO2 – TCCON XCO2 (ppm)
XCO2 (ppm)
Year
GOSAT, daily avg.
TCCON, daily avg.
GOSAT, fit
TCCON, fit

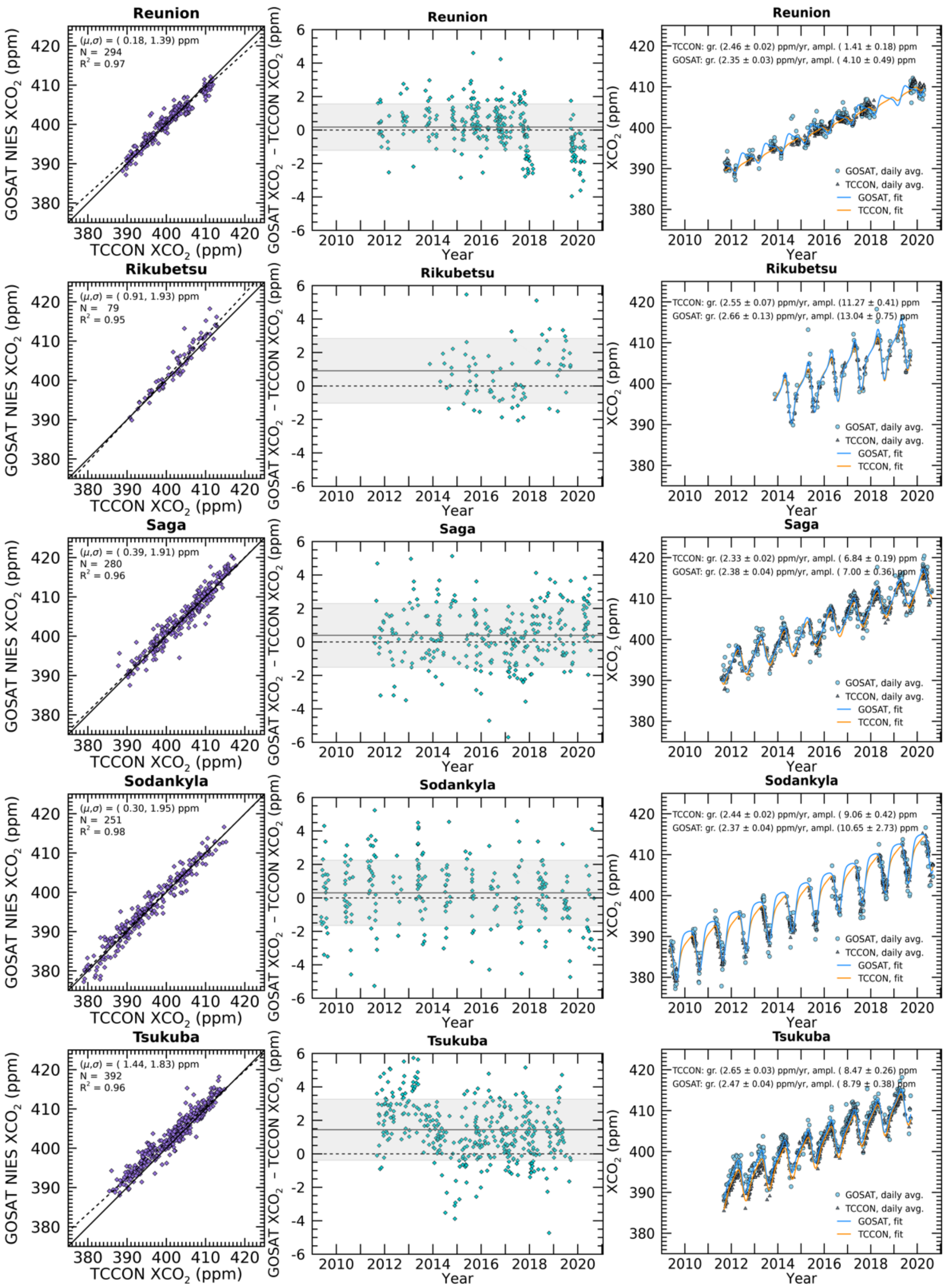
Reunion
(μ,σ) = (0.18, 1.39) ppm
N = 294
R² = 0.97
TCCON: gr. (2.46 ± 0.02) ppm/yr, ampl. (1.41 ± 0.18) ppm
GOSAT: gr. (2.35 ± 0.03) ppm/yr, ampl. (4.10 ± 0.49) ppm
Rikubetsu
(μ,σ) = (0.91, 1.93) ppm
N = 79
R² = 0.95
TCCON: gr. (2.55 ± 0.07) ppm/yr, ampl. (11.27 ± 0.41) ppm
GOSAT: gr. (2.66 ± 0.13) ppm/yr, ampl. (13.04 ± 0.75) ppm
Saga
(μ,σ) = (0.39, 1.91) ppm
N = 280
R² = 0.96
TCCON: gr. (2.33 ± 0.02) ppm/yr, ampl. (6.84 ± 0.19) ppm
GOSAT: gr. (2.38 ± 0.04) ppm/yr, ampl. (7.00 ± 0.36) ppm
Sodankyla
(μ,σ) = (0.30, 1.95) ppm
N = 251
R² = 0.98
TCCON: gr. (2.44 ± 0.02) ppm/yr, ampl. (9.06 ± 0.42) ppm
GOSAT: gr. (2.37 ± 0.04) ppm/yr, ampl. (10.65 ± 2.73) ppm
Tsukuba
(μ,σ) = (1.44, 1.83) ppm
N = 392
R² = 0.96
TCCON: gr. (2.65 ± 0.03) ppm/yr, ampl. (8.47 ± 0.26) ppm
GOSAT: gr. (2.47 ± 0.04) ppm/yr, ampl. (8.79 ± 0.38) ppm
GOSAT NIES XCO2 (ppm)
TCCON XCO2 (ppm)
GOSAT XCO2 – TCCON XCO2 (ppm)
XCO2 (ppm)
Year
GOSAT, daily avg.
TCCON, daily avg.
GOSAT, fit
TCCON, fit

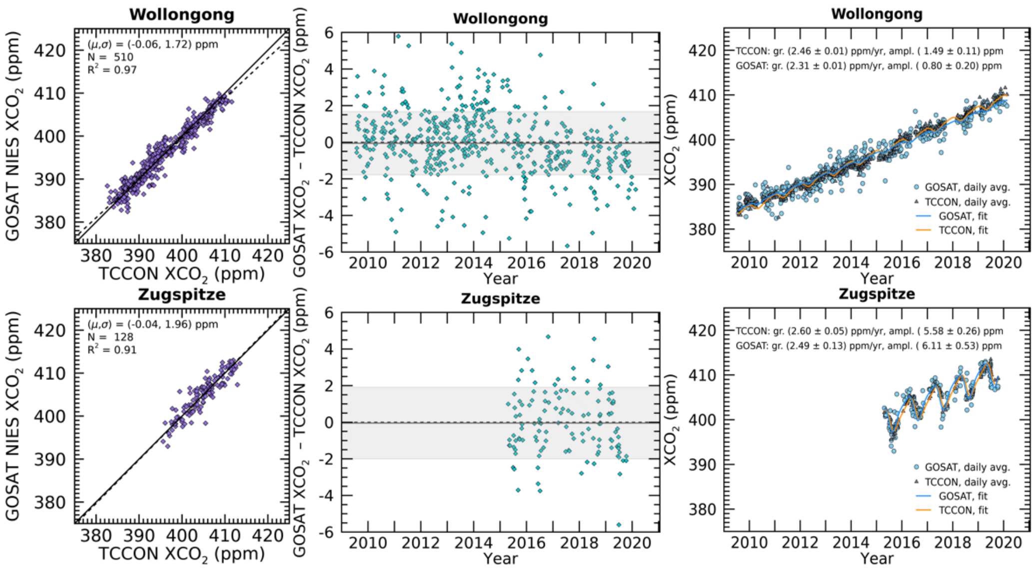

Figure 33: the one-to-one evaluation of the daily-averaged retrieved XCO_2 from GOSAT NIES v02.95 and TCCON GGG2014 (left panel), the bias evaluated as GOSAT–TCCON (middle panel; mean bias is shown with the grey solid line and the standard deviation with the grey shaded area), and XCO_2 seasonal cycle fitting for each co-located time series (right panel).

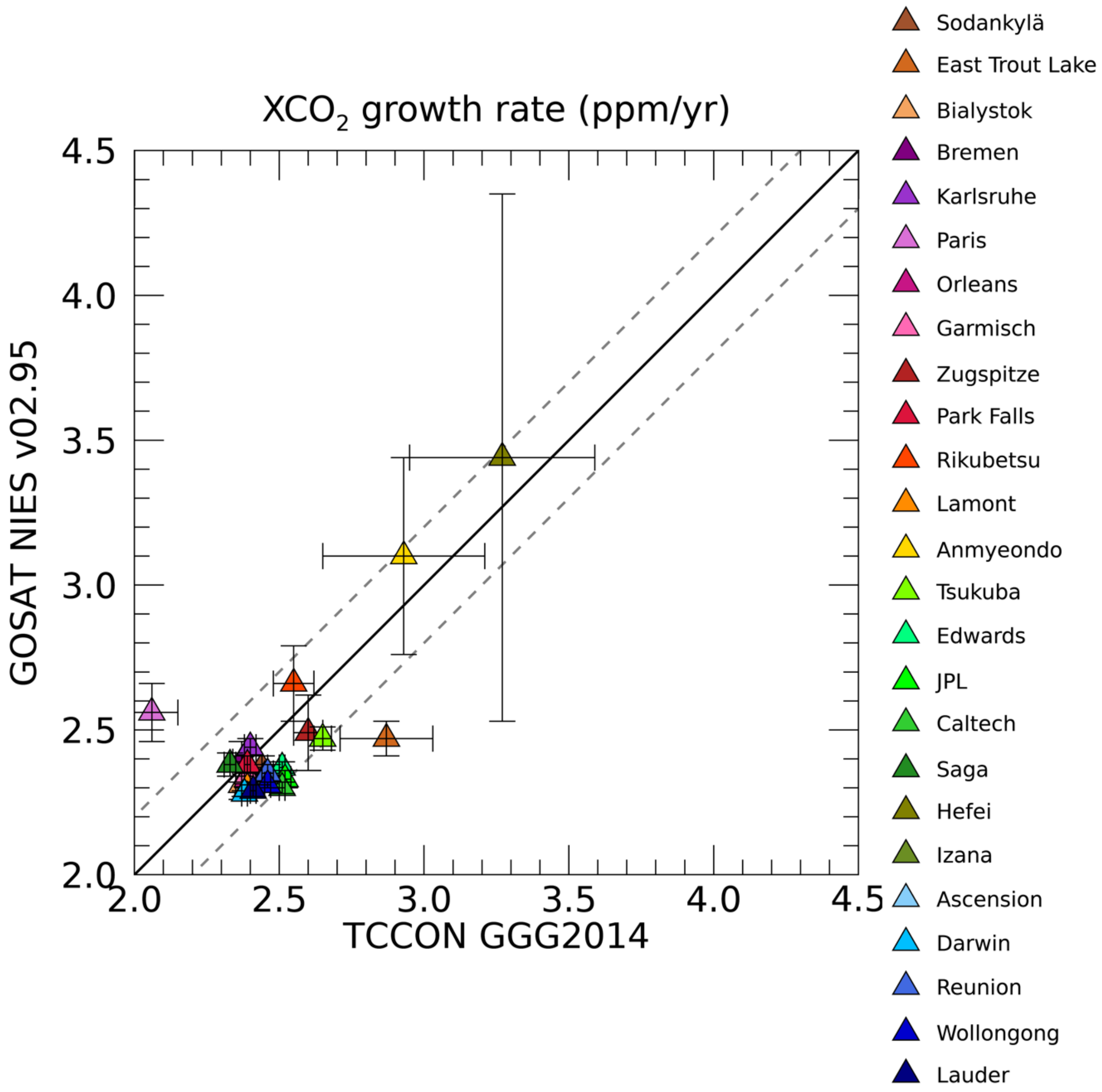

Figure 34: evaluation of the average growth rate (in ppm/year) for co-located GOSAT and TCCON XCO_2 retrievals and based on the seasonal cycle time series fitting. The dashed lines correspond to a deviation of 0.2 ppm/year from the one-to-one line (solid line).

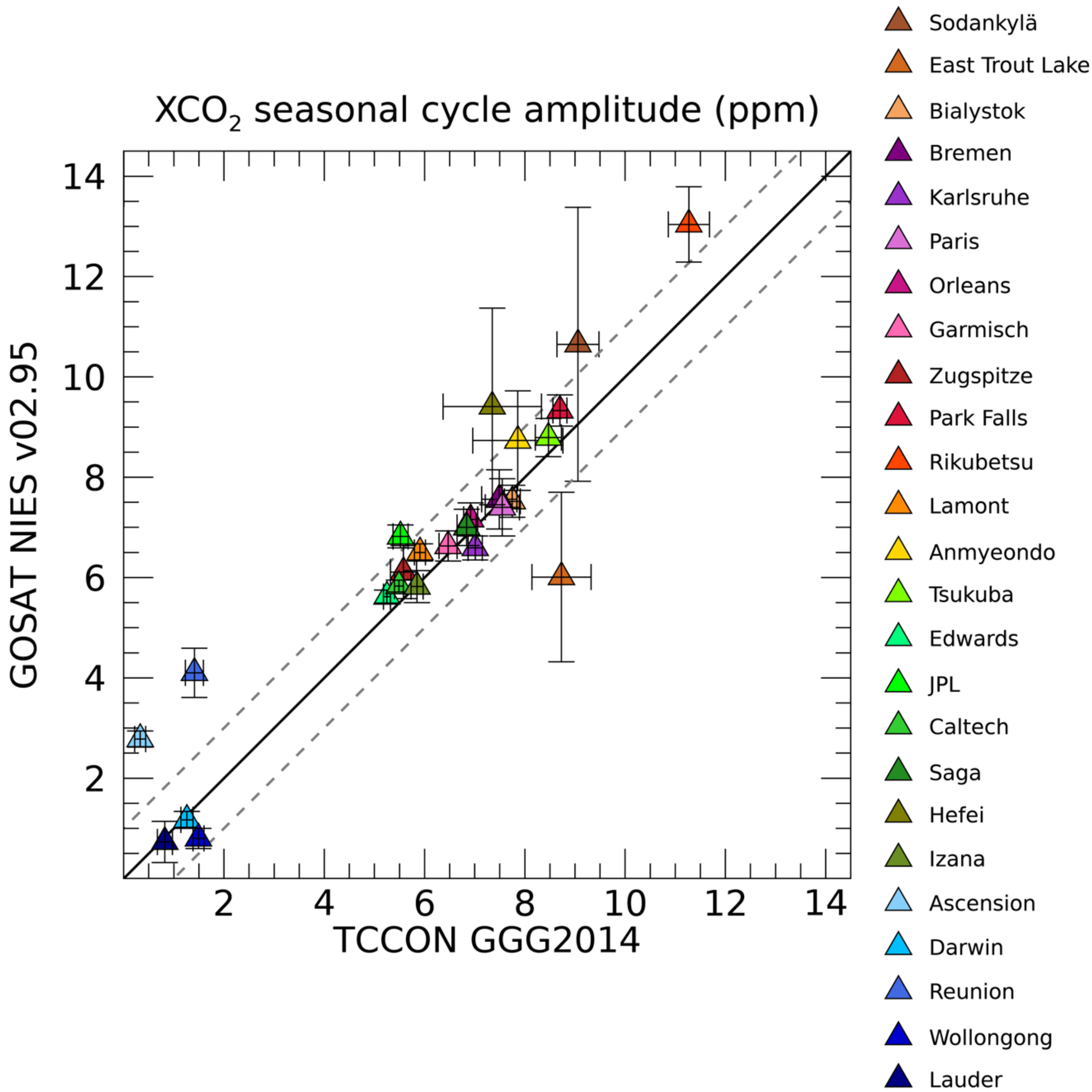

Figure 35: evaluation of the average seasonal cycle amplitude (in ppm) for co-located GOSAT and TCCON XCO_2 retrievals and based on the seasonal cycle time series fitting. The dashed lines correspond to a deviation of 1.0 ppm from the one-to-one line (solid line).

The growth rate is mostly systematically higher for the TCCON, although the differences are not large. The few outliers (e.g., Anmyeondo, Hefei) can be explained by local sources and a short time series which makes it challenging to reliably disentangle the growth rate from the seasonal variability. Based on the growth rate comparison and the XCO_2 difference time series in Figure 33(middle panel), the GOSAT XCO_2 product is stable over time.

The XCO_2 seasonal cycle amplitude depends on the geographical location: in the Southern hemisphere, the seasonal variability in XCO_2 is small, resulting in a shallow seasonal cycle amplitude, generally less than 2 ppm. The seasonal cycle amplitude from GOSAT XCO_2 is not systematically within the error estimates of the ground based TCCON XCO_2 seasonal cycle amplitude in the Southern hemisphere, which may indicate small-scale seasonal biases in the Southern hemisphere GOSAT data. However, to some extent this is also a consequence of the lack of seasonal variability in the Southern hemispheric XCO_2. In the Northern hemisphere, the seasonal cycle amplitude is mostly in a good agreement with the TCCON. The largest differences are seen towards increasing latitudes (e.g., Sodankylä, East Trout Lake) where the seasonal coverage of observations is limited mostly due to the high solar zenith angles in winter. Otherwise, the agreement varies between the sites non-systematically, indicating that the data are not subject to large-scale seasonal biases (at least comparable to the magnitude of the XCO_2 seasonal variability).

3.8.2 GOSAT XCH4 precision and accuracy

The operational, updated GOSAT XCH_4 Level 2 product (GOSAT NIES XCH_4 v02.95bc and v02.96bc) was evaluated against 29 ground-based FTS instruments that participate in the Total Carbon Column Observing Network (TCCON; Wunch et al., 2011; Figure 31). The spatiotemporal co-location criteria for the evaluation were same-day soundings within 2.5 degrees in latitude and 5.0 degrees in longitude, similarly to XCO_2 evaluation. We present an evaluation of the daily mean values which mostly correspond to overpass-averaged statistics.

The biases for daily-averaged GOSAT XCH_4 against 29 ground-based FTS as well as the standard deviations are listed in Table 6 and also presented in Figure 36. Relative biases at most sites are smaller than or equal to 0.5%. An outlier is Zugspitze with a bias of 41 ppb (corresponding to about 2.2%). The origin of the bias remains unknown, and the issue has been reported to the GOSAT team. Standard deviations of the bias vary between 7.2–15.9 ppb. Figure 36 shows that the bias is not systematic globally, or latitudinally dependent, but varies among the evaluation sites and FTS instruments. The resulting statistics show minor improvement over the previous product evaluation (NIES v02.75bc) presented in the last report.

In addition to the evaluation of the bias, i.e., the average difference in daily-averaged GOSAT XCH_4 – TCCON XCH_4, the seasonal cycle amplitude and the growth rate were evaluated at 24 sites using nonlinear time series fitting (see Lindqvist et al., 2015, for methodological details). The time series comparisons as well as the fitted functions for the estimation of the growth rate and the seasonal cycle amplitude are presented in the panels of Figure 37, separately for every site. The seasonal cycle amplitude (in ppb) and the growth rate (slope in ppb/year) are estimated for each FTS comparison, along with statistical error estimates. These are also collectively presented in Figure 38 and Figure 39with statistical uncertainty estimates derived from the parameter fitting procedure.

Table 6: evaluation of GOSAT NIES v02.95 XCH_4 against XCH_4 of ground-based Fourier Transform Spectrometers in the Total Carbon Column Observing Network (TCCON) sites, using the GGG2014 retrieval. The table shows the mean bias (GOSAT – TCCON; in ppb), the relative bias (in %) and the standard deviation (STD; in ppb) at a given site.

TCCON site	Bias	Rel. b. %	STD	TCCON site	Bias	Rel. b. %	STD
Anmyeondo	4.6	0.25	11.3	JPL	-2.5	-0.14	12.1
Ascension	1.2	0.06	7.2	Karlsruhe	1.8	0.10	10.1
Bialystok	4.6	0.25	10.1	Lamont	-2.9	-0.16	12.6
Bremen	3.5	0.19	11.5	Lauder	-2.3	-0.12	10.3
Burgos	7.1	0.38	7.5	Orleans	0.5	0.03	10.1
Caltech	-0.8	-0.04	12.1	Paris	-3.8	-0.21	9.3
Darwin	-0.3	-0.01	8.0	Park Falls	6.7	0.36	9.8
East Trout Lake	4.2	0.22	12.5	Reunion	3.6	0.19	8.7
Edwards	9.4	0.51	12.4	Rikubetsu	6.7	0.36	9.3
Eureka	-5.3	-0.29	15.0	Saga	4.5	0.24	12.0
Four Corners	-7.8	-0.42	15.9	Sodankylä	5.3	0.29	10.8
Garmisch	9.7	0.52	12.2	Tsukuba	6.2	0.33	10.4
Hefei	-1.6	-0.09	14.1	Wollongong	-3.8	-0.20	11.3
Influx	7.3	0.39	8.7	Zugspitze	40.5	2.19	13.3
Izana	13.5	0.73	9.5				

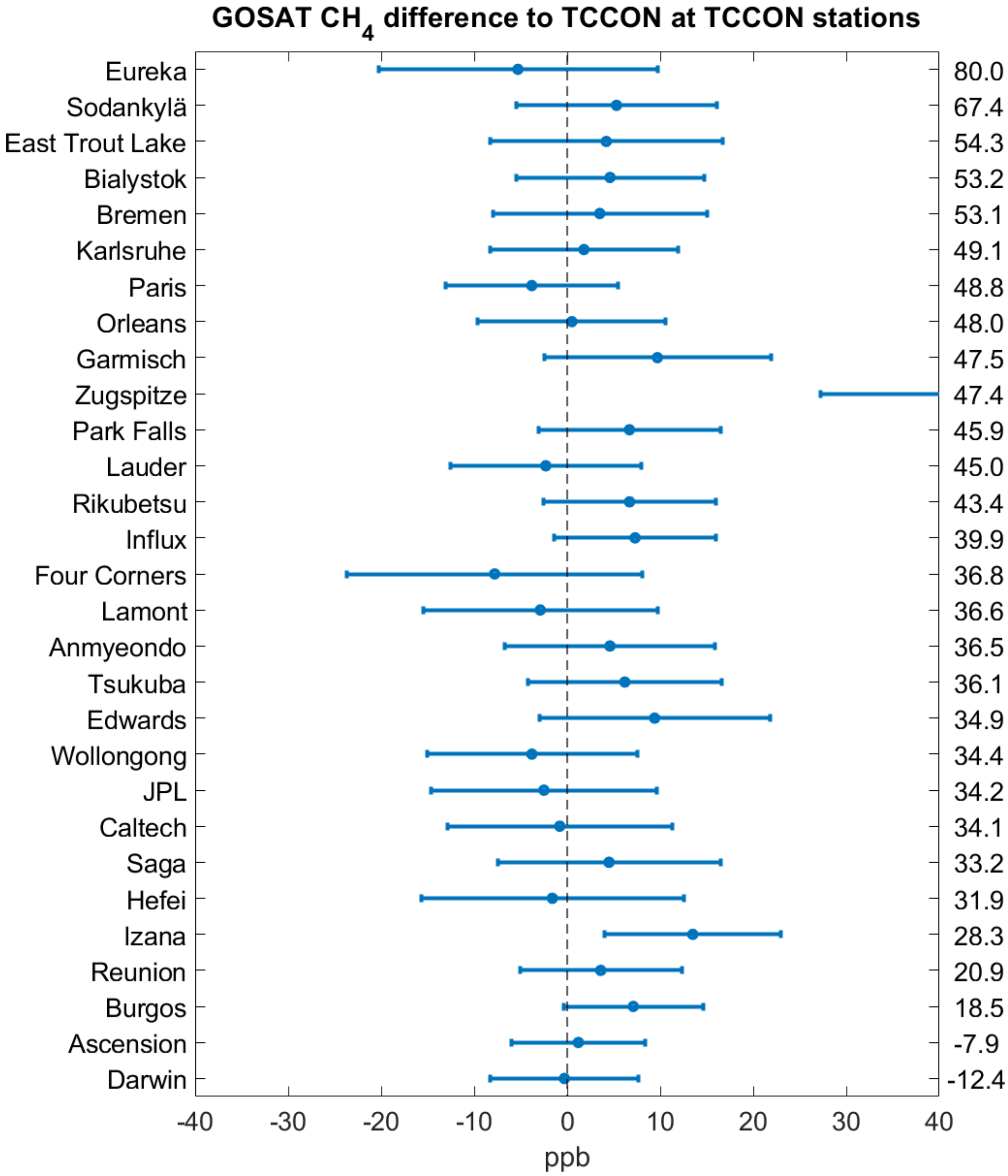

Figure 36: accuracy and precision of GOSAT NIES v02.95 XCH_4 at the TCCON sites, presented as the mean of GOSAT–TCCON daily-averaged XCH_4. The error bars denote the standard deviation (in ppb). The evaluation sites are organised according to their latitude.

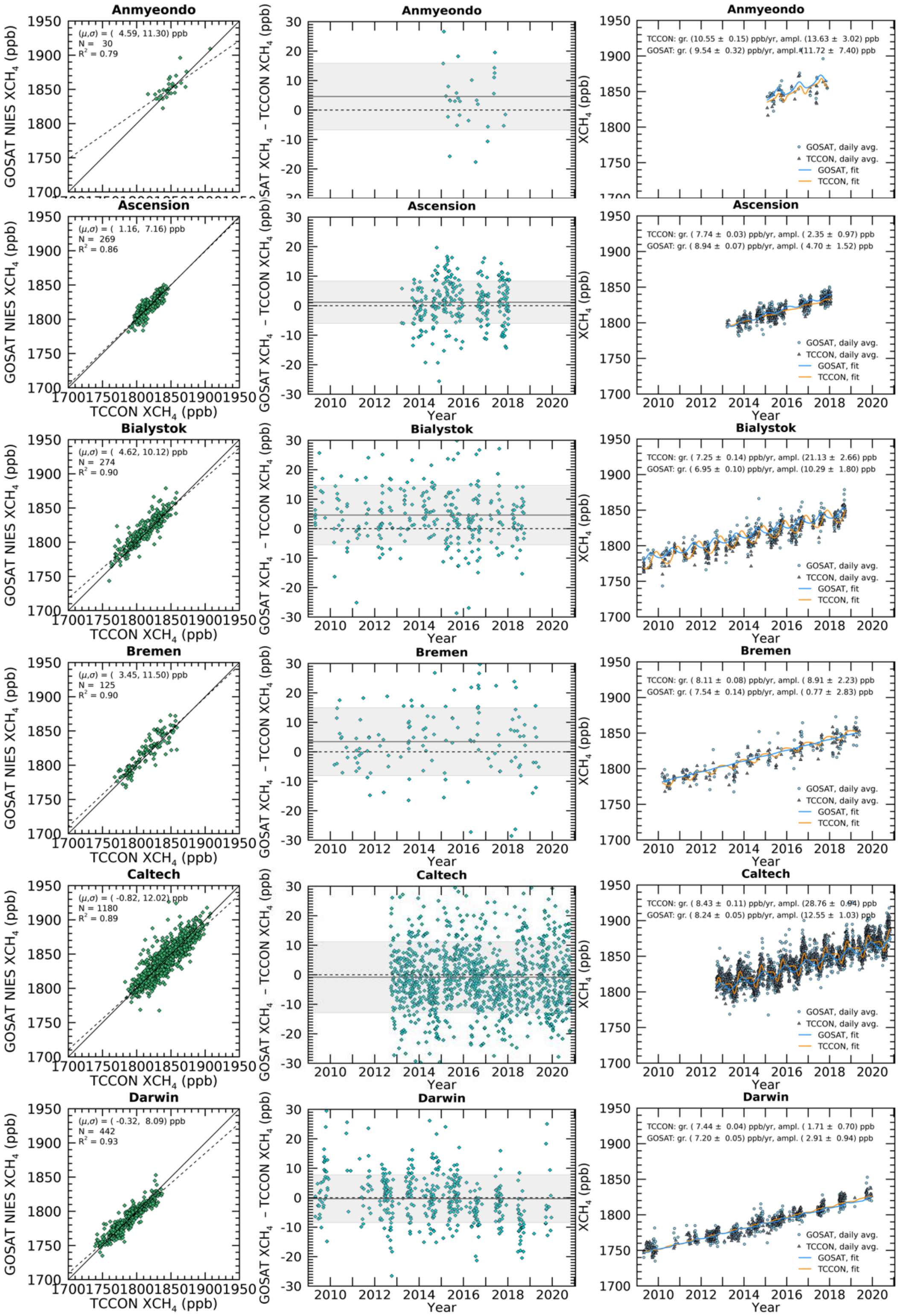
Anmyeondo
(μ,σ) = (4.59, 11.30) ppb
N = 30
R² = 0.79
TCCON: gr. (10.55 ± 0.15) ppb/yr, ampl. (13.63 ± 3.02) ppb
GOSAT: gr. (9.54 ± 0.32) ppb/yr, ampl. (11.72 ± 7.40) ppb
Ascension
(μ,σ) = (1.16, 7.16) ppb
N = 269
R² = 0.86
TCCON: gr. (7.74 ± 0.03) ppb/yr, ampl. (2.35 ± 0.97) ppb
GOSAT: gr. (8.94 ± 0.07) ppb/yr, ampl. (4.70 ± 1.52) ppb
Bialystok
(μ,σ) = (4.62, 10.12) ppb
N = 274
R² = 0.90
TCCON: gr. (7.25 ± 0.14) ppb/yr, ampl. (21.13 ± 2.66) ppb
GOSAT: gr. (6.95 ± 0.10) ppb/yr, ampl. (10.29 ± 1.80) ppb
Bremen
(μ,σ) = (3.45, 11.50) ppb
N = 125
R² = 0.90
TCCON: gr. (8.11 ± 0.08) ppb/yr, ampl. (8.91 ± 2.23) ppb
GOSAT: gr. (7.54 ± 0.14) ppb/yr, ampl. (0.77 ± 2.83) ppb
Caltech
(μ,σ) = (-0.82, 12.02) ppb
N = 1180
R² = 0.89
TCCON: gr. (8.43 ± 0.11) ppb/yr, ampl. (28.76 ± 0.94) ppb
GOSAT: gr. (8.24 ± 0.05) ppb/yr, ampl. (12.55 ± 1.03) ppb
Darwin
(μ,σ) = (-0.32, 8.09) ppb
N = 442
R² = 0.93
TCCON: gr. (7.44 ± 0.04) ppb/yr, ampl. (1.71 ± 0.70) ppb
GOSAT: gr. (7.20 ± 0.05) ppb/yr, ampl. (2.91 ± 0.94) ppb
GOSAT NIES XCH4 (ppb)
TCCON XCH4 (ppb)
GOSAT XCH4 – TCCON XCH4 (ppb)
XCH4 (ppb)
Year
GOSAT, daily avg.
TCCON, daily avg.
GOSAT, fit
TCCON, fit

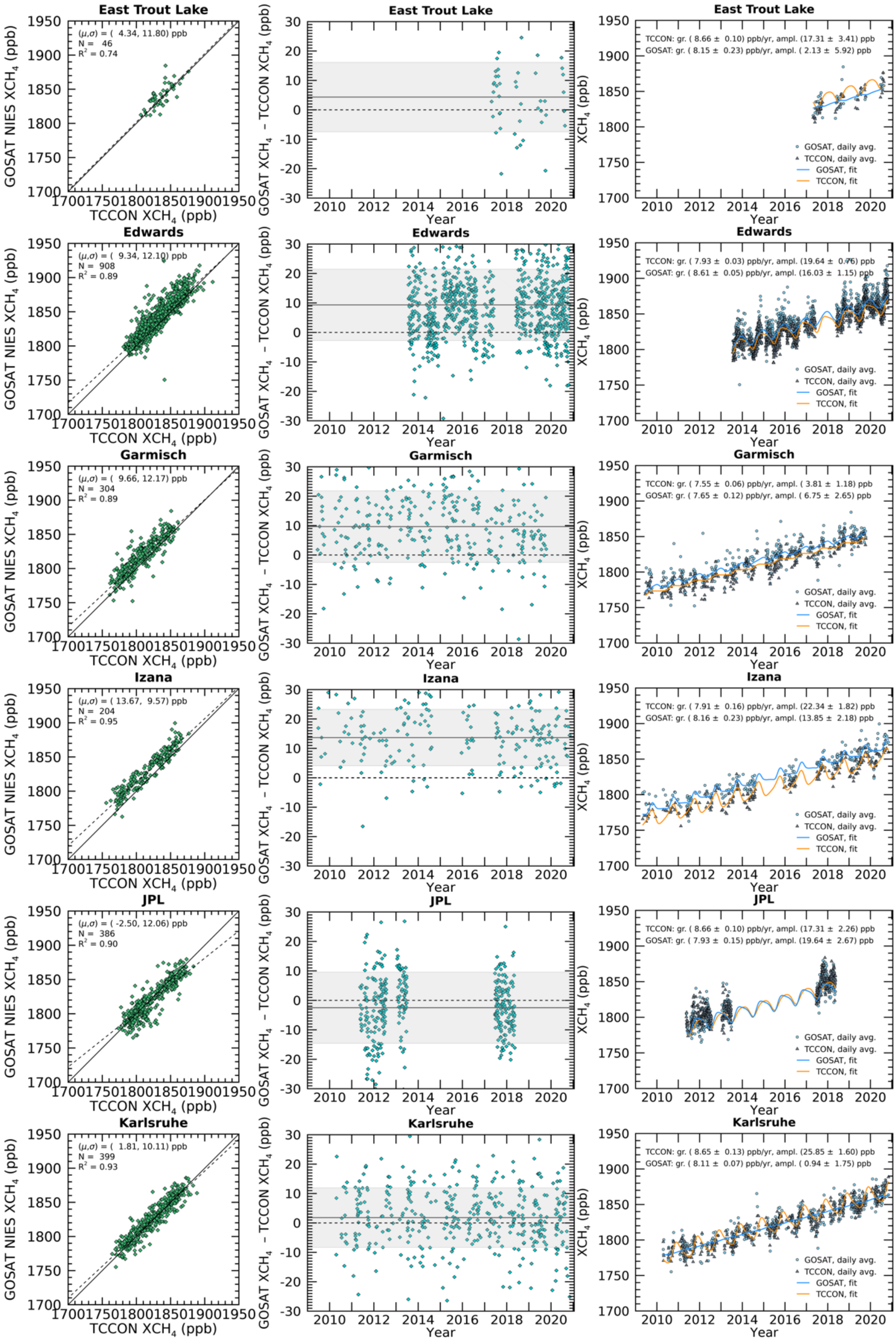
East Trout Lake
(μ,σ) = (4.34, 11.80) ppb
N = 46
R² = 0.74
TCCON: gr. (8.66 ± 0.10) ppb/yr, ampl. (17.31 ± 3.41) ppb
GOSAT: gr. (8.15 ± 0.23) ppb/yr, ampl. (2.13 ± 5.92) ppb
Edwards
(μ,σ) = (9.34, 12.10) ppb
N = 908
R² = 0.89
Garmisch
(μ,σ) = (9.66, 12.17) ppb
N = 304
R² = 0.89
TCCON: gr. (7.55 ± 0.06) ppb/yr, ampl. (3.81 ± 1.18) ppb
GOSAT: gr. (7.65 ± 0.12) ppb/yr, ampl. (6.75 ± 2.65) ppb
Izana
(μ,σ) = (13.67, 9.57) ppb
N = 204
R² = 0.95
TCCON: gr. (7.91 ± 0.16) ppb/yr, ampl. (22.34 ± 1.82) ppb
GOSAT: gr. (8.16 ± 0.23) ppb/yr, ampl. (13.85 ± 2.18) ppb
JPL
(μ,σ) = (-2.50, 12.06) ppb
N = 386
R² = 0.90
TCCON: gr. (8.66 ± 0.10) ppb/yr, ampl. (17.31 ± 2.26) ppb
GOSAT: gr. (7.93 ± 0.15) ppb/yr, ampl. (19.64 ± 2.67) ppb
Karlsruhe
(μ,σ) = (1.81, 10.11) ppb
N = 399
R² = 0.93
TCCON: gr. (8.65 ± 0.13) ppb/yr, ampl. (25.85 ± 1.60) ppb
GOSAT: gr. (8.11 ± 0.07) ppb/yr, ampl. (0.94 ± 1.75) ppb
GOSAT NIES XCH₄ (ppb)
TCCON XCH₄ (ppb)
GOSAT XCH₄ – TCCON XCH₄ (ppb)
XCH₄ (ppb)
Year
GOSAT, daily avg.
TCCON, daily avg.
GOSAT, fit
TCCON, fit

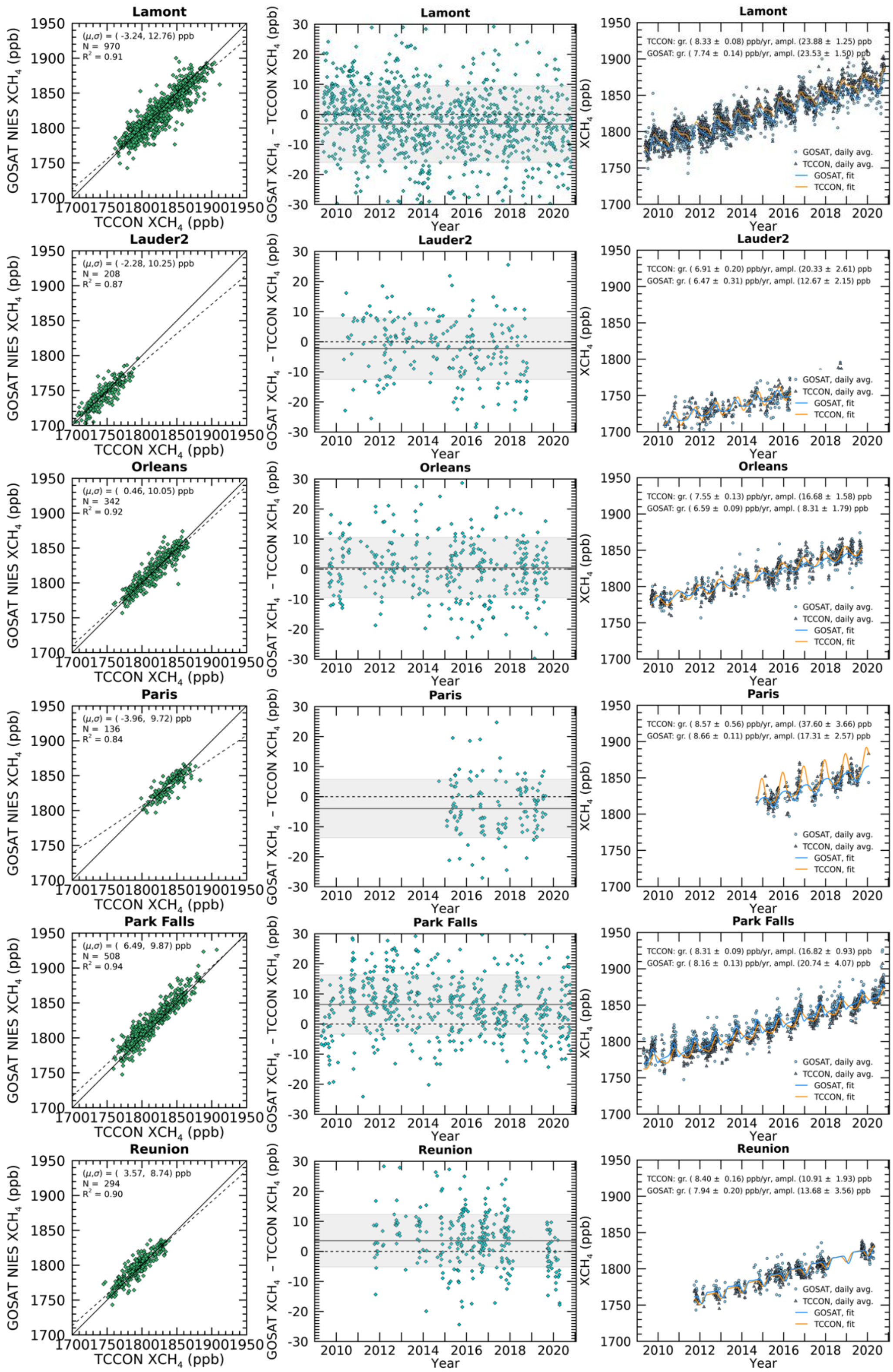
Lamont
(μ,σ) = (-3.24, 12.76) ppb
N = 970
R² = 0.91
TCCON: gr. (8.33 ± 0.08) ppb/yr, ampl. (23.88 ± 1.25) ppb
GOSAT: gr. (7.74 ± 0.14) ppb/yr, ampl. (23.53 ± 1.50) ppb
Lauder2
(μ,σ) = (-2.28, 10.25) ppb
N = 208
R² = 0.87
TCCON: gr. (6.91 ± 0.20) ppb/yr, ampl. (20.33 ± 2.61) ppb
GOSAT: gr. (6.47 ± 0.31) ppb/yr, ampl. (12.67 ± 2.15) ppb
Orleans
(μ,σ) = (0.46, 10.05) ppb
N = 342
R² = 0.92
TCCON: gr. (7.55 ± 0.13) ppb/yr, ampl. (16.68 ± 1.58) ppb
GOSAT: gr. (6.59 ± 0.09) ppb/yr, ampl. (8.31 ± 1.79) ppb
Paris
(μ,σ) = (-3.96, 9.72) ppb
N = 136
R² = 0.84
TCCON: gr. (8.57 ± 0.56) ppb/yr, ampl. (37.60 ± 3.66) ppb
GOSAT: gr. (8.66 ± 0.11) ppb/yr, ampl. (17.31 ± 2.57) ppb
Park Falls
(μ,σ) = (6.49, 9.87) ppb
N = 508
R² = 0.94
TCCON: gr. (8.31 ± 0.09) ppb/yr, ampl. (16.82 ± 0.93) ppb
GOSAT: gr. (8.16 ± 0.13) ppb/yr, ampl. (20.74 ± 4.07) ppb
Reunion
(μ,σ) = (3.57, 8.74) ppb
N = 294
R² = 0.90
TCCON: gr. (8.40 ± 0.16) ppb/yr, ampl. (10.91 ± 1.93) ppb
GOSAT: gr. (7.94 ± 0.20) ppb/yr, ampl. (13.68 ± 3.56) ppb
GOSAT NIES XCH4 (ppb)
TCCON XCH4 (ppb)
GOSAT XCH4 – TCCON XCH4 (ppb)
XCH4 (ppb)
Year
GOSAT, daily avg.
TCCON, daily avg.
GOSAT, fit
TCCON, fit

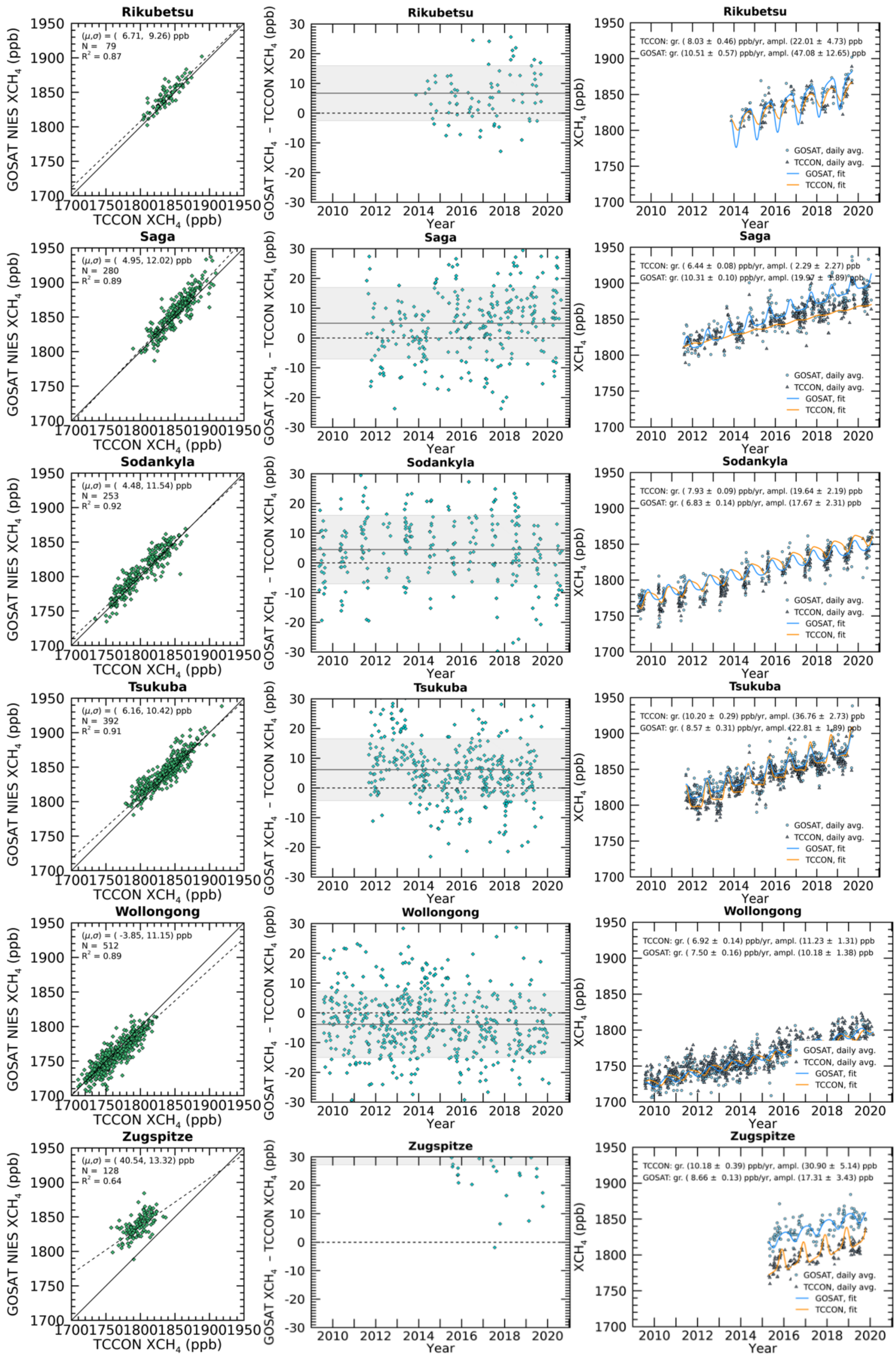

Figure 37: one-to-one evaluation of the daily-averaged retrieved XCH_4 from GOSAT NIES v02.95 and TCCON GGG2014 (left panel), the bias evaluated as GOSAT–TCCON (middle panel; mean bias is shown with the grey solid line and the standard deviation with the grey shaded area), and XCH_4 seasonal cycle fitting for each co-located time series (right panel).

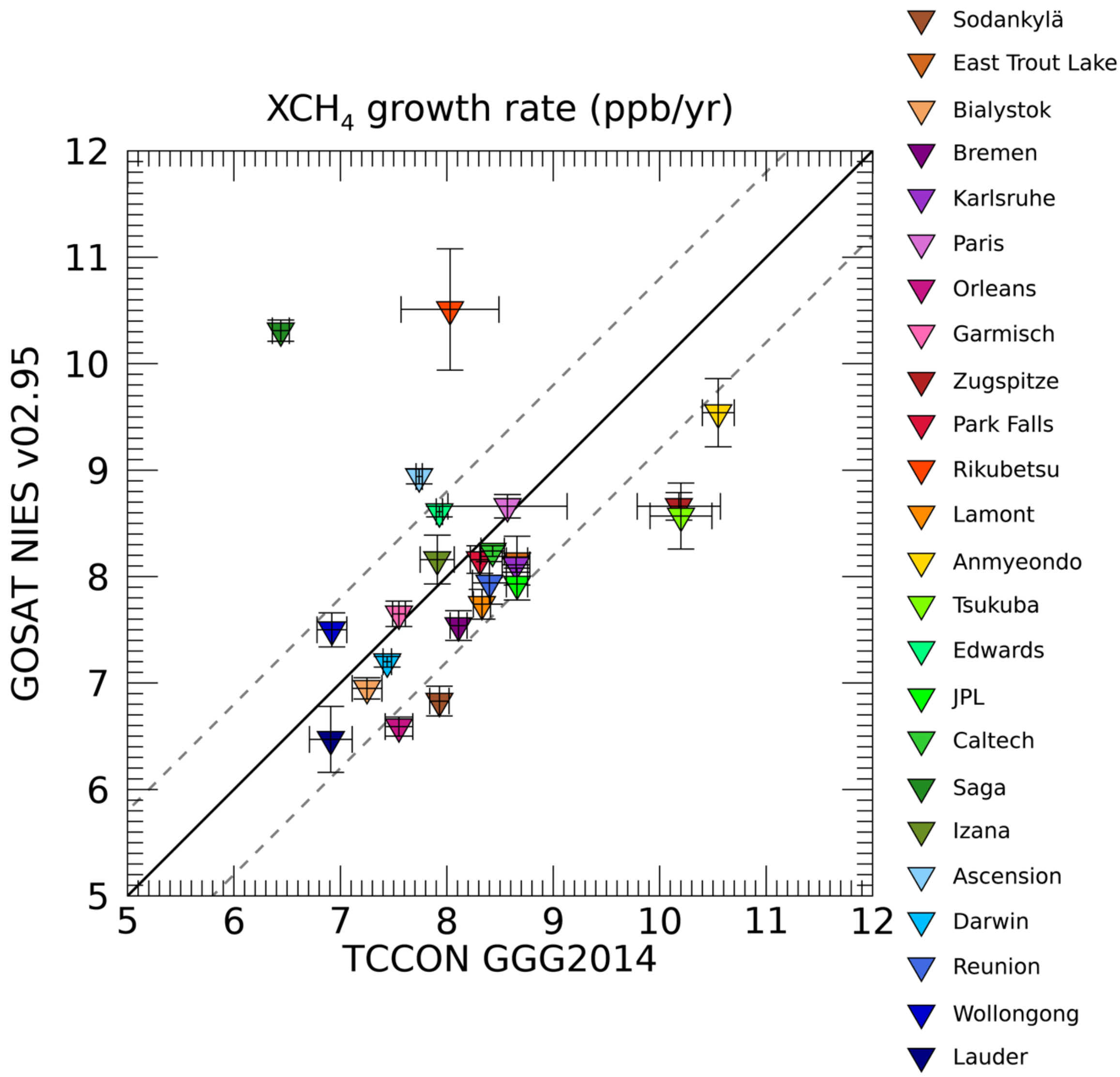

Figure 38: evaluation of the average growth rate (in ppb/year) for co-located GOSAT and TCCON XCH_4 retrievals and based on the seasonal cycle time series fitting. The dashed lines correspond to a deviation of 0.8 ppb/year from the one-to-one line (solid line).

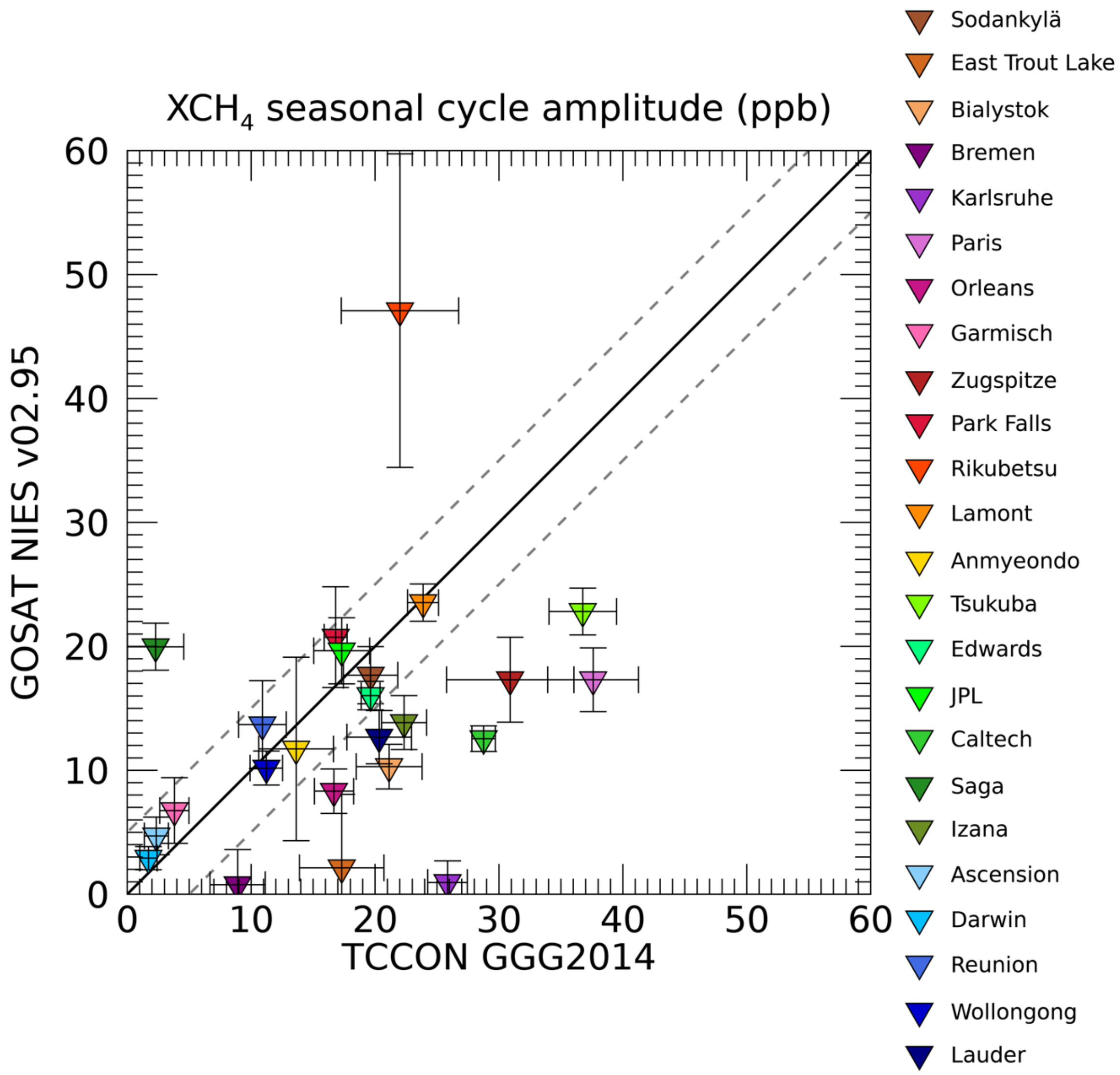

Figure 39: evaluation of the average seasonal cycle amplitude (in ppb) for co-located GOSAT and TCCON XCH_4 retrievals and based on the seasonal cycle time series fitting. The dashed lines correspond to a deviation of 5.0 ppb from the one-to-one line (solid line).

Agreement in the growth rate is generally very good, with only a few outliers where either local emissions are likely to affect the TCCON result more than GOSAT (e.g., Tsukuba) or the time series is not sufficiently long for reliably disentangling the growth rate from seasonal variability. Based on the growth rate comparison and the XCH_4 difference time series in Figure 37(middle panel), the GOSAT XCH_4 product is stable over time.

The XCH_4 seasonal cycle amplitude is highly variable and depends on the geographical location but not systematically according to the latitude such as for CO_2. The seasonal cycle amplitude can be quite sensitive to local sources. Figure 39 shows that the agreement between the GOSAT and TCCON XCH_4 seasonal cycle amplitudes is not very good. However, this does not directly indicate seasonal biases; a closer inspection of Figure 37 time series shows that the fitted seasonal cycles are not necessarily ideal fits to the time series. This has been noted also by Kivimäki et al. (2019) who carry out also a Dynamic Linear Model fitting exercise using Fourier series and a time-dependent growth rate. Thus, the differences in the seasonal cycle amplitude fitting are here interpreted as model deficiencies especially when the time series have significant gaps (e.g., due to the limited seasonal coverage of the data). This interpretation is supported by an analysis of the difference time series in Figure 37which do not generally show systematic seasonal biases. However, even though the seasonal cycle amplitude evaluation produced deviating results, a simultaneous seasonal cycle fitting is considered necessary for the evaluation of the growth rate.

3.9 Evaluation of GOSAT XCO2 and XCH4 Over Snow

At high latitudes, the most significant factor limiting the seasonal coverage of the passive satellite observations is the availability of solar radiation. Another challenge at high latitudes is snow-covered surfaces which absorb strongly in the near-infrared wavelengths, and which have not previously been separately evaluated. To study the GOSAT retrievals over snow, we used NOAA's (U. S. National Oceanic and Atmospheric Administration) IMS (Interactive Multisensor Snow and Ice Mapping System) Daily Northern Hemisphere Snow and Ice Analysis data set in 24 km resolution (U.S. National Ice Center, 2008) to distinguish GOSAT observations made over snow, land, sea, or sea ice. IMS data are a combination of various data products, for example, satellite and in-situ data.

Figure 40shows the amount of data for GOSAT NIES v02.95 XCH_4 product north from latitude 40°N during the entire GOSAT record (left panel) and aggregated at individual months (right panel). Different colours describe the IMS surface classification at the point where the GOSAT observation has been made. A corresponding evaluation was also carried out for XCO_2, but the results were similar and therefore only XCH_4 is presented in this report. However, the XCH_4 retrieval produced slightly more data points over snow than the XCO_2 retrieval. From Figure 40, we can see that the number of observations over snow increases during the time series (2010: total 1242 observations; 2020: total 1752 observations) but on the other hand, the total amount of observations does not increase during the time series. There is minor interannual variability in the total number of observations, but this is mainly related to possible instrument maintenance breaks and interannual variability in cloudiness. When analysing the monthly aggregated time series, the number of observations over snow is the highest in May (total 3436 observations over snow-covered landscape) when there is enough sunlight but still snow on the ground.

Figure 41 and Figure 42 show the retrieval errors, as given in the GOSAT NIES data files, for XCH_4 and XCO_2 observations north from 40°N. The retrieval errors are generally higher for observations over snow compared to observations over land. This is likely related to the snow reflectivity, but in addition, the solar zenith angles are larger during winter and spring compared to summer which also may affect the retrieval errors. The effects of the solar zenith angle and snow reflectivity should be studied in more detail to disentangle their effects which might further advance greenhouse gas retrieval development at high latitudes.

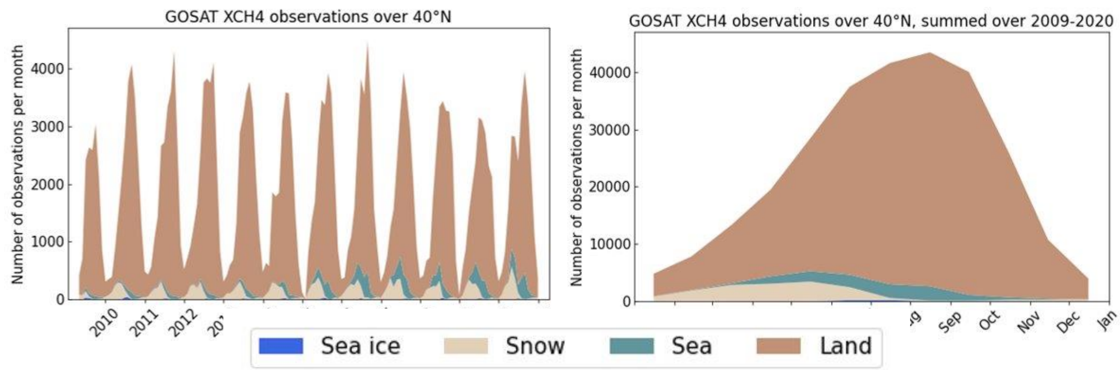

Figure 40: time series of the number of GOSAT NIES v02.95 XCH_4 observations north from 40°N (left) and monthly aggregated number of observations over the entire time series (right). Colours show the surface state at the ground observation footprint.

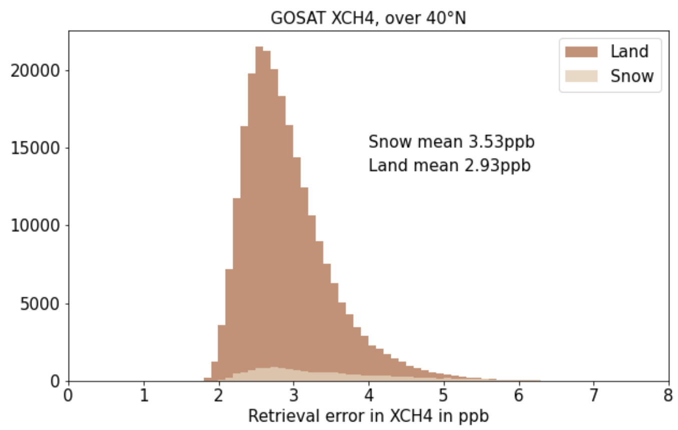

Figure 41: GOSAT NIES v02.95 XCH_4 retrieval errors for observations north from 40°N. Light brown shows the error for observations over snow-covered landscape and dark brown for observations over land.

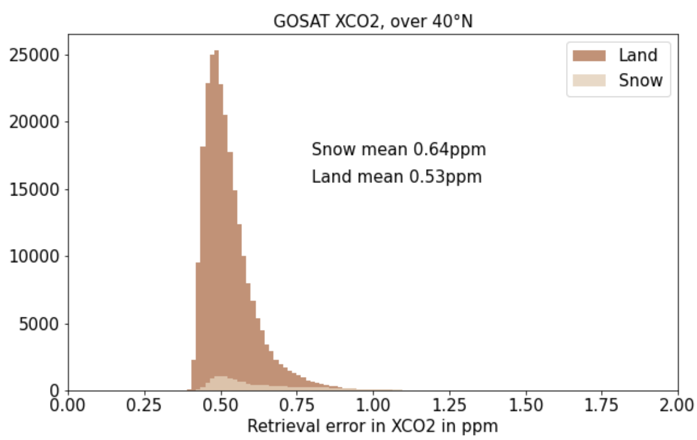

Figure 42: GOSAT NIES v02.95 XCO_2 retrieval errors for observations north from 40°N. Light brown shows the error for observations over snow-covered landscape and dark brown for observations over land.

3.10 Assessment of GOSAT NIES Prior And Posterior Profiles Against AIRCORE Soundings

3.10.1 GOSAT CO2 profiles

FMI has performed regular AirCore profile soundings (Karion et al., 2010) of greenhouse gases, for example, CO_2 and CH_4, at Sodankylä, Northern Finland, since 2013. These measurements provide a cost-efficient method for evaluating the shapes of the prior profiles used in the satellite retrievals.

Figure 43 shows GOSAT NIES v02.95 and TCCON GGG2014 CO_2 prior profiles against 12 AirCore profiles between 2013 and 2019. The TCCON prior profiles and the AirCore measurements are from the same day and location, and the GOSAT profiles are collected from a region within ±2° from the Sodankylä TCCON site. The 12 cases are chosen to be representative to show the seasonal variability of the measured AirCore profiles.

For CO_2, the differences between the profiles are the largest in the lowest parts of the atmosphere, especially for TCCON and AirCore. Seasonal variability is found in the agreement: in late summer and early autumn, the agreement is the weakest. The differences between GOSAT and AirCore are generally smaller.

A new version of the TCCON retrieval (GGG2020) is being developed in the TCCON community and it will include a set of updated prior profiles. Improvement is expected especially for the high-latitude retrievals. The new retrieval version is expected to be published in early 2022 and is likely to reduce the differences observed here.

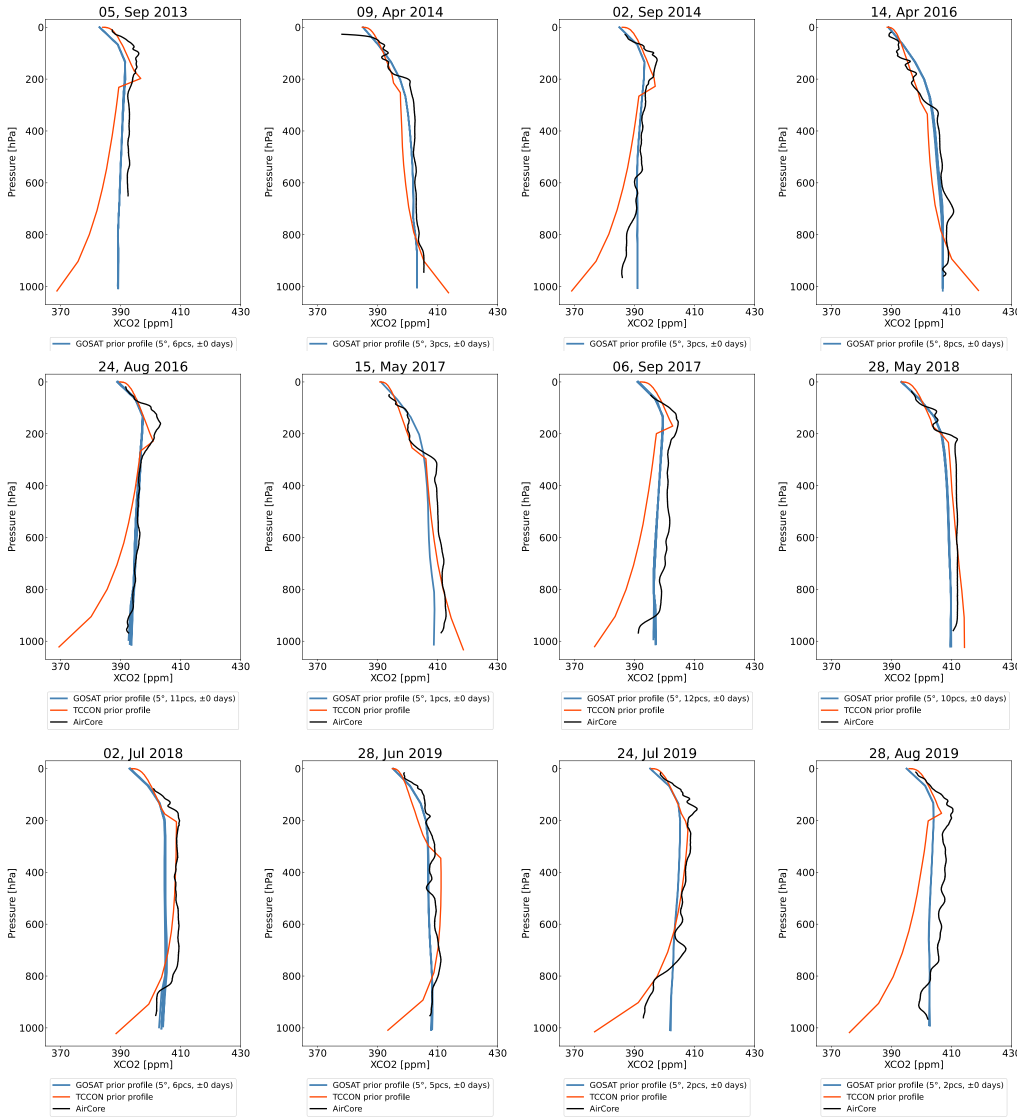

Figure 43: GOSAT NIES v02.95 and TCCON GGG2014 CO_2 prior atmospheric profiles evaluated against the AirCore measurements between 2013 and 2019 at different seasons.

3.10.2 GOSAT CH4 profiles

Figure 44 shows GOSAT NIES v02.95 and TCCON GGG2014 CH_4 prior profiles against measured AirCore profiles for 12 specific cases in 2013–2019. The TCCON prior and AirCore profiles are from the same day and location, and the GOSAT profiles are collected within ±2° from Sodankylä TCCON site. For CH_4, the differences between the profiles are generally the largest in the upper atmosphere where the CH_4 concentration decreases significantly. Especially during a strong polar vortex in late winter or early spring, the true atmospheric state may deviate significantly from the prior profiles. To mitigate this, FMI has developed a dimension-reduction-based CH_4 profile retrieval for FTS spectra (Tukiainen et al., 2016; Karppinen et al., 2020). In addition, this will be considered in the new TCCON GGG2020 retrieval.

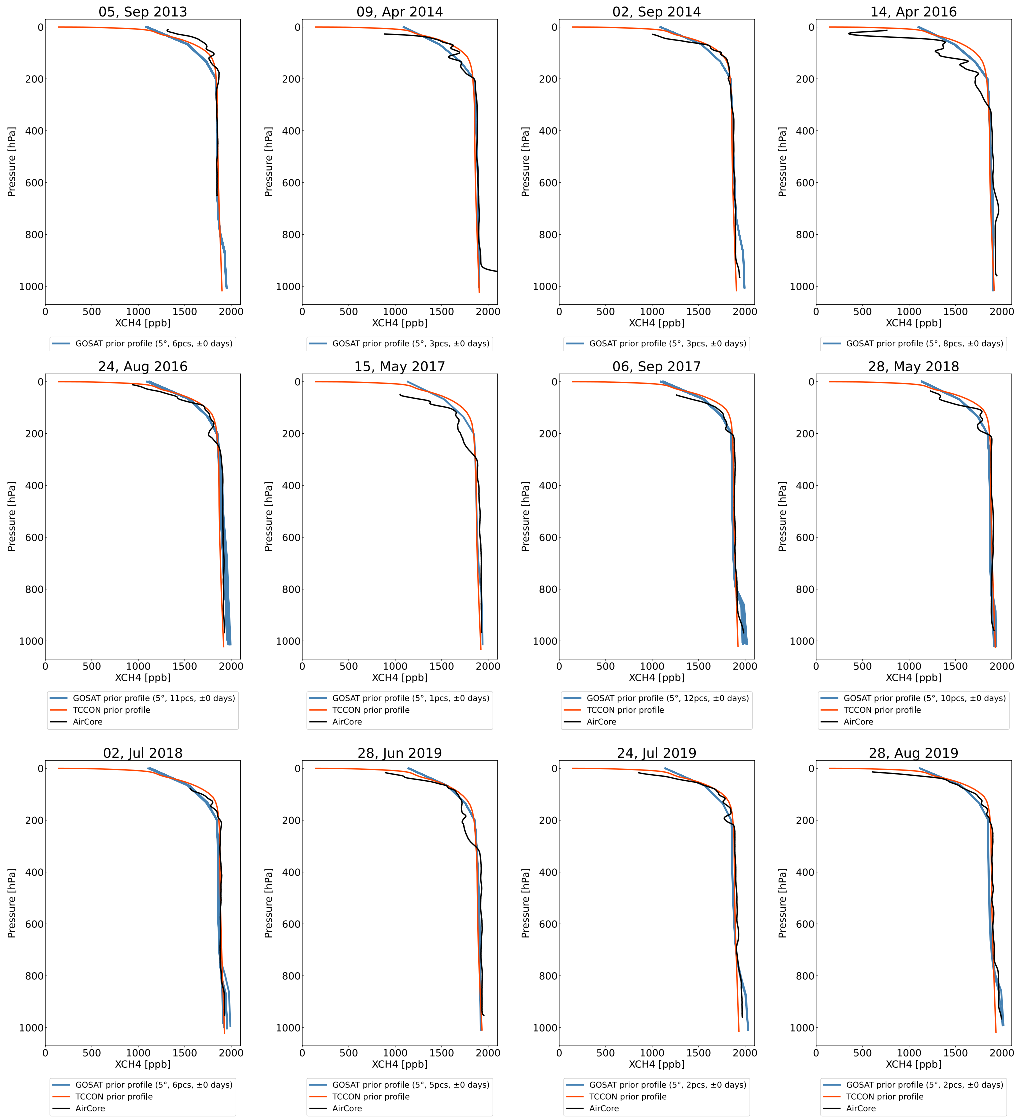

Figure 44: GOSAT NIES v02.95 and TCCON GGG2014 CH_4 prior atmospheric profiles evaluated against AirCore measurements between 2013 and 2019 at different seasons.

4. REFERENCES

[1] C Frankenberg, U. Platt, and T. Wagner. Retrieval of CO from SCIAMACHY onboard ENVISAT: detection of strongly polluted areas and seasonal patterns in global CO abundances. Atmos. Chem. Phys., 4:8425– 8438, 2005.

[2] Wouter Peters, A. R. Jacobson, C. Sweeney, A. E. Andrews, T. J. Conway, K. Masarie, J. B. Miller, L. M. P. Bruhwiler, G. Petron, A. I. Hirsch, D. E. J. Worthy, G. R. van der Werf, J. T. Randerson, P. O. Wennberg, M.C. Krol, and P. P. Tans. An atmospheric perspective on north american carbon dioxide exchange: Carbon- tracker. Proceedings of the National Academy of Science of the United States of America, 104(48):18925– 18930, 11 2007.

[3] A. Butz, S. Guerlet, O. Hasekamp, D. Schepers, A. Galli, I. Aben, C. Frankenberg, J. M. Hartmann, H. Tran, A. Kuze, G. Keppel-Aleks, G. Toon, D. Wunch, P. Wennberg, N. Deutscher, D. Griffith, R. Macatangay, J. Messerschmidt, J. Notholt, and T. Warneke. Toward accurate CO2 and CH4 observations from GOSAT. Geophys. Res. Lett., 38: doi:10.1029/2011GL047888, 2011.

[4] D. Schepers, S. Guerlet, A. Butz, J. Landgraf, C. Frankenberg, O. Hasekamp, J.-F. Blavier, N. M. Deutscher, D. W. T. Griffith, F. Hase, E. Kyro, I. Morino, V. Sherlock, R. Sussmann, and I. Aben. Methane retrievals from Greenhouse Gases Observing Satellite (GOSAT) shortwave infrared measurements: Performance comparison of proxy and physics retrieval algorithms. J. Geophys. Res., 117:D10307, 2012.

[5] P. Veefkind. TROPOMI on the ESA Sentinel-5 Precursor: a GMES mission for global observations of the atmospheric composition for climate and air quality applications. Remote Sens. Envirom., 120:70–83, 2012.

[6] A. Butz, O. P. Hasekamp, C. Frankenberg, and I. Aben. Retrievals of atmospheric CO_2 from simulated space-borne measurements of backscattered near-infrared sunlight: accounting for aerosol effects. Appl. Opt., 48:3322, 2009.

[7] H. Hu, O. Hasekamp, A. Butz, A. Galli, J. Landgraf, J. Aan de Brugh, T. Borsdorff, R. Scheepmaker, and I. Aben. The operational methane retrieval algorithm for TROPOMI. Atmospheric Measurement Techniques, 9:5423–5440, 2016.

[8] O. Hasekamp, H. Hu, A. Galli, P. Tol, J. Landgraf, and Butz A. Algorithm theoretical baseline document for sentinel-5 precursor methane retrieval. Atbd, SRON, Sorbonnelaan 2, 3584 CA Utrecht, The Netherlands, 2019.

[9] Sentinel 5 l2 prototype processors: Algorithm theoretical baseline document: Methane retrieval. Technical report, SRON, 2017.

[10] J. Langen, Y. Meijer, E. Brinksma, B. Veihelmann, and P. Ingmann. Gmes sentinels 4 and 5 mission requirements document. Mrd, ESA.

[11] Requirements for the geophysical validation of sentinel-5 precursor products. techreport, ESA.

[12] Krisna T., Lianghai Wu, Aben I., and Hasekamp O. Algorithm theoretical basis document version 1 (atbdv1) – for products ch4_go2_srpr (v2.0.0, 2019). Technical report, 2021.

[13] Krisna T., Lianghai Wu, Aben I., and Hasekamp O. Product user guide (pug)-for the remotec xch4 gosat2 data product ch4_go2_srpr (v2.0.0, 2021). Technical report, 2021.

[14] Krisna T., Lianghai Wu, Aben I., and Hasekamp O. Product user guide (pug)-for the remotec xch4 gosat2 data product ch4_go2_srfp (v2.0.0, 2021). Technical report, 2021.

[15] Krisna T., Lianghai Wu, Aben I., and Hasekamp O. End-to-end ecv uncertainty budget version 1 (e3ubv1)-for products ch4_go2_srpr (v2.0.0, 2021). Technical report, 2021.

[16] Krisna T., Lianghai Wu, Aben I., and Hasekamp O. End-to-end ecv uncertainty budget version 1 (e3ubv1)-for products ch4_go2_srfp (v2.0.0, 2021). Technical report, 2021.

[17] D. Wunch, G. C. Toon, P. O. Wennberg, S. C. Wofsy, B. B. Stephens, M. L. Fischer, O. Uchino, J. B. Abshire,P. Bernath, S. C. Biraud, J.-F. L. Blavier, C. Boone, K. P. Bowman, E. V. Browell, T. Campos, B. J. Connor, B. C. Daube, N. M. Deutscher, M. Diao, J. W. Elkins, C. Gerbig, E. Gottlieb, D. W. T. Griffith, D. F. Hurst, R. Jiménez, G. Keppel-Aleks, E. A. Kort, R. Macatangay, T. Machida, H. Matsueda, F. Moore, I. Morino, S. Park, J. Robinson, C. M. Roehl, Y. Sawa, V. Sherlock, C. Sweeney, T. Tanaka, and M. A. Zondlo. Calibration of the Total Carbon Column Observing Network using aircraft profile data. Atmospheric Measurement Techniques, pages 1351–1362, 2010.

[18] D Wunch, G. C Toon, J.-F. L Blavier, R. A Washenfelder, J Notholt, B. J Connor, D. W. T Griffith, V Sherlock, and P. O Wennberg. The total carbon column observing network. Philos. T. R. Soc. A., 369(1943):2087– 2112, May 2011.

[19] Haili Hu, Jochen Landgraf, Rob Detmers, Tobias Borsdorff, Joost Aan de Brugh, Ilse Aben, André Butz, and Otto Hasekamp. Toward global mapping of methane with tropomi: First results and intersatellite comparison to gosat. Geophysical Research Letters, 45(8):3682–3689, 2018.

[20] A. Lorente, T. Borsdorff, A. Butz, O. Hasekamp, J. Aan de Brugh, A. Schneider, L. Wu, F. Hase, R. Kivi, D. Wunch, D. F. Pollard, K. Shiomi, N. M. Deutscher, V. A. Velazco, C. M. Roehl, P. O. Wennberg, T. Warneke, and J. Landgraf. Methane retrieved from tropomi: improvement of the data product and validation of the first 2 years of measurements. Atmospheric Measurement Techniques, 14(1):665–684, 2021.

[21] S. Guerlet, A. Butz, D. Schepers, S. Basu, O. P. Hasekamp, A. Kuze, T. Yokota, J.-F. Blavier, N. M. Deutscher, D. W. T. Griffith, F. Hase, E. Kyro, I. Morino, V. Sherlock, R. Sussmann, A. Galli, and I. Aben. Impact of aerosol and thin cirrus on retrieving and validating XCO2 from GOSAT shortwave infrared measurements. J. Geophys. Res., 118:4887–4905, 2013.

[22] M. Inoue, I. Morino, O. Uchino, T. Nakatsuru, Y. Yoshida, T. Yokota, D. Wunch, P. O. Wennberg, C. M. Roehl, D. W. T. Griffith, V. A. Velazco, N. M. Deutscher, T. Warneke, J. Notholt, J. Robinson, V. Sherlock, F. Hase, T. Blumenstock, M. Rettinger, R. Sussmann, E. Kyrö, R. Kivi, K. Shiomi, S. Kawakami, M. De Mazière, S. G. Arnold, D. G. Feist, E. A. Barrow, J. Barney, M. Dubey, M. Schneider, L. T. Iraci, J. R. Podolske, P. W. Hill- yard, T. Machida, Y. Sawa, K. Tsuboi, H. Matsueda, C. Sweeney, P. P. Tans, A. E. Andrews, S. C. Biraud, Y. Fukuyama, J. V. Pittman, E. A. Kort, and T. Tanaka. Bias corrections of gosatswir xco2 and xch4 with tccon data and their evaluation using aircraft measurement data. Atmospheric Measurement Techniques, 9(8):3491–3512, 2016.

[23] Lianghai Wu, Otto Hasekamp, Haili Hu, Jochen Landgraf, Andre Butz, Joost aan de Brugh, Ilse Aben, Dave F. Pollard, David W. T. Griffith, Dietrich G. Feist, Dmitry Koshelev, Frank Hase, Geoffrey C. Toon, Hirofumi Ohyama, Isamu Morino, Justus Notholt, Kei Shiomi, Laura Iraci, Matthias Schneider, Martine de Maziere, Ralf Sussmann, Rigel Kivi, Thorsten Warneke, Tae-Young Goo, and Yao Te. Carbon dioxide retrieval from oco-2 satellite observations using the remotec algorithm and validation with tccon measurements. Atmospheric Measurement Techniques, 11(5):3111–3130, 5 2018.

[24] [Butz et al., 2011] Butz, A., Guerlet, S., Hasekamp, O., Schepers, D., Galli, A., Aben, I., Frankenberg, C., Hartmann, J.-M., Tran, H., Kuze, A., Keppel-Aleks, G., Toon, G., Wunch, D., Wennberg, P., Deutscher, N., Griffith, D., Macatangay, R., Messerschmidt, J., Notholt, J., and Warneke, T.: Toward accurate CO2 and CH4 observations from GOSAT, Geophys. Res. Lett., 38, L14812, https://doi.org/10.1029/2011GL047888, 2011.

[25] [Cogan et al., 2012] Cogan, A. J., Boesch, H., Parker, R. J., Feng, L., Palmer, P. I., Blavier, J.-F. L., Deutscher, N. M., Macatangay, R., Notholt, J., Roehl, C., Warneke, T., and Wunsch, D.: Atmospheric carbon dioxide retrieved from the Greenhouse gases Observing SATellite (GOSAT): Comparison with ground-based TCCON observations and GEOS-Chem model calculations, J. Geophys. Res., 117, D21301, https://doi.org/10.1029/2012JD018087, 2012.

[26] [GOSAT-2 ATBD]GOSAT-2 TANSO-FTS-2 SWIR L2 Retrieval Algorithm Theoretical Basis Document, YOSHIDA Yukio & OSHIO Haruki, NIES-GOSAT2-ALG-20191008-012-00, December 2020, National Institute for Environmental Studies, GOSAT-2 Project, *https://prdct.gosat-2.nies.go.jp/en/documents/ATBD_FTS-2_L2_SWL2_en_00.pdf*, pp. 88, 2020.

[27] [GOSAT-2 Data Users Handbook] GOSAT-2 / IBUKI-2 Data Users Handbook, 1st Edition, October 2020, Japan Aerospace Exploration Agency, National Institute for Environmental Studies, *https://prdct.gosat-2.nies.go.jp/en/documents/GOSAT-2_Data_Users_Handbook_1stEdition_en.pdf*, pp. 101, 2020.

[28] [GOSAT-2 Product Description] NIES GOSAT-2 Product File Format Descriptions, Vol.5, GOSAT-2 TANSO-FTS-2 SWIR L2 Column-averaged Dry-air Mole Fraction Product, October 2020, National Institute for Environmental Studies, GOSAT-2 Project, document NIES-GOSAT2-SYS-20190129-064-01, *https://prdct.gosat-2.nies.go.jp/en/documents/Vol.5_FTS-2_L2_SWFP_ver0104_en_01.pdf*, pp. 12, 2020.

[29] [GOSAT-2 Validation Summary] NIES GOSAT-2 Project, Summary of the GOSAT-2 TANSO-FTS-2 SWIR L2 Column averaged Dry-air Mole Fraction Product Validation, document NIES-GOSAT2-SYS-20201023-013-00, November 2020, *https://prdct.gosat-2.nies.go.jp/en/documents/ValidationResult_FTS-2_L2_SWFP_ver0104_en_00.pdf*, pp. 4, 2020.

[30] [Heymann et al., 2015] Heymann, J., Reuter, M., Hilker, M., Buchwitz, M., Schneising, O., Bovensmann, H., Burrows, J. P., Kuze, A., Suto, H., Deutscher, N. M., Dubey, M. K., Griffith, D. W. T., Hase, F., Kawakami, S., Kivi, R., Morino, I., Petri, C., Roehl, C., Schneider, M., Sherlock, V., Sussmann, R., Velazco, V. A., Warneke, T., and Wunch, D.: Consistent satellite XCO_2 retrievals from SCIAMACHY and GOSAT using the BESD algorithm, Atmos. Meas. Tech., 8,2961–2980, https://doi.org/10.5194/amt-8-2961-2015, 2015.

[31] [Krisna et al., 2020] Krisna, T. C., I. Aben, J. Landgraf, L. Wu, O. Hasekamp, ESA Climate Change Initiative "Plus" (CCI+) Algorithm Theoretical Basis Document Version 1 [32] (ATBDv1) for productsCO2_GO2_SRFP (v1.0.0) & CH4_GO2_SRFP (v1.0.0), Technical Report, version 1.2, pp. 40, 3-Dec-2020, 2020.

[33] [Noël et al., 2020] Noël, S., Reuter, M., Buchwitz, M., Borchardt, J., Hilker, M., Bovensmann, H., Burrows, J. P., Di Noia, A., Suto, H., Yoshida, Y., Buschmann, M., Deutscher, N. M., Feist, D. G., Griffith, D. W. T., Hase, F., Kivi, R., Morino, I., Notholt, J., Ohyama, H., Petri, C., Podolske, J. R., Pollard, D. F., Sha, M. K., Shiomi, K., Sussmann, R., Te, Y., Velazco, V. A., and Warneke, T.: XCO_2 retrieval for GOSAT and GOSAT-2 based on the FOCAL algorithm, Atmos. Meas. Tech. Discuss., *https://doi.org/10.5194/amt-2020-453*, in review, 2020.

[34] [Reuter et al., 2020] Reuter, M., Buchwitz, M., Schneising, O., Noel, S., Bovensmann, H., Burrows, J. P., Boesch, H., Di Noia, A., Anand, J., Parker, R. J., Somkuti, P., Wu, L., Hasekamp, O. P., Aben, I., Kuze, A., Suto, H., Shiomi, K., Yoshida, Y., Morino, I., Crisp, D., O'Dell, C. W., Notholt, J., Petri, C., Warneke, T., Velazco, V. A., Deutscher, N. M., Griffith, D. W. T., Kivi, R.,

Pollard, D. F., Hase, F., Sussmann, R., Te, Y. V., Strong, K., Roche, S., Sha, M. K., De Maziere, M., Feist, D. G., Iraci, L. T., Roehl, C. M., Retscher, C., and Schepers, D.: Ensemble-based satellite-derived carbon dioxide and methane column-averaged dry-air mole fraction data sets (2003-2018) for carbon and climate applications, Atmos. Meas. Tech., 13, 789-819, https://doi.org/10.5194/amt-13-789-2020, 2020.

[35] [Suto et al., 2020] Suto, H., Kataoka, F., Kikuchi, N., Knuteson, R. O., Butz, A., Haun, M., Buijs, H., Shiomi, K., Imai, H., and Kuze, A.: Thermal and near infrared sensor for carbon observation Fourier-transform spectrometer-2 (TANSO-FTS-2) on the Greenhouse Gases Observing Satellite-2 (GOSAT-2) during its first year on orbit, Atmos. Meas. Tech. Discuss., 2020, 1–51, *https://doi.org/10.5194/amt-2020-360*, *https://amt.copernicus.org/preprints/amt-2020-360/*, 2020.

[36] [Wunch et al., 2010] Wunch, D., Toon, G. C., Wennberg, P. O., Wofsy, S. C., Stephens, B. B., Fischer, M. L., Uchino, O., Abshire, J. B., Bernath, P., Biraud, S. C., Blavier, J.-F. L., Boone, C., Bowman, K. P., Browell, E. V., Campos, T., Connor, B. J., Daube, B. C., Deutscher, N. M., Diao, M., Elkins, J. W., Gerbig, C., Gottlieb, E., Griffith, D. W. T., Hurst, D. F., Jiménez, R., Keppel-Aleks, G., Kort, E. A., Macatangay, R., Machida, T., Matsueda, H., Moore, F., Morino, I., Park, S., Robinson, J., Roehl, C. M., Sawa, Y., Sherlock, V., Sweeney, C., Tanaka, T., and Zondlo, M. A.: Calibration of the Total Carbon Column Observing Network using aircraft profile data, Atmos. Meas. Tech., 3, 1351–1362, https://doi.org/10.5194/amt-3-1351-2010, 2010.

[37] [Wunch et al., 2011] Wunch, D., Toon, G. C., Blavier, J.-F. L., Washenfelder, R. A., Notholt, J., Connor, B. J., Griffith, D. W. T., Sherlock, V., and Wennberg, P. O.: The Total Carbon Column Observing Network, Philos. T. R. Soc. A, 369, 2087–2112, https://doi.org/10.1098/rsta.2010.0240, 2011.

[38] [Yoshida et al., 2013] Yoshida, Y., Kikuchi, N., Morino, I., Uchino, O., Oshchepkov, S., Bril, A., Saeki, T., Schutgens, N., Toon, G. C., Wunch, D., Roehl, C. M., Wennberg, P. O., Griffith, D. W. T., Deutscher, N. M., Warneke, T., Notholt, J., Robinson, J., Sherlock, V., Connor, B., Rettinger, M., Sussmann, R., Ahonen, P., Heikkinen, P., Kyrö, E., Mendonca, J., Strong, K., Hase, F., Dohe, S., and Yokota, T.: Improvement of the retrieval algorithm for GOSAT SWIR XCO_2 and XCH_4 and their validation using TCCON data, Atmos. Meas. Tech., 6, 1533–1547, https://doi.org/10.5194/amt-6-1533-2013, 2013.

[39] Boesch, H., Liu, Y., Tamminen, J., Yang, D., Palmer, P.I., Lindqvist, H., Cai, Z., Che, K., Di Noia, A., Feng, L., Hakkarainen, J., Ialongo, I., Kalaitzi, N., Karppinen, T., Kivi, R., Kivimäki, E., Parker, R.J., Preval, S., Wang, J., Webb, A.J., Yao, L., and Chen, H.: Monitoring Greenhouse Gases from Space, Remote Sens., 13, 2700, 2021.

[40] Karion, A., Sweeney, C., Tans, P. and Newberger, T.: AirCore: An innovative atmospheric sampling system. Journal of Atmospheric and Oceanic Technology, 27(11), pp.1839-1853, 2010.

[41] Karppinen, T., Lamminpää, O., Tukiainen, S., Kivi, R., Heikkinen, P., Hatakka, J., Laine, M., Chen, H., Lindqvist, H., and Tamminen, J.: Vertical distribution of Arctic methane in 2009–2018 using ground-based remote sensing, Remote Sens., 12, 917, 2020.

[42] Kivimäki, E., Lindqvist, H., Hakkarainen, J., Laine, M., Sussmann, R., Tsuruta, A., Detmers, R., Deutscher, N., Dlugokencky, E. J., Hase, F., Hasekamp, O., Kivi, R., Morino, I., Notholt, J., Pollard, D. F., Roehl, C., Schneider, M., Sha, M. K., Velazco, V. A., Warneke, T., Wunch, D., Yoshida, Y., and Tamminen, J.: Evaluation and analysis of the seasonal cycle and variability of the trend from GOSAT methane retrievals, Remote Sens., 11, 882, 2019.

[43] Lindqvist, H., O'Dell, C. W., Basu, S., Boesch, H., Chevallier, F., Deutscher, N., Feng, L., Fisher, B., Hase, F., Inoue, M., Kivi, R., Morino, I., Palmer, P. I., Parker, R., Schneider, M.,

Sussmann, R., and Yoshida, Y.: Does GOSAT capture the true seasonal cycle of carbon dioxide? Atmos. Chem. Phys., 15, 13023–13040, 2015.

[44] Taylor, T. E., O'Dell, C. W., Crisp, D., Kuze, A., Lindqvist, H., Wennberg, P. O., Chatterjee, A., Gunson, M., Eldering, A., Fisher, B., Kiel, M., Nelson, R. R., Merrelli, A., Osterman, G., Chevallier, F., Palmer, P. I., Feng, L., Deutscher, N. M., Dubey, M. K., Feist, D. G., Garcia, O. E., Griffith, D., Hase, F., Iraci, L. T., Kivi, R., Liu, C., De Mazière, M., Morino, I., Notholt, J., Oh, Y.-S., Ohyama, H., Pollard, D. F., Rettinger, M., Roehl, C. M., Schneider, M., Sha, M. K., Shiomi, K., Strong, K., Sussmann, R., Té, Y., Velazco, V. A., Vrekoussis, M., Warneke, T., and Wunch, D.: An eleven year record of XCO2 estimates derived from GOSAT measurements using the NASA ACOS version 9 retrieval algorithm, Earth Syst. Sci. Data Discuss. [preprint], https://doi.org/10.5194/essd-2021-247, in review, 2021.

[45] Tukiainen, S., Railo, J., Laine, M., Hakkarainen, J., Kivi, R., Heikkinen, P., Chen, H. and Tamminen, J.: Retrieval of atmospheric CH4 profiles from Fourier transform infrared data using dimension reduction and MCMC. Journal of Geophysical Research: Atmospheres, 121(17), pp.10-312, 2016.

[46] U.S. National Ice Center. 2008, updated daily. IMS Daily Northern Hemisphere Snow and Ice Analysis at 1 km, 4 km, and 24 km Resolutions, Version 1. [24km resolution]. Boulder, Colorado USA. NSIDC: National Snow and Ice Data Center. doi: https://doi.org/10.7265/N52R3PMC. [Date Accessed: 27 Jan 2021].